

ROLE OF SUBERIN FOR DEFENSE RESPONSES IN POTATO

Dissertation

Zur Erlangung des
Doktorgrades der Naturwissenschaften (Dr. rer. nat.)

der

Naturwissenschaftlichen Fakultät III
Agrar- und Ernährungswissenschaften,
Geowissenschaften und Informatik

der Martin-Luther-Universität Halle-Wittenberg

Vorgelegt

von Elvio Henrique Benatto Perino
geboren am 18.07.1988 in Ourinhos – Brasilien

Gutachter (-in):

1. Prof. Dr. Sabine Rosahl
2. Prof. Dr. Holger Bruno Deising
3. Prof. Dr. Jens Boch

Halle (Saale), 06th Mar. 2023.

INDEX

1. INTRODUCTION.....	9
1.1. <i>Solanum tuberosum</i> and <i>Phytophthora infestans</i>	9
1.2. Breeding and genome editing for resistance in <i>Solanum tuberosum</i>	11
1.3. Plant-pathogen interactions and the role of Pep13	15
1.4. The role of periderm and suberin in plant defense	16
1.5. Suberin biosynthesis and the putative biosynthetic genes in <i>Solanum tuberosum</i>	18
1.5.1. The ABC transporter StABCG1	24
1.5.2. Regulation of the suberin pathway and transcription factors	26
1.6. Aim of this study.....	27
2. MATERIAL AND METHODS.....	28
2.1. <i>Solanum tuberosum</i>	28
2.2. <i>Nicotiana benthamiana</i>	28
2.3. <i>Phytophthora infestans</i> , plant inoculation assays and biomass	28
2.4. <i>Escherichia coli</i> , vector cloning and selection of transformants	30
2.5. <i>Agrobacterium tumefaciens</i> transformation.....	31
2.6. Media	32
2.7. PCR.....	33
2.8. Golden Gate cloning.....	34
2.8.1. Construction of vectors <i>pPVS3:GFP</i> and <i>pPVS3:GUS</i>	34
2.8.2. Simultaneous overexpression of the putative suberin biosynthetic genes <i>StABCG1</i> , <i>StFHT</i> , <i>StCYP86A33</i> and <i>StKCS6</i>	35
2.8.3. Overexpression of the putative suberin biosynthetic genes via <i>AtMYB39</i> transcription factor under control of 35S promoter	38

2.8.4.	Use of CRISPR/Cas9 technology for editing the transporter <i>StABCG1</i> , involved in suberin deposition	38
2.9.	Transient expression in <i>Solanum tuberosum</i> and <i>Nicotiana benthamiana</i>	39
2.10.	Stable transformation of <i>Solanum tuberosum</i>	40
2.11.	Wounded leaves and tubers and microscopy	41
2.12.	Analyses	41
2.12.1.	Genotype confirmation of the <i>StABCG1</i> -CrisprCas plants	41
2.12.2.	Pep13 infiltration.....	42
2.12.3.	RNAseq	42
2.12.4.	Illumina sequencing.....	43
2.12.5.	GUS staining	43
2.12.6.	NightShade (GFP detection)	43
2.12.7.	RT-qPCR/Gene expression.....	44
2.12.8.	Untargeted metabolite profiling.....	45
2.12.9.	Assessment of tuber weight in <i>StABCG1</i> -CrisprCas plants.....	45
2.12.10.	Resistance of <i>StABCG1</i> -CrisprCas tubers to wounds during storage..	46
3.	RESULTS.....	47
3.1.	Suberin is formed in <i>S. tuberosum</i> leaves under different treatments	47
3.2.	Suberin biosynthetic genes are induced after Pep13 infiltration in <i>Solanum tuberosum</i> leaves (RNAseq data).....	49
3.3.	Suberin-related genes are differentially expressed after Pep13 infiltration.....	50
3.4.	Suberin-related genes are differentially expressed after wounding.....	53
3.5.	Suberin-related genes are differentially expressed after <i>Phytophthora infestans</i> inoculation.....	55
3.6.	Suberin transporter <i>StABCG1</i> was edited with CRISPR/Cas9.....	57
3.6.1.	<i>StABCG1</i> knockout mutants were identified by Illumina sequencing.....	59

3.6.2. Pep13-infiltrated <i>StABCG1</i> -CrisprCas plants have defective suberin formation	60
3.6.3. Wounded leaves of <i>StABCG1</i> -CrisprCas plants have defective suberin formation	63
3.6.4. Wounded <i>StABCG1</i> -CrisprCas leaves show dramatic changes in metabolites profile	66
3.6.5. <i>StABCG1</i> -CrisprCas plants have defective suberin formation after <i>Phytophthora infestans</i> infection	69
3.6.6. Tubers from <i>StABCG1</i> -CrisprCas plants have defective suberin formation....	73
3.6.7. Tuber of <i>StABCG1</i> -CrisprCas plants had an acquired resistance after <i>Phytophthora infestans</i> inoculation	76
3.7. Activation of suberin biosynthetic genes	77
3.7.1. Expression of the betalain pathway via TALE triggers necrosis in <i>Solanum tuberosum</i>	78
3.7.2. TAL-effector hinders stable transformation in <i>Solanum tuberosum</i>	80
3.7.3. Expression of the transcription factor <i>AtMYB39</i> induces enhanced suberin formation in <i>Solanum tuberosum</i>	84
4. DISCUSSION	87
4.1. Transcriptomic data revealed putative suberin biosynthesis genes	87
4.2. Use of CrisprCas9 technology in <i>Solanum tuberosum</i>	92
4.3. <i>StABCG1</i> -CrisprCas plants have defective suberin formation	94
4.3.1. Browning in the <i>StABCG1</i> -CrisprCas plants	96
4.4. <i>AtMYB39</i> expressing potato plants had enhanced suberin formation	99
5. SUMMARY	102
6. ZUSAMMENFASSUNG	104
7. REFERENCES	106

8.	APPENDICES	119
8.1.	Supplementary figures	119
8.2.	Primers Table	120
8.3.	Plasmids and constructs table.....	123
9.	NOTE OF THANKS.....	125
10.	EIDESSTÄTTLICHE ERKLÄRUNG / DECLARATION UNDER OATH.....	127
11.	CURRICULUM VITAE	128

LIST OF ABBREVIATIONS

4CL	<i>4-coumarate:CoA ligase</i>
5GT	glucosyltransferase
<i>A. thaliana</i>	<i>Arabidopsis thaliana</i>
<i>A. tumefaciens</i>	<i>Agrobacterium tumefaciens</i>
ABA	Abscisic acid
ABC	ATP-binding-cassette
ABCG	ATP-binding-cassette-G-transporters
<i>Achn</i>	<i>Actinidia chinensis</i>
ACT	<i>agmatine coumaroyl transferase</i>
AHC	Alkyl hydroxycinnamates
ANAC	<i>no apical meristem activation factor in Arabidopsis</i>
ASFT	suberin feruloyl transferase
<i>At</i>	<i>Arabidopsis thaliana</i>
ATMT	<i>Agrobacterium tumefaciens</i> -mediated transformation
BAHD	family group of acyltransferases (Benzyl alcohol O-acetyltransferase; anthocyanin O-hydroxycinnamoyltransferase; N-hydroxycinnamoyl/benzoyltransferase; deacetylindoline 4-O-acetyltransferas)
BAK	<i>Brassinosteroid-Insensitive 1-Associated Receptor Kinase</i>
<i>bHLH</i>	<i>basic helix-loop-helix</i>
bp	base pairs
Bv	<i>Beta vulgaris</i>
C##	chain composed from ## carbons
CA	coumaroyl agmatine
CafNor	caffeoyl noradrenaline
CafPut	caffeoyl putrescine
Cas9	Clustered Regularly Interspaced Short Palindromic Repeats-associated nuclease
CBF	<i>C-repeat binding factor</i>
CER	<i>β-Ketoacyl-Coenzyme A Synthase</i>
CO	coumaroyl octopamine
CoA	Coenzyme A
cols.	colleagues
CouNor	coumaroyl noradrenaline
CRISPR	Clustered Regularly Interspaced Short Palindromic Repeats
CT	coumaroyl tyramine
CUT	<i>Cuticular β-ketoacyl-Coenzyme A Synthase</i>
CYP	cytochrome P450
d	days
dai	days after inoculation
daw	days after wounding
DMR	<i>Downy mildew resistance</i>

DNA	Deoxyribonucleic acid
DOD	3,4-dihydroxyphenylalanine 4,5-dioxygenase
<i>E. coli</i>	<i>Escherichia coli</i>
EFR	elongation factor receptor
<i>elf</i>	elongation factor
ETI	effector-triggered immunity
EV	Empty vector
FA	feruloyl agmatine
FACT	Fatty Alcohol:Caffeoyl-CoA Caffeoyl Transferase
FAE	Fatty acid elongation
FAR	fatty acyl-CoA reductases
FHT	fatty alcohol hydroxycinnamoyl transferase
Fig.	Figure
flg22	flagelin 22
FLS	flagellin-sensing
FNor	feruloyl noradrenaline
FO	feruloyl octopamine
FT	feruloyl tyramine
G3P	Glycerol-3-phosphate
GBSS	<i>Granule-bound Starch Synthase</i>
GFP	green fluorescent protein
<i>Gh</i>	<i>Gossypium hirsutum</i>
GPAT	glycerol 3-phosphate transferase
gRNA	guide Ribonucleic acid
h	hours
HCAAs	hydroxycinnamic acid amides
HDS	<i>1-hydroxy-2-methyl-2-(E)-butenyl-4-diphosphate Synthase</i>
indels	insertions and/or deletions
Kan	kanamycin
KSC	3-ketoacyl CoA synthase
LAC	<i>laccase</i>
LACSs	Long-chain acyl-CoA synthetases
<i>Le</i>	<i>Lycopersicon esculentum</i>
LOX1	<i>lipoxygenase</i>
Mas	mannopine synthase
<i>Md</i>	<i>Malus domestica</i>
MYB	<i>myeloblastosis viral oncogene</i>
<i>N. benthamiana</i>	<i>Nicotiana benthamiana</i>
<i>Nb</i>	<i>Nicotiana benthamiana</i>
NBD	nucleotide-binding domain
NHEJ	non-homologous end-joining
NLR	nucleotide-binding domain leucine-rich repeat
Nos	nopaline synthase
Ocs	octopine synthase
<i>P. crispum</i>	<i>Petroselinum crispum</i>
<i>P. infestans</i>	<i>Phytophthora infestans</i>

PAMP	Pathogen-Associated Molecular Patterns
PCR	Polymerase chain reaction
PDR	Pleiotropic drug resistance
PHO	Phosphate
PM	Plasma membrane
<i>PPO</i>	<i>Polyphenol oxidase</i>
<i>PR</i>	<i>pathogenesis-related protein</i>
<i>PRB1B</i>	<i>pathogenesis-related protein B1B</i>
<i>PRP</i>	<i>Probable glutathione S-transferase</i>
PRRs	pattern recognition receptors
PS	Polyester synthase
PTI	pattern-triggered immunity
<i>PVS</i>	<i>putative vetispiradiene synthase</i>
qPCR	quantitative polymerase chain reaction
<i>Qs</i>	<i>Quercus suber</i>
<i>R. solanacearum</i>	<i>Ralstonia solanacearum</i>
rel. units	relative units
RNA	Ribonucleic acid
RNAseq	Ribonucleic acid sequencing
ROS	reactive oxygen species
<i>Rpi-blb</i>	<i>Phytophthora infestans-bulbocastanum</i>
<i>S. bulbocastanum</i>	<i>Solanum bulbocastanum</i>
<i>S. demissum</i>	<i>Solanum demissum</i>
<i>S. stoloniferum</i>	<i>Solanum soloniferum</i>
<i>S. tuberosum</i>	<i>Solanum tuberosum</i>
<i>Sb</i>	<i>Solanum bulbocastanum</i>
<i>SBE</i>	<i>Starch-Branching Enzymes</i>
<i>SBR</i>	<i>Starch-Branching</i>
<i>Sc</i>	<i>Saccharomyces cerevisiae</i>
SEM	Standard error of the mean
sgRNA	single guide Ribonucleic acid
SSR2	<i>Sterol Side-chain Reductase</i>
<i>St</i>	<i>Solanum tuberosum</i>
<i>Ta</i>	<i>Triticum aestivum</i>
TAL	transcription activator-like
TALEs	transcription activator-like effectors
TF	transcription factor
<i>THT</i>	<i>tyramine hydroxycinnamoyl transferase</i>
TMD	transmembrane domain
VLCFA	very long-chain fatty acids
WBC	White-brown complex
WT	wild-type
ZFNs	Zinc-finger nucleases

1. INTRODUCTION

1.1. *Solanum tuberosum* and *Phytophthora infestans*

Potato (*Solanum tuberosum*) is the third most important food crop in the world (Barrell et al., 2013) with worldwide production higher than 359 million tonnes per year, according to the Food and Agriculture Organization Corporate Statistical Database (2020) (FAO, 2021; Clasen et al., 2016), and a harvested area estimated at 19 million ha in 2017 (FAO, 2021). China leads as the largest potato producer with 4.2 million ha in 2020, or 21.7 % of the total production, followed by India, Ukraine, Russia, USA, and Germany in sixth place with an annual production of 11 million tonnes (FAO, 2021). Potato is an important tuber crop in Germany, exporting in 2020 a total of 5.42 million tonnes of potatoes as fresh goods or in the form of processed products (BMEL, 2021).

Potato is a very important dietary source of carbohydrates, after crops like wheat, rice, and maize, containing a high nutritional value, source of vitamins and potassium (Fogelman et al., 2019). Potato is also one of the major crops used as source for starch production (Andersson et al., 2017), and for other processed products such as potato chips and french fries (Clasen et al., 2016). In Germany, the production of starch from potatoes is the most important purpose in this field. Following the Federal Ministry of Food and Agriculture of Germany (BMEL, 2021), about 23 % of the harvested potato is used for starch production.

The cultivated potato (*Solanum tuberosum*) traces its origin to South America. The landraces show huge differences in tuber colors and shapes, leaf, flower, and growth habit variations. The number of sets of chromosomes in these species ranges from diploid to pentaploid (Spooner et al., 2007), but most varieties of known potatoes are tetraploid and have heterogeneous progeny, as the example of *S. tuberosum*. Using potato tuber or stem propagation as the current practice, helps maintaining the genetic conformity (Diémé et al., 2013).

Late blight, caused by the oomycete *P. infestans*, is until today a constant threat to the global potato and tomato production (Leesutthiphonchai et al., 2018), which leads to

a state annual cost that can reach US\$ 10 billion, including about US\$ 1.5 billion for chemical control (Haverkort et al., 2009).

Despite improvements in education, hygiene, pest controls, and knowledge of pathogens and hosts, the management of late blight remains a continuous challenge (Leesutthiphonchai et al., 2018).

The disease cycle of *P. infestans* involves sporangia spread by the wind or the rain to different host plants. The zoospores released from the sporangia have flagella, allowing further movement on water layers on leaves or soil. Upon landing on a suitable place, such as a host leaf surface, the zoospores encyst, germinating into a germ tube and forming an appressorium (Judelson and Blanco, 2005). Following ideal conditions, over the leaf surface, the pathogen starts the asymptomatic biotrophic phase, forming primary hyphae in the intercellular space and also feeding structures, such as haustoria (Fig. 1). Under favorable environmental conditions, the pathogen switches to the necrotrophic phase and promotes further colonization and necrosis of the host tissues. Under optimal conditions, sporulation is triggered a day later, when sporangiophores emerge from stomata cells, followed by sporangia formation and release of zoospores (Leesutthiphonchai et al., 2018) (Fig. 1).

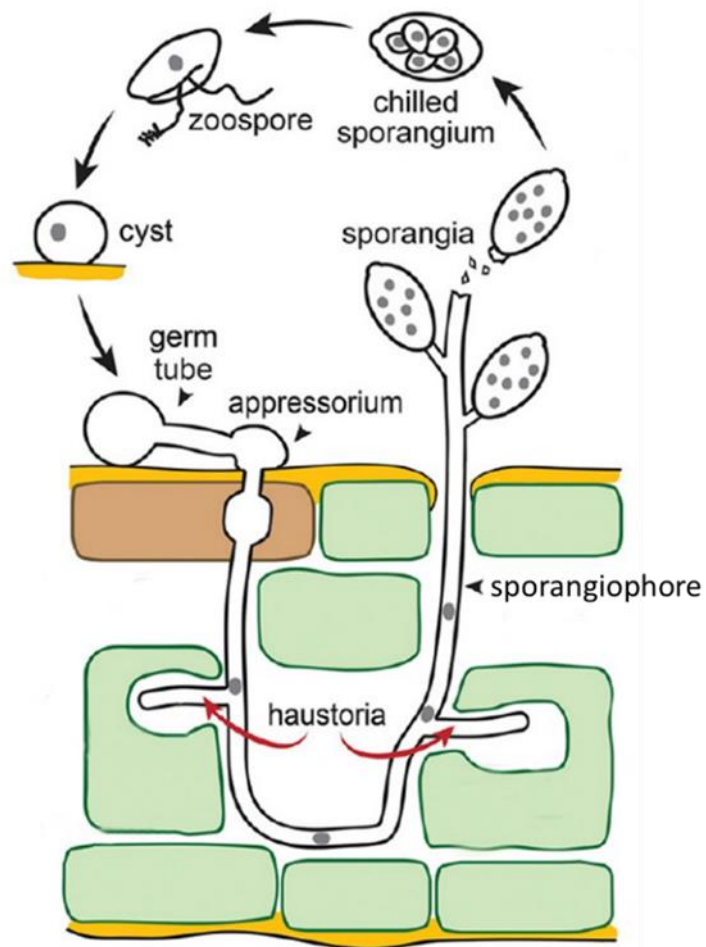


Figure 1: Disease cycle of *Phytophthora infestans* on leaf surface. Sporangia are spread through the wind or rain to other host plants, the infection proceeds after germ tube and appressorium formation. Under ideal conditions, the sporangiophore emerges forming new sporangia. Figure adapted from Leesutthiphonchai et al. (2018).

1.2. Breeding and genome editing for resistance in *Solanum tuberosum*

Because of their strong adaptability, pathogens can cause great economic losses (Nowicki et al., 2012). *P. infestans* proliferation can be greatly favored by appropriate environmental conditions, such as lower temperatures and high humidity (Wu et al., 2020). Also, sexual reproduction in *P. infestans* contributes to a higher genetic diversity (Paro et al., 2012). Nowadays, chemical treatments such as systemic fungicides or insecticides are used against infestations. However, these measures are only effective within a limited range, since the increasing use of chemical agents and fungicides may promote a

selection pressure, resulting in *P. infestans* strains with increasing resistance to fungicides, as well as pollution of the environment, consequently affecting human health (Paro et al., 2012; Gisi et al., 2011; Gisi and Cohen, 1996).

An attempted solution to this problem is to produce varieties of resistant plants. Plant breeders have long-sought sources of genetic resistance to late blight disease. However, due to tetraploidy and high heterozygosity of the cultivated *S. tuberosum*, traditional crossbreeding can greatly slow down the production of new varieties (Muthoni et al., 2015). Approximately 100,000 new genotypes are generated in the process of creating a new variety (Nicolia et al., 2015) and so traditional breeding methods require years to generate a resistant potato plant (Lindhout et al., 2011). This difficulty could be circumvented by clonal propagation, which is commonly used in potato, but this method produces plants with identical genotypes (Nadakuduti et al., 2019). However, identical genotypes in crop cultivation is disadvantage, since genetic diversity is an essential resource for crop breeding to better adapt agriculture to conditions, such as global climate change and consumer preferences (Hufford et al., 2019). This genetic diversity can also increase agricultural productivity, generating resistance against biotic and abiotic stresses, such as pathogen disease or salt stress (Lemmon et al., 2018).

Resistance in *Solanum* spp. against pathogens may be attributed to the presence of multiple resistance genes, which are required to provide broader resistance (Enciso-Maldonado et al., 2021). Sources of resistance have been reported in wild potatoes where a number of resistant genes were identified (Karki et al., 2021), including several species previously described as resistant to late blight, such as *S. bulbocastanum*, *S. stoloniferum* (Bachmann-Pfarbe et al., 2019) and *S. demissum* (Reddick, 1930). For example, several resistance genes were identified in the Mexican wild potato *S. demissum*. Some of these genes were transferred into the cultivated potato species by crossing and backcrossing (Machida-Hirano, 2015). However, new strains of *P. infestans* have overcome it (Bradeen and Kole, 2016), for example, there are now many variants of different lineage, each of the lineage have at least 19 different genotypes (Cooke and Lees, 2004). Despite being important sources of resistance genes, some wild potato, such as *S. bulbocastanum*, are diploid ($2n = 2x = 24$) and cannot be conventionally crossed with tetraploid cultivated potato species (Rakosy-Tican, 2020).

A possible alternative is genetic engineering, which provides an effective method of introducing crop improvements in potatoes. Some of these resistance genes were previously cloned into the cultivated potato species, such as the Resistance to *Phytophthora infestans-bulbocastanum* 1 and 2 from *S. bulbocastanum* (*SbRpi-blb1* and *SbRpi-blb2*; Gillund et al., 2013), which can recognize a wide range of isolates of *P. infestans* and have been proven effective in the field (BASF, 2011; Oh et al., 2009).

Diverse techniques were successfully employed for site-directed mutagenesis in genome editing purposes for diploid plants, for example barley, rice, soybean, tomato, and maize, providing a precise and specific editing of DNA sequences in the genome (Nicolia et al., 2015). Among these techniques, the three mostly studied are Zinc-finger nuclease (ZFNs), Transcription activator-like effector nucleases (TALENs) and the recently described CRISPR/Cas. ZFNs consists of an artificial restriction enzyme – a fusion of a zinc finger protein with the cleavage domain of the *FokI* restriction enzyme (Urnov et al., 2010). Two zinc finger proteins recognize a specific sequence in the DNA, binding the strands, allowing the fused *FokI* endonuclease to create an active dimer that cleaves the DNA in the target loci (Zhang et al., 2019a). ZNFs have an excessive off-targeting because of the restricted number of zinc fingers that may be constructed in a single ZFN (usually 2 to 6; Cornu et al.; 2008), which was changed later, introducing a spacer between the fusion of the domains, leading to an increase of the site specificity from 12 to 36 bp (Miller et al., 2007; Szczepek et al., 2007). Still, ZFNs design is time consuming and has a poor targeting density (Yildiz et al., 2021). According to Eck (2018), there are no reports of ZFNs genome editing in solanaceous, and no reports were found up to now.

A simpler alternative is the *Xanthomonas* spp. effector strategy given by the transcription activator-like effectors (TALEs), which induces the expression of specific host genes (Boch et al., 2009). TALENs are a fusion of a DNA-binding domain, in this case from TALEs, and a non-specific cleavage domain of *FokI* endonucleases (Yildiz et al., 2021; Zhang et al., 2019a). The primary difference is that, unlike ZFNs, each TALE repeat recognizes single nucleotides rather than 3-base pair sites (Yildiz et al., 2021), in a modular and predictable mode (Scholze and Boch, 2010). However, TALEs are easier to design and to modify than zinc finger proteins, making TALENs encompass more

possibilities for genome editing than ZFNs (Zhang et al., 2019a). Sawai et al. (2014) pioneered the successful use of TALENs in a tetraploid cultivated potato by editing the Sterol Side-chain Reductase 2 (*StSSR2*) in all four alleles. Another important example is given by Nicolia et al. (2015), who used transient TALEN expression in protoplasts to perform site-directed mutagenesis in a tetraploid potato. These studies highlighted in the past that the site directed mutagenesis might be employed as a new potato breeding strategy as well as for functional investigation of critical genes to increase long-term potato production (Yildiz et al., 2021; Nicolia et al., 2015).

The newest tool for genome-editing is the Clustered Regularly Interspaced Short Palindromic Repeats (CRISPR)/Cas9 system for targeted genome modifications, which has been shown to be the most powerful method due to its high gene-specificity, a user-friendly and a cost-efficient technique of producing target-specific mutations (Nadakuduti et al., 2019). With a short single-guide RNA (sgRNA), a 20 bp sequence complementary to the target region, a promoter and a sgRNA scaffold, in combination with a Cas9 nuclease (Jinek et al., 2012), it is possible to cleave the double-strand in a target region of choice. When the cell recognizes the damaged DNA, a repair mechanism is activated, either by the non-homologous end-joining (NHEJ) pathway or the precise homologous recombination pathway (Nadakuduti et al., 2019; Britt, 1999). NHEJ is susceptible to errors and often leads to inserts or deletions (indels), which may cause a knockout of gene function (Andersson et al., 2017). The first time that the CRISPR/Cas9 technique was successfully used in higher plants was in 2013 (Li et al., 2013; Nekrasov et al., 2013; Shan et al., 2013). However, up to now there are not many reports using CRISPR/Cas technique in tetraploid potato. For example, Butler et al. (2016) had used geminivirus replicons to increase the copy number of CRISPR/Cas9 in diploid and tetraploid potato and Zhou et al. (2017) showed by knock-outing using CRISPR/Cas9 that the *StMYB44* is involved in the regulation of Phosphate1 (*StPHO1*) in potato.

The major challenges are for polyploid crops, such as wheat (*Triticum aestivum* L.) and potato (*Solanum tuberosum* L.). The presence of multiple alleles of a certain gene as well as gene duplications result in a high number of possible targets in a single cell (Nicolia et al., 2015). Genetic modification, in which a genetic material is integrated or modified into/from the genome of the plant, has been a widely

used method in potato research for a long time (Barrell et al., 2013). However, since the European Commission has requested its Scientific Advice Mechanism to review the new breeding techniques in agricultural biotechnology, it has restricted commercialization of the developed genetically modified plants (Ruffell, 2018).

1.3. Plant-pathogen interactions and the role of Pep13

The interactions between pathogens and plants is one of the oldest species interactions and had changed evolution of plant defense. In response to pathogens and insect attacks, plants usually activate both constitutive and induced defenses. Both defenses respond to infection through different morphological, biochemical, and molecular mechanisms (Thordal-Christensen, 2020). Jones and Dangl (2006) have proposed a model for plant-pathogen interaction, named zig-zag model. When a pathogen first comes in contact with its host, conserved Pathogen-Associated Molecular Patterns (PAMP) are recognized by pattern recognition receptors (PRRs), localized in the plant plasma membrane, triggering the pattern-triggered immunity (PTI). To avoid it, pathogens can, for example, manipulate immunity proteins, such as the PRRs, or immunity signaling components (Thordal-Christensen, 2020). In this case, effector-triggered immunity (ETI) is activated, which uses nucleotide-binding domain leucine-rich repeat (NLR) receptors to detect secreted effectors of pathogens (Pruitt et al., 2021). Eliminating or developing new effectors, pathogens can overcome the ETI response, starting all over (Thordal-Christensen, 2020). PTI and ETI are directly involved in the transcriptional regulation of defense genes. In addition, ETI can also program cell death response, called the hypersensitive reaction (Hatsugai et al., 2017).

PAMPs are characteristic of a certain microbial species. An example is the bacterial protein flagellin (*flg22*), which is very well characterized in *Arabidopsis* and also the translation elongation factor Tu (*elf18*), which are recognized by the plant receptor kinases *FLS2* and *EFR*, respectively. Both use the Brassinosteroid-Insensitive 1-Associated Receptor Kinase 1 (*BAK1*) as a co-receptor (Monaghan and Zipfel, 2012; Robatzek and Saijo, 2008).

The PAMP known as Pep13 was demonstrated to elicit defense responses in parsley (Nürnberg et al., 1994). This peptide consists of 13 amino acids (VWNQPVRGFKVYE) and was identified as a component of an extracellular cell wall transglutaminase in *Phytophthora sojae* (Brunner et al., 2002; Nürnberg et al., 1994). Pep13 is highly conserved among the genus *Phytophthora* and does not exist in plants. The 13 amino acids motif is essential for the enzymatic activity of the transglutaminase and is also crucial for the elicitor activity in *Petroselinum crispum* and *S. tuberosum* (Halim et al., 2004; Brunner et al., 2002; Nürnberg et al., 1994; Parker, 1991). An exchange on the second amino acid from W to A (W2A - VANQPVRGFKVYE) leads to a reduction in elicitor and enzymatic activity in comparison to Pep13 (Nürnberg et al., 1994).

Halim et al. (2004) showed that infiltration of potato leaves with Pep13 causes accumulation of jasmonic (JA) and salicylic (SA) acid and the development of cell death. After Pep13 infiltration, transgenic potato plants with modified JA or SA showed a reduced defense response (Halim et al., 2009; Halim et al., 2004). The hypersensitive response observed in potato after Pep13 infiltration appears to be specific, especially because *P. crispum*, *Solanum lycopersicum* and *Arabidopsis thaliana* showed no signs of cell death after the same treatment (Halim et al., 2004; Brunner et al., 2002). In addition, infection with *P. infestans* in potato plants after treatment with Pep13 results in systemic resistance (Halim, 2006).

A number of genes involved in plant defense has been described to be activated after Pep13 treatment, like *St4CL*, *StPRP1*, *StTHT*, *StPRB1B*, *StPR1*, *StPR5* and *StLOX1* (Halim et al., 2004; Brunner et al., 2002). RNAseq (Ulrike Smolka – IPB/Halle, Germany, personal communication) and microarray (Altmann, 2009) data from our group have shown more than 3,200 and 1,200 genes, respectively, to be differentially expressed at least 3-fold in potato plants after Pep13 treatment, compared to the W2A control. Of these, more than 800 genes are overexpressed in both studies.

1.4. The role of periderm and suberin in plant defense

The periderm, as the first line of defense for plants, is an effective barrier in secondary shoot axes, roots, and tubers of potato plants. The periderm replaces the

epidermis as the outermost tissue during secondary growth. In the immature periderm, the phellogen is unstable and fragile, subsequently separating outwardly the suberized phellem and inwardly the underlying phelloderm. These tissues together form the periderm (Fig. 2A) (Campilho et al., 2020; Barel and Ginzberg, 2008; Lenzian, 2006; Lulai and Freeman, 2001; Reeve and Hautala, 1970). In potato tubers, the phellogen originates from the epidermal and subepidermal cells of the epidermis (Barel and Ginzberg, 2008; Reeve and Hautala, 1970).

Lipophilic barriers, such as suberin, create a special tissue covering all aerial surfaces and underground root organs (Franke and Schreiber, 2007). Due to its barrier function in root, shoot and leaf endoderm, suberin separates the plant body from the environment, allowing plants to survive in terrestrial habitats (Schreiber et al., 2005). Suberized cell walls form physiologically vital plant-environment interfaces, preventing uncontrolled water loss, nutrient depletion (Franke and Schreiber, 2007; Franke et al., 2005), and exchange of gases and solutes (Cohen et al., 2017).

Other than constitutively, suberin is also formed in the tissues as a result of external stimuli, as a response to abiotic stresses, such as salt concentration (Ranathunge et al., 2011; Krishnamurthy et al., 2009; Enstone et al., 2002), nutrient deficiency (Barberon et al., 2016), waterlogging (Kotula et al., 2017) and heavy metal toxicity (Degenhardt and Gimmler, 2000) or biotic stresses, such as wounding (Lulai and Corsini, 1998) and pathogen infection (Lanoue et al., 2010; Ranathunge et al., 2008; Thomas et al., 2007). For example, after being injured or infected by pathogens, a new periderm will form around the damaged or dead epidermal cells as a protective layer (Lulai and Neubauer, 2014; Buskila et al., 2011). Thus, during storage, an intact and suberized tuber periderm (Fig. 2B) is the main barrier to prevent diseases, insect attack, dehydration and tuber rot (Lulai, 2007; Schreiber et al., 2005; Lulai and Freeman, 2001).

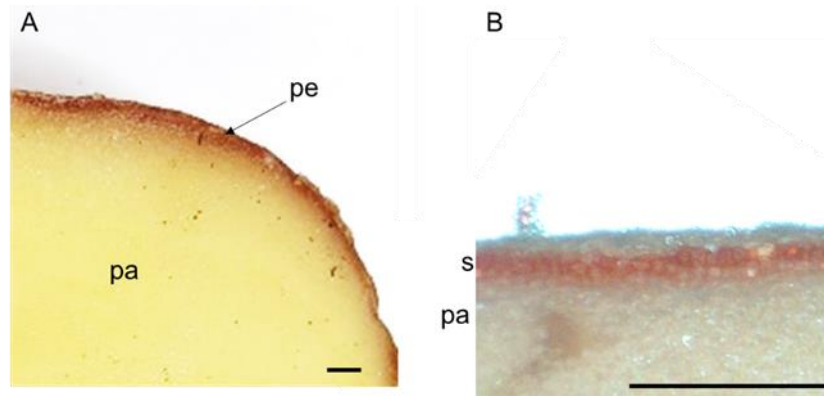


Figure 2: Structure of the potato tuber periderm. (A) Longitudinal section of a potato tuber, showing the periderm (pe) and the parenchyma (pa). (B) Microscopic view of the potato periderm after SudanIII staining showing the suberized phellem (s) and the starch-containing storage parenchyma (pa). Bars correspond to 1 mm (the author).

A recent study suggests a correlation between the enhanced suberin formation and resistance against pathogens (Campilho et al., 2020). Suberin is a heteropolymer composed of polyaliphatic linked with polyphenolic components (Vishwanath et al., 2015; Bernards, 2002). The polyaliphatic domain is mostly composed of long chain fatty acids, primary alcohols, and glycerol (Beisson et al., 2012; Franke et al., 2005), while the polyphenolic domain contains hydroxycinnamic acid derivatives, with ferulate being the major aromatic constituent of suberin in *Arabidopsis*, potato, and many other plants (Franke et al., 2005; Bernards and Razem, 2001; Bernards et al., 1995).

1.5. Suberin biosynthesis and the putative biosynthetic genes in *Solanum tuberosum*

Up to now, the genes encoding enzymes involved in suberin biosynthesis are: (I) β -ketoacyl-CoA synthases, e.g. KCS2/DAISY (Lee et al., 2009; Franke et al., 2008) and KCS20 (Lee et al., 2009); (II) fatty acid cytochrome P450 oxidase, e.g. CYP86A1 (Höfer et al., 2008) and CYP86B1 (Compagnon et al., 2009; Molina et al., 2009); (III) fatty acyl-CoA reductases, e.g. FARs (Vishwanath et al., 2013a; Domergue et al., 2010); (IV) glycerol 3-phosphate transferase 5, e.g. GPAT5 (Beisson et al., 2007; Li et al., 2007), along with those responsible for the inclusion of aromatic monomers, such as aliphatic suberin feruloyl transferase, e.g. ASFT (Gou et al., 2009; Molina et al., 2009). In the last

years, (V) ATP-binding-cassette-G-transporters, e.g., ABCG2, ABCG6, and ABCG20 have shown to be necessary for the formation of suberin (Yadav et al., 2014). For potato plants, the genes described are, respectively, KCS6 (Serra et al., 2009a), CYP86A33 (Serra et al., 2009b), FAR3 (Vulavala et al., 2017), GPAT3 (Vulavala et al., 2019), FHT (Serra et al., 2010) and ABCG1 (Landgraf et al., 2014).

Most of the enzymes involved in the suberin formation from Arabidopsis and some from potato were identified by characterizing mutants with altered suberin composition (Vishwanath et al., 2015). In figure 3, a simplified model of suberin biosynthesis in Arabidopsis is shown (Vishwanath et al., 2015).

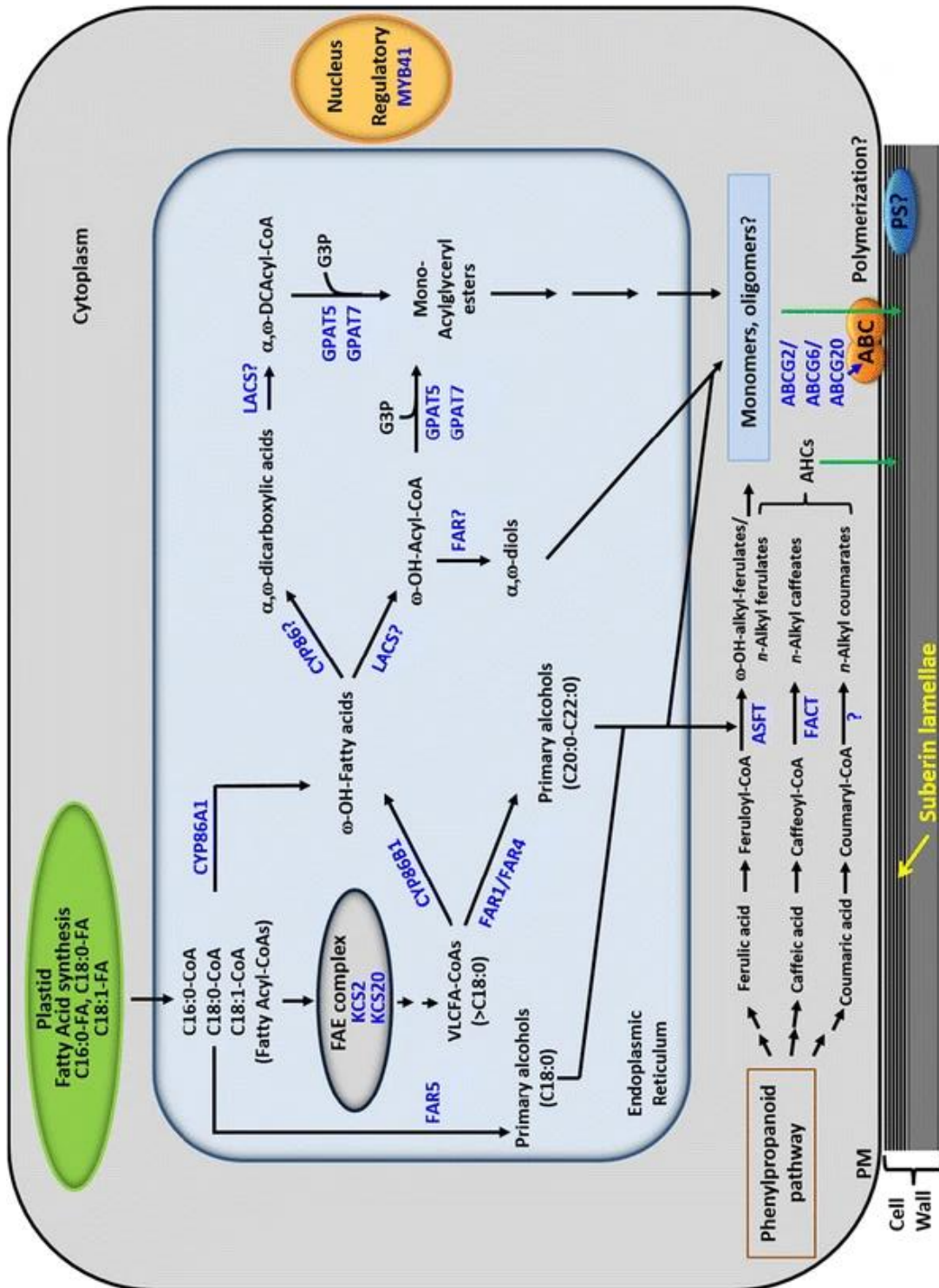


Figure 3: Model of suberin formation. Fatty acid elongation (FAE); Very long-chain fatty acids (VLCFAs); Fatty acyl reductases (FARs); Cytochrome P450 enzymes (CYPs); Glycerol-3-phosphate (G3P); Glycerol 3-phosphate acyltransferases (GPATs); Long-chain acyl-CoA synthetases (LACSs); ATP-binding-cassette (ABC); Plasma membrane (PM); Polyester synthase(s) (PS); Alkyl hydroxycinnamates (AHCs); ASFT (Aliphatic Suberin Feruloyl Transferase); FACT (Fatty Alcohol:Caffeoyl-CoA Caffeoyl Transferase). (Vishwanath et al., 2015).

Biosynthesis of long chain fatty acids by a fatty acid elongase (FAE) complex occurs in the endoplasmic reticulum. The first condensation phase is catalyzed by a Ketoacyl-CoA synthase (KCS). The KCS was described to be the limiting factor for fatty acid extension (Serra et al., 2009a).

Arabidopsis contains 21 KCS genes (Joubes et al., 2008). Since saturated long chain fatty acids are found in several biosynthetic pathways (suberin, wax, and sphingolipid), these enzymes can act in different metabolic routes. For example, KCS enzymes, such as the ones encoded by *AtKCS6* (also known by *AtCER6*, *AtCUT1*) (Millar et al., 1999) and *AtKCS1* (Todd et al., 1999), were described to be involved in the biosynthesis of epidermal wax components in Arabidopsis. *LeCER6*, for instance, is involved in the synthesis of epidermal waxes in tomato fruits (Leide et al., 2007; Vogg et al., 2004). Todd et al. (1999) suggest that *AtKCS1* is also involved in suberin synthesis in roots.

In the potato tuber periderm, biosynthesis of long-chain suberin monomers and wax compounds in potato tuber periderm is dependent on *StKCS6* (Serra et al., 2009a), which has high homology to *LeCER6*, *AtCER6/CUT1/KCS6*, *AtCER60/KCS5* and *GhCER6*. Silencing of *StKCS6* results in tubers with a significant decrease in aliphatic compounds with chain length of C28 and accumulation of C26 and lower. *In vitro* studies in yeast have shown that *AtKCS5/AtCER60* produces C26, C28 and C30 fatty acids (Trenkamp et al., 2004), while *GhCER6*, from *Gossypium hirsutum*, homologous to *AtCER6*, can complement the *ScElo3*, from *Saccharomyces cerevisiae*, in elongation of fatty acids (Qin et al., 2007).

Subsequently, the fatty acids are hydroxylated by cytochrome P450s enzymes (P450s), producing hydroxyacids, hydroperoxides, epoxides, aldehydes, ketones and α,ω -diacids (Pinot and Beisson, 2010), which can be used as monomers for polymerization in cutin or suberin (Kolattukudy, 1981). Like CYP86 and CYP94 (Werck-Reichhart and Feyereisen, 2000), recent studies have identified other P450s families acting on fatty acids, such as CYP74 (Stumpe and Feussner, 2006), CYP77 (Sauveplane et al., 2009), CYP703 (Morant et al., 2007), CYP704 (Li et al., 2010), CYP709 (Kandel et al., 2005). Soler et al. (2007) reported the involvement of P450s in fatty acid metabolism in protective biopolymers, such as cutin and suberin.

Knockout of *AtCYP86A1* showed that the C16, C18 and C18:1 suberin monomers in the root were reduced, and the total aliphatic suberin content decreased by 60 %. *CYP86A1* had been localized in the endoplasmic reticulum of root endodermal cells (Höfer et al., 2008).

In accordance to Höfer et al. (2008), silencing of the *StCYP86A33* gene in *Solanum tuberosum* showed a 60 % reduction of the aliphatic suberin load in the periderm, including C18:1 ω -hydroxyacid (reduction of about 70 %) and C18:1 α,ω -diacid (about 90 %) monomers in comparison with wild-type, and increased permeability of the periderm, especially in old tubers (Serra et al., 2009b).

Later, an aromatic component is added to the precursors of suberin. The aromatic domain of suberin in Arabidopsis, potato and many other plants are composed of hydroxycinnamates, such as ferulate, *p*-coumarate, and/or sinapate (Gou et al., 2009; Franke et al., 2005; Bernards et al., 1995). Graça and Pereira (2000) suggest ferulate esters as precursors of suberin.

Gou et al. (2009) and Serra et al. (2010) have described the fatty ω -hydroxyacid/fatty alcohol hydroxycinnamoyl transferase (FHT) in Arabidopsis and potato tubers, respectively. These enzymes were classified as acyltransferases of the BAHD family and are described to be responsible for catalyzing the formation of aromatic esters in lipidic polymers (Wang et al., 2017), using hydroxycinnamoyl-CoA esters as acyl donors (Serra et al., 2010).

Serra et al. (2010) showed that potato tubers deficient in *FHT* have an alteration in the composition of the periderm, reduction of ferulate in suberin and waxes, besides increased water loss, rough scabbed skin, and impaired skin maturation in tubers. In the same work, they suggest that *FHT*, which accumulates in the phellogen cell layer (Boher et al., 2013), is a strong candidate for esterifying ferulic acid to suberin monomers. Similarly, *At5g41040* (orthologue of *StFHT* in Arabidopsis) T-DNA mutations in the gene encoding FHT showed low content of ferulate in suberin and increased water permeability in the root and seed coat (Gou et al., 2009; Molina et al., 2009). Before suberin deposition, *StFHT* is already active in the phellogen cells in potato (Boher et al., 2013) and Arabidopsis (Naseer et al., 2012). Boher et al. (2013) also suggest that low levels of FHT may rapidly offer new ferulate esters if eventually the phellogen receives some stimuli for

phellem differentiation. The loss of phenolic suberin by knocking down or knocking out *At5g41040* alters the permeability and sensitivity of seeds and roots to salt stress, highlighting that the suberin aromatics are important in the function of the polymer (Gou et al., 2009), because the aromatic units of suberin are covalently linked with the aliphatic domain through ester bonds (Gou et al., 2009; Pollard et al., 2008).

According to the model from Vishwanath et al. (2015), activated fatty acids are also reduced by FARs to primary alcohols. Domergue et al. (2010) had described FAR1, FAR4 and FAR5 to be involved in the primary alcohol formation in Arabidopsis. Editing each of these genes leads to a chain-length-specific reduction of primary alcohols (Domergue et al., 2010) in roots and seeds from Arabidopsis. In addition, the permeability was higher in seed coat in the triple mutant *atfar1atfar3atfar5* (Vishwanath et al., 2013a).

Yang et al. (2010) described that the ω -hydroxy fatty acids and α,ω -dicarboxylic acids are linked or esterified with glycerol and/or ferulic or coumaric acid. This esterification of ω -hydroxy fatty acids and α,ω -dicarboxylic acids with glycerol-3-phosphate to sn-2-monoacylglycerols is catalyzed by acyl-CoA-dependent glycerol-3-phosphate acyltransferases (GPATs).

Current hypotheses regarding the transport of suberin monomers to the cell wall include transport through secretory pathways by lipophilic bodies (Vishwanath et al., 2015) or, according to the models from Vishwanath et al. (2015) and Franke and Schreiber (2007), transport via ABC transporters (Landgraf et al., 2014, Bernards et al., 1999), where they are polymerized via GDSL lipases, to form a suberin macromolecule (Ursache et al., 2021).

ATP binding cassette (ABC) transporters are capable of transporting different substrates across biological membranes (Shanmugarajah et al., 2019). For example, 130 genes in Arabidopsis are divided into eight ABC subfamilies (Sanchez-Fernandez et al., 2001; Higgins, 2001). The largest one is the ABCG subfamily, which contains 28 half-size (white-brown complex, WBC) and 15 full-size (pleiotropic drug resistance, PDR) transporters. The ABCG subfamily is characterized by their reverse domain organization, in which the nucleotide-binding domain (NBD) is fused with the transmembrane domain (TMD) at the N-terminus (Fig. 4). In addition, the WBC protein is active only after dimerization (Verrier et al., 2008).

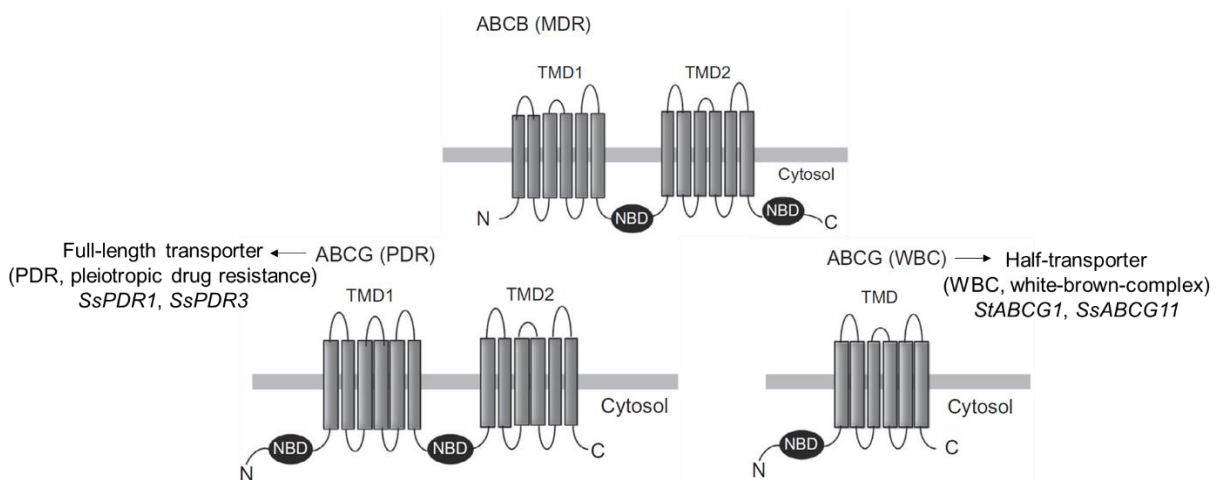


Figure 4: Domain structures of ABC transporters. ABCG transporters have the reverse orientation of the nucleotide-binding domain (NBD) and transmembrane domain (TMD). Pleiotropic drug resistance (PDR) are full-length transporters; White-brown complex (WBC) are half-transporters. Figure adapted from Shoji et al. (2014).

Based on the potato genome sequence (Diambra, 2011), from the 250 ABC transporters found about 130 belong to the subfamily G (Andolfo et al., 2015). From these, 25 have their place in the PDR group, and 112 belong to the WBC.

1.5.1. The ABC transporter StABCG1

Landgraf et al. (2014) had identified the *StABCG1* as the suberin precursor transporter from *S. tuberosum*, sharing high sequence identity with the suberin transporters from *Arabidopsis*, *AtABCG1* and *AtABCG16*.

StABCG1 contains two exons (744 and 1509 bp) and one intron (97 bp). The gene encodes an ABC (ATP-binding cassette) half-transporter (WBC) of subfamily G of 750 amino acids with a P-loop-containing ATP hydrolase region on the first exon and six transmembrane domains on the second exon (Landgraf et al., 2014).

StABCG1 was one of 800 expressed genes that were transcriptionally induced after treatment with Pep13. In addition to Pep13, *StABCG1* is also induced in response wounding and infection with *P. infestans* (Landgraf, 2016). Landgraf et al. (2014) had identified that the expression of *StABCG1* occurs mainly in the tuber periderm and in the roots, more exactly the protein is localized at the plasma membrane.

Downregulation of the *StABCG1* shows a changed morphology of roots and tuber periderm with partially collapsed and disorganized cell layers (Fig. 5). In addition, the tubers of the *StABCG1*-RNAi plants show a substantial reduction in their weight after storage compared to tubers of control plants (WT and EV) (Landgraf, 2016).

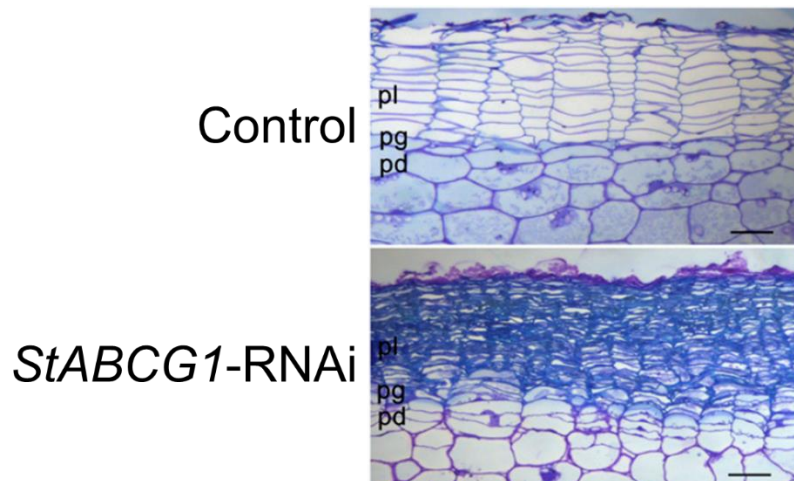


Figure 5: Microscopy of cross sections of tuber periderm of wild-type (Control) and *StABCG1*-RNAi. pl, phellem; pg, phellogen; pd, phelloderm. Bars = 80 μ m. Figure adapted from Landgraf et al. (2014).

Landgraf (2016) showed *StABCG1*-RNAi plants lack suberin after Pep13 infiltration or *P. infestans* infection in leaves compared to the control plants. The author also showed that these transformed plants show larger necrosis after Pep13 infiltration in comparison to the controls (WT and EV).

Metabolomic analyses revealed that the suppression of *StABCG1* expression induces a reduction of aliphatic components in suberin and accumulation of suberin precursors in the soluble semipolar extracts of the tuber periderms, such as ω -feruloyloxy fatty acids and ω -feruloyloxy fatty acid glycerol esters (Landgraf, 2016). Landgraf (2016) and Landgraf et al. (2014) suggest that a lack of aliphatic suberin, as well as ferulic acid, in the tuber periderm leads to a defective water barrier, highlighting the importance of *StABCG1* in the suberin deposition.

1.5.2. Regulation of the suberin pathway and transcription factors

The regulation of the suberin pathway started to be studied in the last years, in this time several regulators have been associated with suberin biosynthesis. For example, *AtMYB41* (Kosma et al., 2014) or *AtANAC046* (Mahmood et al., 2019) under control of the 35S promoter can activate the formation of aliphatic suberin by increasing the transcript levels of suberin-related genes. The knock-out of *AtMYB107* or *AtMYB9* in *Arabidopsis* had resulted in seeds with a significant reduction in suberin monomers and altered levels of other seed coat-associated metabolites (Lashbrooke et al., 2016). In addition, Shukla et al. (2021) had recently reported that in *Arabidopsis* the transcription factors *AtMYB41*, *AtMYB53*, *AtMYB92* and *AtMYB93*, which are all constitutively expressed in the endodermis, are induced in response to ABA, and the quadruple mutant has a dramatic reduction in the endodermal suberin formation and decrease of suberin monomers in roots. Notably, after ABA treatment, these mutants were not able to produce suberin. Cohen et al. (2020) had described a new promising transcription factor called *AtMYB39*. In this study, besides the higher suberin deposition on *Arabidopsis* roots, and the overexpression of the suberin-related genes, such as *AtASFT*, *AtGPAT5* and *AtCYP86B1*, by overexpressing *AtMYB39*, its transient expression in leaves of *Nicotiana benthamiana* led to a deposition of suberin-like lamellae. Thus, Cohen et al. (2020) showed that a transcription factor can induce suberin formation on leaves.

Genes encoding Transcription factors (TFs), like the MYB genes, serve as key regulators for biological processes. They have a great role in modifying complex traits in organisms, such as responses to biotic and abiotic stresses, development, differentiation, and defense. Apart from *Arabidopsis*, a number of MYBs had been demonstrated to regulate the suberin biosynthesis in other species. The *QsMYB1* from cork oak (*Quercus suber*) has been shown to control the expression of a number of suberin biosynthesis genes, including different members of the ABCG gene family, which were described to be involved in the transport of suberin monomers (Capote et al., 2018). Considerable suberin deposition was found in leaves of *N. benthamiana* after transient expression of *MdMYB93* from apple (*Malus domestica*), and expression of *MdMYB93* also leads to upregulation of the suberin-related genes (*KCS*, *CYP86*, *GPAT* and *LACS*) (Legay et al., 2016). Recently,

Wahrenburg et al. (2021) had reported that transient expression of *StMYB74* or *StMYB102* of *S. tuberosum* in *N. benthamiana* leaves resulted in a higher amount of suberin, with subcellular deposition identical to that of naturally occurring suberin.

1.6. Aim of this study

The overall goal of this study was to elucidate the role of the biopolymer suberin in defense responses of potato. Several publications so far proposed a correlation between suberin production and plant defense, however, most studies contain correlative data, and very few showed actual functional data. A number of studies showing suberin-deficient plants was reported, but very few investigated their responses against pathogens and wounding. Therefore, a concise description on the defense responses on plants either containing or not suberin is of significant interest.

To assess the importance of suberin, it was necessary to generate plants lacking suberin, as well as plants with enhanced suberin formation. One way to achieve this is to generate both loss- and gain-of-function mutants, by generating CRISPR/Cas9-edited potato plants with decreased suberin formation (loss-of-function) and plants with enhanced suberin formation (gain-of-function).

2. MATERIAL AND METHODS

2.1. *Solanum tuberosum*

Potato plants (*Solanum tuberosum* cv. *Desirée*) were propagated *in vitro* and in soil as described previously (Landgraf et al., 2014). For *in vitro* propagation, stem cuttings were cultured in 2MS medium (Table 1), and grown in a phytochamber under long day conditions (16 h of light ($140 \mu\text{mol}\cdot\text{m}^{-2}\cdot\text{s}^{-1}$) at 22 °C). Potato plants were transferred to steam-sterilized soil and grown for four weeks in a phytochamber with 16 h light ($\approx 140 \mu\text{mol}\cdot\text{m}^{-2}\cdot\text{s}^{-1}$) at 20 °C and 60 % relative humidity. Four-week-old plants were transferred to 10 L pots, filled with soil and grown for approximately 2 months in the greenhouse for tuber production. Tubers were harvested from 12-week-old plants and stored at room temperature before analysis.

2.2. *Nicotiana benthamiana*

Three-week-old tobacco plants (*Nicotiana benthamiana*) were used for transient expression. *N. benthamiana* plants were grown in a greenhouse under long day conditions (16 h of light at 20-22 °C).

2.3. *Phytophthora infestans*, plant inoculation assays and biomass

A GFP-expressing strain of *Phytophthora infestans* (CRA208m2) (Si-Ammour et al., 2003) was cultivated and propagated in plastic pots (8x9x10 cm – HxWxL) on oat bean medium (Table 1) at 18 °C in the dark. Zoospores were prepared from cultures grown for 12 days. Plates were flooded with 10 mL of sterile water and incubated at 4 °C to release zoospores. The resulting suspension was filtrated with a nylon net filter (20 μm) in a falcon tube, zoospores were counted using a Luna Automated Cell counter (Logos Biosystems, Annandale, USA) and adjusted to 1×10^5 zoospores/mL. For leaf infection assays, droplets containing 10 μL were inoculated onto the abaxial side of potato leaves of 3-week-old

plants if not stated otherwise. Inoculated leaves were covered with plastic bags for 24 hours to maintain moisture and induce germination.

For *P. infestans* biomass, six inoculated sites on potato leaves (\varnothing 0.6 cm) and also 60 μ L of zoospore suspension, used for inoculation, were collected in a different 2 mL eppendorf tube and immediately frozen in liquid nitrogen. Following Eschen-Lippold et al. (2007), after addition of an external standard plasmid (NOX), DNA was extracted using the DNeasy PlantMini Kit (QIAGEN, Hilden, Germany). The primers PIO8-3-3F and PIO8-3-3R (Supplementary table 1) as well as the Universal ProbeLibrary #73 (04688961001, ROCHE, Basel, Switzerland) were used for amplification and detection of *P. infestans* DNA. A fragment from *P. infestans* genomic DNA was amplified using the primers O8-3 and O8-4 (Supplementary table 1; Judelson and Tooley, 2000) was amplified and cloned into pCR2.1, as described by Eschen-Lippold et al. (2007), and used as standard curves. PCR was carried out using the Taqman[®] Universal PCR Master Mix (Applied Biosystems, Waltham, USA). The amplification conditions were initial denaturation at 95 °C for 10 minutes, followed by 40 cycles at 95 °C for 15 seconds and 60 °C for 1 minute. Relative amounts of *P. infestans* DNA in the samples were calculated using the Bio-Rad CFX Maestro (Bio-Rad, Hercules, USA) or ABI Prism 7000 Sequence Detection-Software, including the external standard and the data from the standard curve. The data was normalized by the amount of standard plasmid contained in the samples. The amplification and detection of the standard plasmid was performed similarly to the *P. infestans*, using the primers NOXF and NOXR (Supplementary table 1) and the Universal ProbeLibrary #4 (04685016001. ROCHE, Basel, Switzerland).

For tuber inoculation, a disinfection with 1 % sodium hypochlorite for 20 min was performed, and then the tubers were washed 2 times in sterile water and let dry for 10 minutes at room temperature. Both ends of each tuber were cut with a sterile scalpel and the inner part was collected with a cork borer (\varnothing 1.8 cm). The cylinder collected was then cut with a sterile scalpel into 0.5 cm disks and stored in 12-wells petri dishes. Before laying the tuber disks in the petri dish, each well was prepared with a filter paper disk with 500 μ L sterile water to maintain high humidity. Droplets containing 20 μ L of *P. infestans* suspension (1×10^5 zoospores/mL) were inoculated onto each tuber disk 0, 3, 7, and 14 days after wounding. Fluorescence of *P. infestans* was measured in

NightSHADE LB985 (Berthold, Bad Wildbad, Germany) (see section 2.12.6). This analysis was performed in two replicates. For each replicate at least 4 tuber disks from each line (WT, EV and five different *StABCG1*-CrisprCas lines) were used and 2 tuber disks for each line were used as control (no inoculation).

2.4. *Escherichia coli*, vector cloning and selection of transformants

Escherichia coli strain DH5 α was served as recipient strain to carry the plasmids used for the assembly of the constructs used in this work. Lysogeny Broth (LB) medium containing 100 mg/L of specific antibiotics was used in solid (LA) and liquid form (LB) (Table 1). LA plates containing specific antibiotics were used to propagate colonies of transformed competent cells. LB with specific antibiotics was used for the propagation of overnight starter cultures. Bacteria were cultivated in a horizontal shaker at 200 rpm (for liquid cultures) at 36 °C for 16 hr.

All transformations of *E. coli* used in this work were based on the recommendations for GoldenGate cloning (Marillonnet and Grütznér, 2020). Fifteen microliters of the ligation mixture were pipetted into 50 μ L of competent cells and incubated on ice for 15 min, followed by a heat shock at 42 °C for 60 s and immediately incubated on ice for 2 minutes, followed by addition of 250 μ L of SOC medium (Table 1). The culture was incubated in a shaker at 180 rpm and 37 °C for one hour. Fifty microliters of the culture were plated on LA plates (Table 1) containing a selection antibiotic and incubated at 37 °C overnight. Single colonies were isolated in a new Petri dish containing LA medium with an appropriate antibiotic.

To identify positive *E. coli* clones, plasmid extraction from single colonies was performed (Plasmid Midi Kit, QIAGEN, Hilden, Germany), 0.5-1 μ g of DNA was cleaved using 1 U of restriction enzyme in a 10 μ L reaction overnight. The fragment sizes were then separated in 1 % (w/v TAE) agarose gel and electrophoresis. The restriction enzymes used are listed in supplementary table 2. The selected plasmids were transferred to *A. tumefaciens* (see section 2.5), which were selected by colony PCR (see section 2.7). The respective clone was then used for stable plant transformation (see section 2.10).

2.5. *Agrobacterium tumefaciens* transformation

The production and transformation of competent cells was carried out according to Höfgen and Willmitzer (1988). *Agrobacterium tumefaciens* competent cells (strains AGL0, AGL1 (Lazo et al., 1991) or GV3101 (Holsters, et al., 1980); 200 µL aliquots) were kindly provided by Ulrike Smolka (IPB/Halle, Germany). Stored cells were thawed on ice before transformation. Competent agrobacteria were mixed with 5 µg of the target plasmid. The cultures were incubated on ice for 5 minutes, in liquid nitrogen for 5 minutes, and at 37 °C for 5 minutes, successively. One milliliter of YEB medium (Table 1) was added and the mixture was incubated at 180 rpm, 28 °C for 1-3 hours. One hundred microliters of the culture was plated onto Petri dishes containing YEB-medium mixed with the appropriate antibiotics and incubated at 28 °C for 2 days. Single colonies were isolated in a new Petri dish containing YEB-medium with the appropriate selection antibiotic. Agrobacteria carrying the final constructs were used for stable transformation and transient expression in plants. Liquid YEB medium (Table 1) containing 100 mg/L specific antibiotic was used for cultivation of transformed cells. The bacteria were cultivated in a horizontal shaker at 200 rpm at 28 °C for 2 days.

2.6. Media

All media used on this work is described on the Table 1.

Table 1: Media used on this work.

2MS (Murashige and Skoog, 1962)	0.44 % MS-Salt (Duchefa, Haarlem, NL) 58.4 mM Sucrose pH 5.0 0.6 % (w/v) Plant agar
3MS (Murashige and Skoog, 1962)	87.65 mM Sucrose 2.3 mM MES 0.44 % (w/v) MS-Salt (Duchefa, Haarlem, NL) pH 5.8 0.6 % (w/v) Plant agar
75K (Shoot-inducing medium)	0.1 % Vitamin solution (5 % (w/v) nicotinic acid, 5 % (w/v) Pyridoxine-HCl, 10 % (v/v) Thiamine-HCl, 20 % (w/v) Glycine) 0.25 mg/mL Carbenicillin 0.002 mg/mL Zeatin riboside 0.02 µg/mL NAA (C ₁₂ H ₁₀ O ₂) 0.02 µg/mL GA3 (Gibberellic acid) in GMS (see below)
76K (Callus-inducing medium)	0.1 % (v/v) Vitamin solution (5 % (w/v) nicotinic acid, 5 % (w/v) Pyridoxine-HCl, 10 % (v/v) Thiamine-HCl, 20 % (w/v) Glycine) 0.1 mg/mL Carbenicillin 0.1 µg/mL BAP (C ₁₂ H ₁₁ N ₅) 5 µg/mL NAA (C ₁₂ H ₁₀ O ₂) in GMS (see below)
GMS	88.8 mM Glucose 2.3 mM MES 0.44 % (w/v) MS-Salt (Duchefa, Haarlem, NL) pH 5.8 7.5 % (w/v) Plant agar
Induction medium	60.3 mM K ₂ HPO ₄ 33 mM KH ₂ PO ₄ 7.6 mM (NH ₄) ₂ SO ₄ 1.7 mM Na ₃ C ₆ H ₅ O ₇ ·2H ₂ O 1 mM MgSO ₄ 5.55 mM Glucose 5.55 mM Fructose 0.4 % (w/v) Glycerin 10 mM MES pH 5,6 Add before use 50 µg/ml Acetosyringone
Infiltration medium	10 mM MES pH 5,4 10 mM MgCl ₂ Add before use 150 µg/ml Acetosyringone

LA	1 % (w/v) Bacto-tryptone 0.5 % (w/v) Bacto-Yeast Extract 85.6 mM NaCl 1.5 % (w/v) Agar
LB	1 % (w/v) Bacto-tryptone 0.5 % (w/v) Bacto-Yeast Extract 85.6 mM NaCl
Oat Bean Medium	3.4 % (w/v) Bean flour 1.7 % (w/v) Oat flour 24.8 mM Sucrose 49 mM Agarose
SOC	2 % (w/v) Bacto-tryptone 20 mM Glucose 0.5 % (w/v) Yeast extract 10 mM NaCl 2.5 mM KCl 10 mM MgCl ₂ 10 mM MgSO ₄
YEB	0.5 % (w/v) Beef extract 0.1 % (w/v) Yeast extract 0.5 % (w/v) Peptone 1.46 mM Sucrose 2.0 mM MgSO ₄ 1.5 % (w/v) agar

All solutions were autoclaved at 121 °C for 30 min before use, except vitamins, antibiotics, hormones and micronutrients solutions, which were sterile filtrated.

2.7. PCR

All PCRs performed in this work were conducted with 1 U of DreamTaq™-DNA-Polymerase (Fermentas), 0.1 μM of the described primers (Supplementary table 1) approximately 50 ng of genomic DNA in a final volume of 20 μL. The amplification conditions were initial denaturation at 95 °C for 3 minutes, followed by 35 cycles of denaturation at 95 °C for 30 seconds, 30 seconds at the annealing temperature recommended by the manufactureres and extension at 72 °C for 1 min/kb, followed by a final extension at 72 °C for 10 minutes. PCR products were visualized after 1 % (w/v TAE) agarose gel electrophoresis with GelRed (Biotium, Fremont, USA) or Midori Green (NIPPON Genetics EUROPE, Düren, Germany) under UV-light.

For *E. coli* colony PCR, an adaptation of the same method was used. Instead of the DNA, a single colony was used, and RNA-free-water was added. On the other hand, for *A. tumefaciens* colony PCR, a single colony was incubated in 10 µL of 20 mM NaOH at 37 °C for 8 minutes. For a 20 µL PCR reaction, 1 µL of the suspension was used.

2.8. Golden Gate cloning

The Golden Gate Cloning method (Engler and Marillonnet, 2013; Werner et al., 2012; Weber et al., 2011; Engler et al., 2009; Engler et al., 2008) was used for all constructs generated in this work.

The primer sequences created for the amplification of the fragments for the golden gate assembly are listed in supplementary table 1. The assembly reactions were conducted with 20 U of T4-ligase (Promega), 10 U of the specific enzyme (*Bsal* or *BbsI* from BioLabs, Heidelberg, Germany), 20 fmol of each plasmid or DNA fragment in a final volume of 15 µL. The reactions were conducted with 20 cycles of 37 °C for 5 minutes and 16 °C for 5 minutes, followed by denaturation at 50 °C for 5 minutes and 80 °C for 5 minutes. All constructs were then cloned in *E. coli* and verified with at least 3 different restriction enzymes or sent for sequencing at Eurofins (Ebersberg, Germany) (Supplementary table 2).

2.8.1. Construction of vectors *pPVS3:GFP* and *pPVS3:GUS*

The *StPVS3* promoter described by Yamamizo et al. (2016) is a pathogen-inducible promoter and it was chosen to control the activities of the studied genes in this work (*StABCG1*, *StFHT*, *StCYP86A33* and *StKCS6*). However, Yamamizo et al. (2016) did not describe the variety of *S. tuberosum* used in their work. In the present work *S. tuberosum* cv. *Desirée* was used to conduct all experiments. Since *S. tuberosum* is tetraploid and has high heterozygosity, to confirm the functionality of *pPVS3* of *S. tuberosum* cv. *Desirée*, the *StPVS3* promoter (Yamamizo et al., 2016) was fused to the GUS and also GFP reporter genes and tested for *P. infestans* and wounding sites. The

2618 bp promoter *StPVS3* was divided into two parts, named pAGR21 (1402 bp) and pAGR22 (1217 bp), due a *BbsI* site in the sequence. In order to remove the restriction site, a mutation from A to T was performed between the two fragments at position 1401. For the construct pAGR21, the primers 27 and 28 were used and for pAGR22, the primers 29 and 30 (Supplementary table 1). Each fragment was cloned into vector pAGM1311, and subsequently cloned into pICH41295, forming the construct pAGR23.

The full promoter was cloned in vectors carrying a GFP and GUS gene, pAGM38499 and pAGM38501, respectively, leading to the final constructs pAGR33 (*pPVS3:GFP*) and pAGR34 (*pPVS3:GUS*), which were subsequently transferred to *S. tuberosum* via *Agrobacterium tumefaciens*-mediated transformation (ATMT). All plants generated in this study were named as EPXX, where XX is the number of the plasmid and EP referring to the initials of the author. Accordingly, the plants carrying the GFP and GUS cassette were named EP33 and EP34, respectively.

2.8.2. Simultaneous overexpression of the putative suberin biosynthetic genes *StABCG1*, *StFHT*, *StCYP86A33* and *StKCS6*

In order to generate potato plants with enhanced expression of suberin biosynthetic genes, a first construct called pAGR45 was generated, harboring the four suberin-associated genes *StKCS6* (1738 bp), *StCYP86A33* (1925 bp), *StFHT* (1735 bp – allele A2; 1607 bp – allele A3), and *StABCG1* (2253 bp). Each gene was assembled under control of a minimal promoter containing the TAL effector (pICH71037) and different terminators, *StKCS6* with 35S (pICH41414), *StCYP86A33* with Nos (pICH41421), *StFHT* with Ocs (pICH41432) and *StABCG1* with Mas (pICH77901). These independent constructs, with promoter, gene, and terminator were named pAGR38, pAGR39, pAGR40 (A2 and A3) and pAGR41, respectively, and they were mounted into positions 2 (pICH47742), 3 (pICH47751), 4 (pICH47761), and 5 (pICH47772) of the binary vector pAGM37443, respectively. Position 1 was occupied by the Kanamycin resistance construct pICH67131, position 6 (pICH47781) harbored the pAGR42 construct, containing the *StPVS3* promoter (pAGR23 – see section 2.8.1) joined to the TAL effector (pICH73103) and G7 terminator (pICH72400), and position 7 (pICH47791) contained

linker EL6 (pICH41822), forming the final constructs pAGR45A2 and pAGR45A3 (for the different alleles of *StFHT*) (Fig. 6). An empty vector of this construct was called pAGR44 and contained the linker EL5 (pICH41800) at position 6 instead of the TAL effector construct, and so not promoting the expression of the built-in suberin-related genes. A variation of the empty vector pAGR44 was generated and named pAGR51, by replacing each TAL effector binding site (pICH71037) for the promoter *StPVS3* (pAGR23) in the independent constructs pAGR38, pAGR39, pAGR40 (A2 and A3) and pAGR41, which were then named pAGR47, pAGR48, pAGR49 (A2 and A3) and pAGR50, respectively, in order to promote independent and induced expression of each gene in the final construct. A final control vector pAGR46 contained only the Kanamycin resistance construct (pICH67131) in position 1, the TAL effector construct (pAGR42) in position 2 and linker EL2 (pICH41744) in position 3, in order to observe only the effect of the TAL effector expression in the plants. The constructs pAGR44, pAGR45 (A2 and A3), pAGR46 and pAGR51 were used to obtain the transformed plants EP44, EP45 (A2 and A3), EP46, and EP51, respectively.

For the assembly, the genes *StFHT*, *StCYP86A33* and *StKCS6* were individually obtained from the genomic DNA of *S. tuberosum*, and *StABCG1* from a cDNA previously generated in our group. Both alleles from *StFHT* (A2 and A3) were fully amplified with the primers 44/45, cloned into pICH41308 and forming the constructs pAGR30A2 and pAGR30A3, respectively, which contain a mutation from G to A at position 1708 and 1580, respectively. Similarly, the 2253 bp *StABCG1* was fully obtained with the primers 46/47 and cloned into pICH41308, forming construct pAGR35. The 1925 bp *StCYP86A33* was amplified in two steps, generating the constructs pAGR24 (1660 bp, primers 31/32) and pAGR25 (267 bp, primers 33/34), and promoting a mutation from A to C at position 1661 to avoid the original *Bsal* site. Each smaller fragment was cloned into the vector pAGM1311, and joined in pICH41295, forming the construct pAGR26. Similarly, the 1738 bp *StKCS6* was split into the constructs pAGR27 (1531 bp, primers 35/36) and pAGR28 (208 bp, 37/38) in order to introduce a mutation from T to A at position 1531 to avoid the *Bsal* site. Each smaller fragment was cloned into the vector pAGM1311, and joined in pICH41295, forming the construct pAGR29. All primers can be found in supplementary table 1.

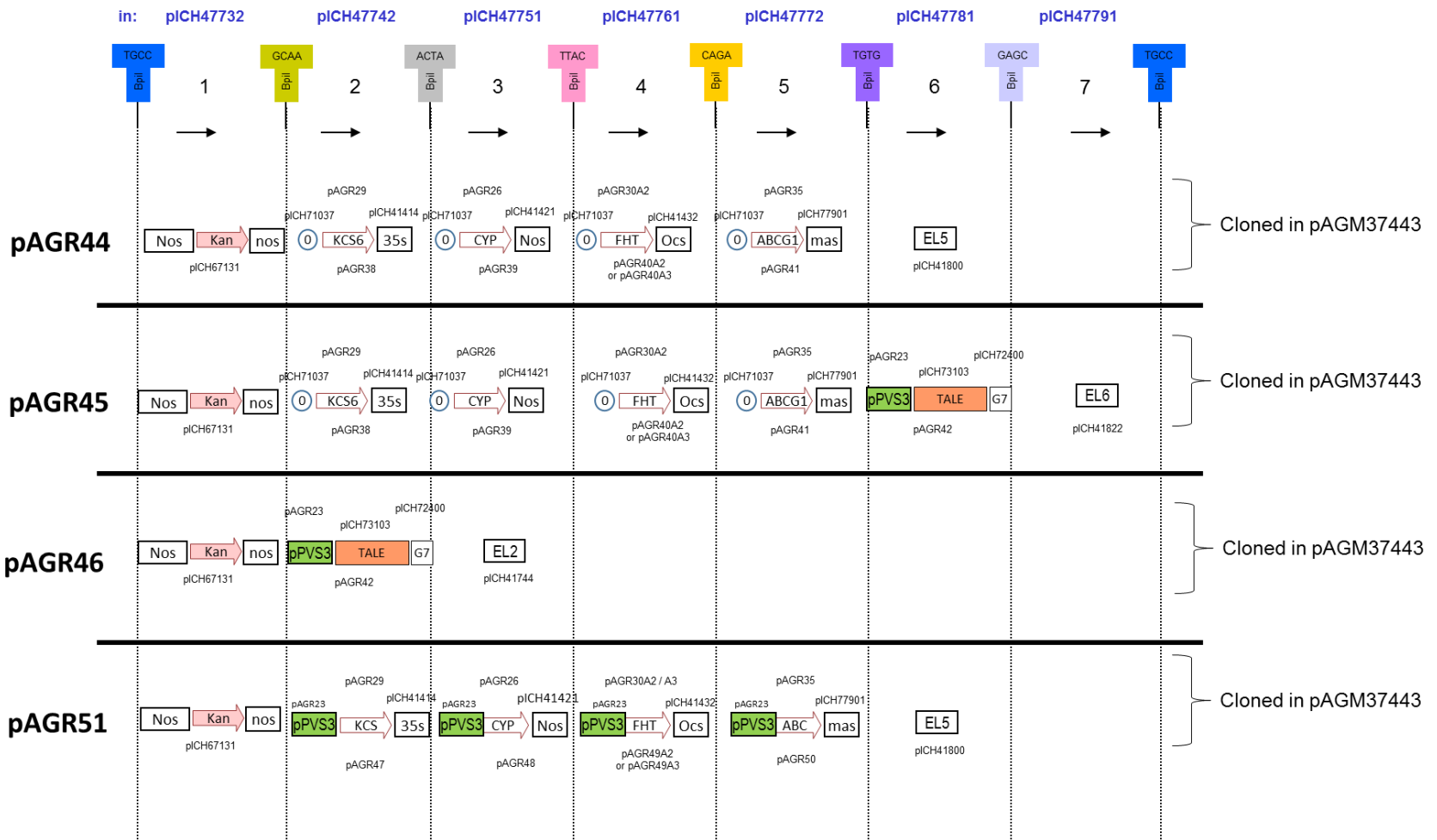


Figure 6: Recombinant plasmids used for transformation of *Solanum tuberosum*, assembled via Golden Gate cloning. Nos, nopaline synthase promoter/terminator; Kan, kanamycin resistance gene; pPVS3, putative vetispiradiene synthase 3 promoter; KCS6, CYP (*CYP86A33*), FHT and ABCG1 genes from *S. tuberosum*; 35S, *CaMV* 35S terminator; Ocs, octopine synthase terminator; mas, mannopine synthase terminator; TALE, Transcription activator-like effector; 0, TAL effector binding site; G7, *Agrobacterium tumefaciens* g7 terminator; EL2, EL5 and EL6, linkers; Golden Gate assembled for the constructs pAGR44, pAGR45, pAGR46 and pAGR51.

2.8.3. Overexpression of the putative suberin biosynthetic genes via *AtMYB39* transcription factor under control of 35S promoter

A second approach to promote enhanced suberin formation in potato plants was via the overexpression of the transcription factor *AtMYB39*. The 1083 bp *AtMYB29* gene (Cohen et al., 2020) was synthesized by ThermoFisher Scientific – GeneArt (Waltham, USA), the plasmid was named 20ABQQQP. Construct pAGR102 was assembled with *AtMYB39* under control of 35S promoter (pICH51266) and the 35S terminator (pICH41414), forming construct pAGR90, which was mounted into position 2 (pICH47742) of the binary vector pAGM37443. Position 1 contained the Kanamycin resistance construct pICH67131 and position 3 (pICH47751) contained the linker EL2 (pICH41744) (Fig. 7).

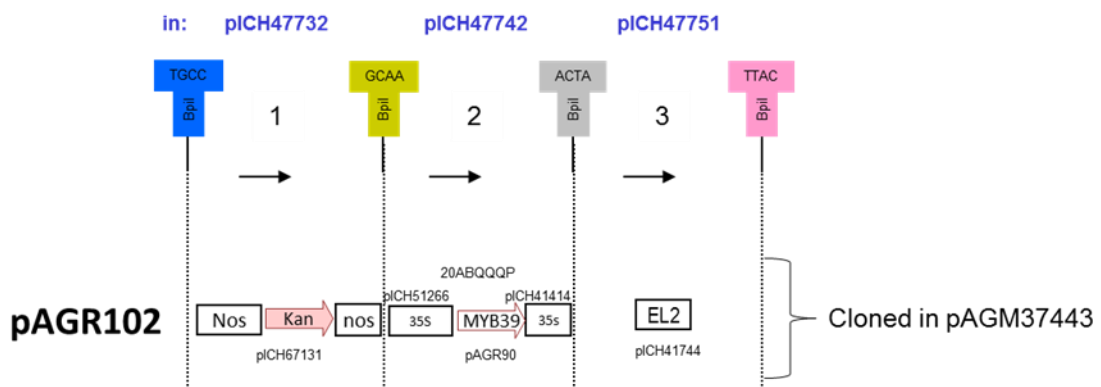


Figure 7: Recombinant plasmids used for transformation of *Solanum tuberosum*, assembled via Golden Gate cloning. Nos, nopaline synthase promoter/terminator; Kan, kanamycin resistance gene; 35S, CaMV 35S promoter/terminator; EL2, Linker; Golden Gate assembled for the construct pAGR102.

2.8.4. Use of CRISPR/Cas9 technology for editing the transporter *StABCG1*, involved in suberin deposition

To analyze loss of function of the *StABCG1* gene, CRISPR/Cas9 technology was applied to obtain *StABCG1* knockout *S. tuberosum* plants. The allele found in *S. tuberosum* cv. Desirée contained 2350 bp, including two exons and one intron. Figure 8 shows a scheme of the structure of the *StABCG1* gene. The encoded protein

contains two ATP binding sites and at the first amino acids of an ABC transporter-type domain, a characteristic sequence from ABC transporters. The exon2 codes for six transmembrane domains. The 20 bp gRNA chosen for the transformation is homologous to the sequence localized 414 bp downstream from the start codon, located in the exon1.

The cassette used for leaf disk transformation in *S. tuberosum* was designed by Ulrike Smolka (IPB/Halle, Germany), it was named pAGM31061 and contained the CRISPR/Cas9 system (ncas9-NLS, kindly provided by Dr. Sylvestre Marillonnet, IPB/Halle, Germany) and a gRNA under control of the *AtU6* promoter. The construct was transferred to plants through *Agrobacterium tumefaciens*-Mediated transformation (Ulrike Smolka and Maximilian Faber, IPB/Halle, Germany). One hundred sixty-five transformed plants were obtained, from these 5 (#132, #142, #143, #149 and #155) were selected by Ulrike Smolka and Maximilian Faber to be further analyzed.

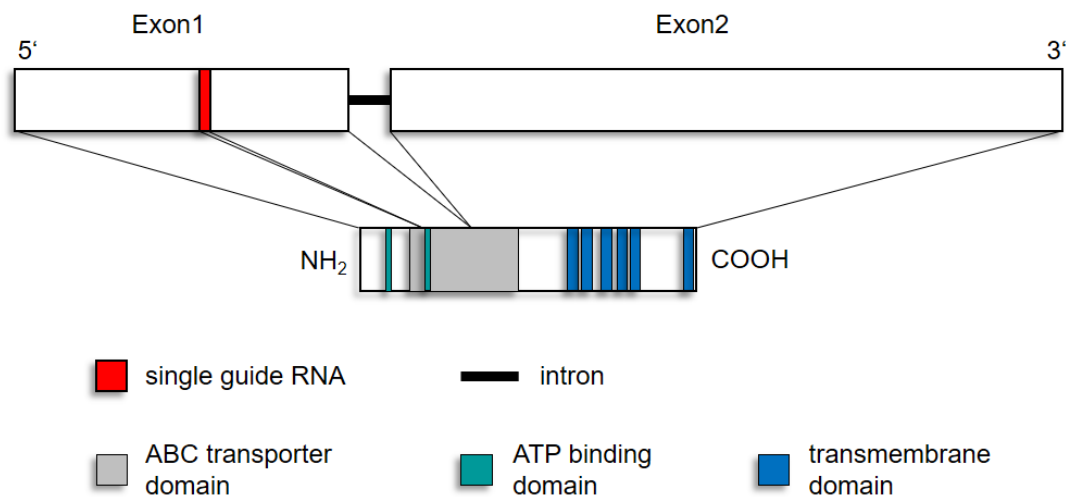


Figure 8: Structure of *StABCG1* gene and respective protein. Gray bars represent the ABC transporter-type domain; Red bar represents the homologous sequence of the designed gRNA; Green bars represent the ATP binding sites; Blue bars represent transmembrane domains. Predictions were based on UniProt (<https://www.uniprot.org> - M1C5V2), MyHits (<https://myhits.sib.swiss>) and Prosite (<https://prosite.expasy.org>).

2.9. Transient expression in *Solanum tuberosum* and *Nicotiana benthamiana*

Agrobacterium tumefaciens-mediated transient expression assays were based on Van den Ackerveken et al. (1996) and Marois et al. (2002). For transient expression in

S. tuberosum, three to four weeks-old WT plants were used. A suspension of *Agrobacterium tumefaciens* GV3101 carrying the target plasmid was grown in 5 mL YEB medium (Table 1), containing the corresponding antibiotics, at 28 °C and 200 rpm for 2 days. The culture was centrifuged at 2,300 g for 10 minutes at room temperature, the supernatant was discarded and the pellet was resuspended in 5 mL of Induction Medium (Table 1) containing acetosyringone (50 µg/mL) and the appropriate antibiotics. The cells were cultivated at 28 °C and 200 rpm for 4-5 hours, followed by a centrifugation step for 10 minutes at 2,300 g, and the supernatant was discarded again. The pellet was resuspended in 5 mL of infiltration medium (Table 1) with acetosyringone (150 µg/mL) for measuring the OD600, which was diluted to 0.2, using infiltration medium with acetosyringone (150 µg/mL). The suspension was stored at room temperature for at least 1 hour before infiltration into potato or tobacco leaves.

2.10. Stable transformation of *Solanum tuberosum*

All stable transformations used in this work were based on Feltkamp et al. (1995). *Agrobacterium tumefaciens* carrying the target plasmid was grown in 20 mL YEB medium (Table 1) with the corresponding antibiotic for 2 days at 160 rpm at 28 °C. The culture was centrifuged at 4000 x g for 10 min at 4 °C, carefully washed in 20 mL of 10 mM MgCl₂, centrifuged at 4000 x g for 10 min at 4 °C, and resuspended in 10 mL of 3MS medium (Table 1).

Sterile leaves of potato plants were cut, scratched with a scalpel, and placed abaxial surface upwards in Petri dishes on top of 10 mL 3MS medium containing 100 µL of the *A. tumefaciens* culture. The Petri dishes were incubated at 22 °C for 2 days in the dark.

To induce callus formation, the leaves were transferred to solid 76K medium (Table 1; callus-inducing medium) and incubated in a phytochamber under long day conditions (16 h of light (140 µmol·m⁻²·s⁻¹) at 22 °C) for 1 week under sterile conditions.

The leaves were then transferred to solid shoot-inducing 75K medium (Table 1) every 2 weeks to induce sprouts growth and incubated in the phytochamber (see section 2.1). Sprouted leaf calli were cut off and inserted in a sterile solid 3MS medium

(Table 1), mixed with the appropriate antibiotic, and incubated in a phytochamber (see section 2.1).

To identify transformed plants, DNA was extracted from each line (DNeasy® Plant Mini Kits, QIAGEN, Hilden, Germany), and used for PCR (see section 2.7), aiming to amplify a part of the transgene.

2.11. Wounded leaves and tubers and microscopy

To check for suberin formation after wounding, leaves of *S. tuberosum* were stained with SudanIII (Smit et al., 2000). Leaves from 3-week-old WT, EV and transformed plants were wounded with a cork borer (Ø 0.6 cm). Samples were collected with a larger cork borer (Ø 1.3 cm) at the indicated time point, destained in four overnight steps at different concentrations of ethanol (50 %, 70 %, 100 % and 50 % - v/v). Tubers of controls (WT and EV) and transformed plants were manually cut into thin layers with a sterile scalpel. All samples were stained with SudanIII at 70 °C for 30 min, and at room temperature for 3 days, then analyzed microscopically with a Nikon AZ100 stereo microscope (Amstelveen, Netherlands) under bright light.

For the *AtMYB39* expressing potato plants, 20 wounded leaf samples of each line were used per experiment. Each sample was divided in four parts, leading a total of 80 samples per line. Photos were taken and randomized using the Bulk Rename Utility software and rated by two different people according to the intensity of red in the wounded layer: no suberin formation; low suberin formation; intermediary suberin formation; high suberin formation.

2.12. Analyses

2.12.1. Genotype confirmation of the *StABCG1*-CrisprCas plants

In order to verify editing of the alleles of the *StABCG1*-CrisprCas plants, the Guide-it™ sgRNA *In Vitro* Transcription Kit (Takara Bio, Kusatsu, Japan) was used to synthesize a gRNA with the primer 67 (Supplementary table 1), according to the manufacturer's

instructions. Genomic DNA was obtained from leaves and tubers from 2 plants of each of the 5 lines (#132, #142, #143, #149 and #155), WT and EV. An individual PCR from each sample was performed with Terra PCR Direct Polymerase (Takara Bio), using the primers 39 and 40 (Supplementary table 1), according to the manufacturer's instructions. An *in vitro* cut with Cas9 and the specific gRNA was performed using the Guide-it™ Genotype Confirmation Kit (Takara Bio), according to the manufacturer's instructions. The fragment sizes were then checked in 1 % (w/v TAE) agarose gel and electrophoresis.

2.12.2. Pep13 infiltration

The PAMP Pep-13 (VWNQPVRGFKVYE) was infiltrated in the abaxial side of potato leaves of 3-week-old plants at the concentration of 100 µM. The same concentration of W2A (VANQPVRGFKVYE), a nearly inactive peptide, was used as a control. The third and fourth leaves were infiltrated 6 times with about 0.5 mL of the solution per infiltration site.

2.12.3. RNAseq

The third leaf of *S. tuberosum* was infiltrated with 100 µM Pep13 as described in section 2.12.2, and 100 µM W2A was used as control. Eight leaf disks (Ø 0.6 cm) were collected with a cork borer 4 hours and 12 hours after the treatment. RNA was extracted from each sample (RNeasy Mini Kit, QIAGEN, Hilden, Germany) and sent to Novogene (Sacramento, USA), which performed the RNAseq analyses. The data was converted to a table by Dr. Benedict Athmer (IPB/Halle, Germany).

Three samples from periderm from freshly harvested tubers from the plant *StABCG1-CrisprCas #142* and the WT were collected for RNA extraction. RNA was extracted from each sample (RNeasy Mini Kit, QIAGEN, Hilden, Germany) and sent to EUROFINs (Ebersberg, Germany), which performed the RNAseq analyses. The data was evaluated by Dr. Sarah Scharfenberg (IPB/Halle, Germany).

All RNA extractions were performed by Ulrike Smolka (IPB/Halle, Germany). For each experiment, 3 biological replicates for each line/treatment were used.

2.12.4. Illumina sequencing

Genomic DNA was obtained from leaves of the 5 lines of *StABCG1*-CrisprCas plants and WT. PCR was performed using primers 132 and 133 (Supplementary table 1). These primers contain a tail, which is homologous to the Novogene (Sacramento, USA) tagged-primers for Illumina sequencing. Later, a nested PCR was performed using the Novogene tagged-primers. The PCR products were purified using the QIAquick PCR Purification Kit (QIAGEN, Hilden, Germany), diluted to the same concentration and mixed in an Eppendorf 2 mL tube. The samples were sent to Novogene (Sacramento, USA) for Illumina sequencing. The results were analyzed in the online tool CRISPResso2 (<https://crispresso.pinelloolab.partners.org>), with help of Dr. Khabat Vahabi (IPB/Halle, Germany).

2.12.5. GUS staining

The activity of the previously described *StPVS3* promoter (Yamamizo et al., 2016) was tested with the *pPVS3*:GUS construct (pAGR34) both by transient expression and stable transformation (EP34 plants) using GUS staining (Blume and Grierson, 1997; Jefferson et al, 1987). Detached leaves were submerged in a 5-bromo-4-chloro-3-indolyl- β -D-glucuronide (1 mM X-Gluc) solution, under vacuum for 1 hour and incubated at 38 °C overnight. Leaves were destained in different concentrations of ethanol as follow: 10 minutes in 70 % ethanol solution (v/v), two times overnight in 100 % ethanol, and 10 minutes in 50 % ethanol solution (v/v) at room temperature.

2.12.6. NightShade (GFP detection)

The activity of the previously described *StPVS3* promoter (Yamamizo et al., 2016) was tested with the *pPVS3*:GFP construct (pAGR33) by transient expression and stable transformation (EP33) and analyzed in NightSHADE LB985 (Berthold, Bad Wildbad, Germany) under GFP filter (475 nm for excitation filter and 520 nm for emission filter). The

same conditions were used to measure *P. infestans* fluorescence inoculated on tuber disks (see section 2.11).

2.12.7. RT-qPCR/Gene expression

Eight treatment sites on potato leaves were collected (\varnothing 0.6 cm) and immediately frozen in liquid nitrogen. Three biological replicates were collected, each containing ~100 mg fresh leaf weight. Uninfected and water treated leaves served as controls for *P. infestans* analyses, and W2A was used as control for Pep13 treatments. RNeasy Plant Mini Kit (QIAGEN, Hilden, Germany) was used for total RNA extraction – according to the manufacturer’s instructions. RNA samples were treated with RNase-free DNase Set (QIAGEN, Hilden, Germany) and the quality was tested with a Nanodrop (ThermoFisher Scientific, Waltham, USA).

The isolated RNA was transcribed into cDNA using Oligo dT with the RevertAid H Minus First Strand cDNA Synthesis Kit (ThermoFisher Scientifics, Waltham, USA). Quantitative PCR was measured on a CFX96™ Real-Time System (Bio-Rad, Hercules, USA). Reactions were performed using the Roche Universal Probe Library, Probe #31 and primers 55/56 for amplification of *StKCS6*; Probe #66 and primers 57/58 for *StCYP86A33*; Probe #133 and primers 59/60 for *StFHT*; Probe #35 and primers 61/62 for *StABCG1*; Probe #162 and primers *EF1alphaF/EF1alphaR* for the endogenous elongation factor *StEF1 α* ; Probe #145 and primers 126/127 for the *AtMYB39*. Relative transcript levels were calculated using the MxPro qPCR software (Stratagene). Reactions were also performed using EVAGreen Dye (Biotium, Fremont, USA) at the same conditions before, primers 136/137 for amplification of *StFAR1*; primers 134/135 for *StFAR3*; primers 138/139 for *StKCS11*; primers 140/141 for *StGPAT4*; primers 142/143 for *StPPO*; primers 144/145 for *StLAC14*. Relative transcript levels were calculated using the Bio-Rad CFX Maestro (Bio-Rad, Hercules, USA). All primers can be found in supplementary table 1.

For Roche Universal Probe Library and EVAGreen reaction, the amplification conditions were initial denaturation at 95 °C for 15 minutes, followed by 40 cycles with denaturation at 95 °C for 15 seconds, 20 seconds at 60 °C (manufacturer’s annealing

temperature) and extension at 72 °C for 20 seconds, followed by a final denaturation at 95 °C for 1 minute, 30 seconds at 55 °C and 30 seconds at 95 °C. The fluorescence was measured at the end of each cycle and the dissociation curve at the end of the reaction.

Expression of *StEF1α* was used as a reference.

2.12.8. Untargeted metabolite profiling

The 3rd and 4th leaves from 3 different plants of WT and five different *StABCG1*-CrisprCas (#132, #142, #143, #149 and #155) lines were wounded with a cork borer (Ø 6 mm). Ten days later, ten wounded areas were isolated per sample using a larger cork borer (Ø 1 cm). Two samples from each plant were pooled mixing fragments from the 3rd and 4th leaves. For control, non-wounded leaves from new plants were collected. Dr. Karin Gorzolka (IPB/Halle, Germany) performed a methanol extraction and the Liquid Chromatography-Mass Spectrometry measurements as described by Gorzolka et al. (2020).

2.12.9. Assessment of tuber weight in *StABCG1*-CrisprCas plants

Freshly harvested tubers from the greenhouse from WT, EV and five different *StABCG1*-CrisprCas (#132, #142, #143, #149 and #155) lines were individually weighed 0, 7, 14, 21 and 35 days after harvesting. This analysis was performed in three replicates. At least 74 tubers from each line were weighed, totaling a number of 216 from the controls (WT and EV) and 462 tubers from the *StABCG1*-CrisprCas lines.

In a separate experiment, tubers freshly harvested from the greenhouse of WT, EV and five different *StABCG1*-CrisprCas (#132, #142, #143, #149 and #155) lines were divided into two different-sized fractions with a sterile scalpel and stored at room temperature. The bigger and smaller fractions were individually weighed up to 10 days after wounding. This analysis was performed in two replicates. Three tubers from each line were used for each replicate.

2.12.10. Resistance of *StABCG1*-CrisprCas tubers to wounds during storage

Freshly harvested tubers from the greenhouse from WT, EV and five different *StABCG1*-CrisprCas (#132, #142, #143, #149 and #155) lines were wounded with a sterile potato peeler, stored in a non-sterile paper bag and analyzed for loss of weight up to 14 days after wounding. This analysis was performed in two replicates. Two tubers from each line were used for each replicate.

In a separated analysis, freshly harvested tubers from the greenhouse from WT and one *StABCG1*-CrisprCas (#142) line tubers were totally peeled with a sterile potato peeler, stored in a non-sterile paper box at room temperature and analyzed for phenotypes up to 7 days. This analysis was performed only once and can be considered preliminary. Two tubers from each line were used.

3. RESULTS

To address the importance of suberin for pathogen responses, leaves and tubers from the cultivated potato were analyzed after wounding and *P. infestans* inoculation. In addition, leaves were also analyzed after Pep13 infiltration. Furthermore, plants with decreased suberin deposition and plants with enhanced suberin formation were generated and analyzed.

3.1. Suberin is formed in *S. tuberosum* leaves under different treatments

In an effort to know if suberin is formed in leaves, three different conditions were compared, and leaves were either infiltrated with Pep13 to induce necrosis (Fig. 9A), wounded with a cork borer (Fig. 9C) and inoculated with *P. infestans* (Fig. 9E). Pep13 infiltration showed earlier necroses formation at 1 day after infiltration while the inoculation with *P. infestans* took 3 days to show the first symptoms. Photos were taken 7 days after each treatment, samples were collected and stained for suberin with SudanIII, showing a red layer in the lesions between the health tissue and the treatment, indicating the presence of suberin in all treatments (Fig. 9B, D and F).

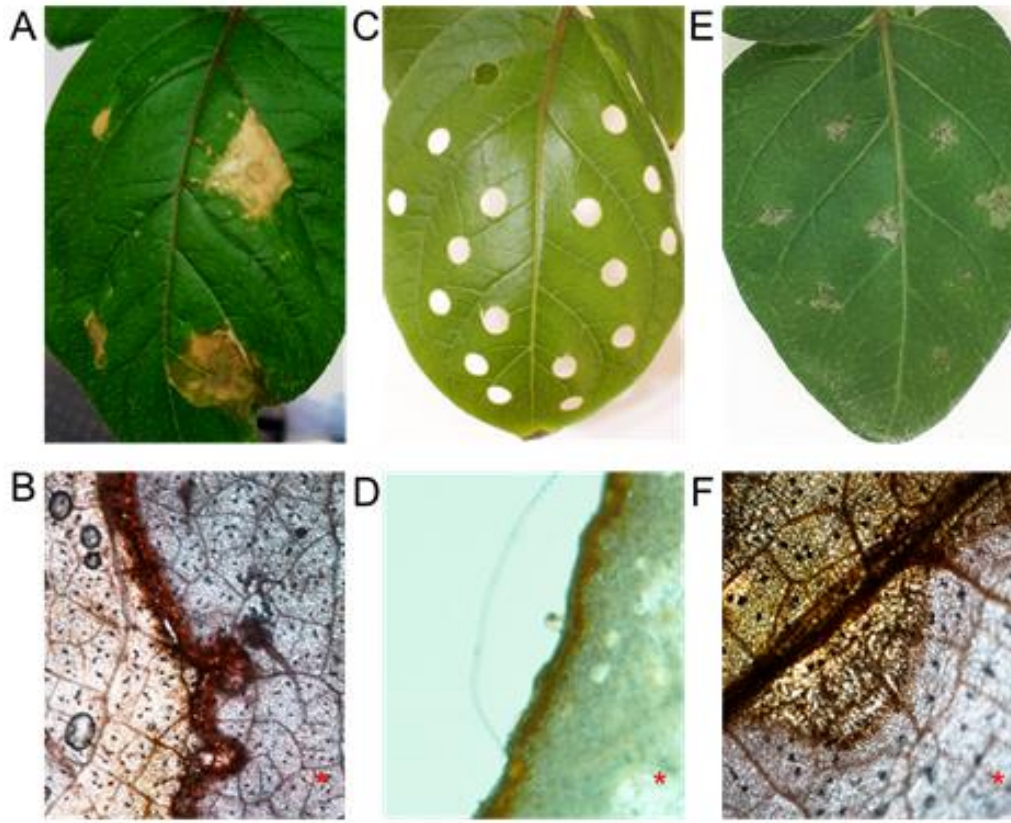


Figure 9: Suberin is formed in potato leaves after Pep13 infiltration, wounding or *P. infestans* inoculation. Leaves of 3-week-old plants grown in a phytochamber from the cultivated potato were used for infiltration of 100 μ M Pep13 (**A/B**), wounding with a 6 mm (\varnothing) cork borer (**C/D**) and inoculation of 10 μ L of a 1×10^5 zoospores/mL suspension (**E/F**). Seven days after each treatment, the treated area was isolated using a 1 cm (\varnothing) cork borer, stained with SudanIII and subjected to bright light microscopy (**B**: Pep13 infiltration; **D**: wounding; **F**: *P. infestans* inoculation). Red asterisks indicate the healthy tissue. Bars = 0.5 mm.

To check the time of suberin production, wounded leaves were analyzed daily for up to 7 days. Microscopy of SudanIII-stained lesions showed first visible suberin at 4 days after wounding, when red coloration was formed around the wounded site, whereas from the 5th day onwards a very strong and defined red layer was found in all samples (Fig. 10).

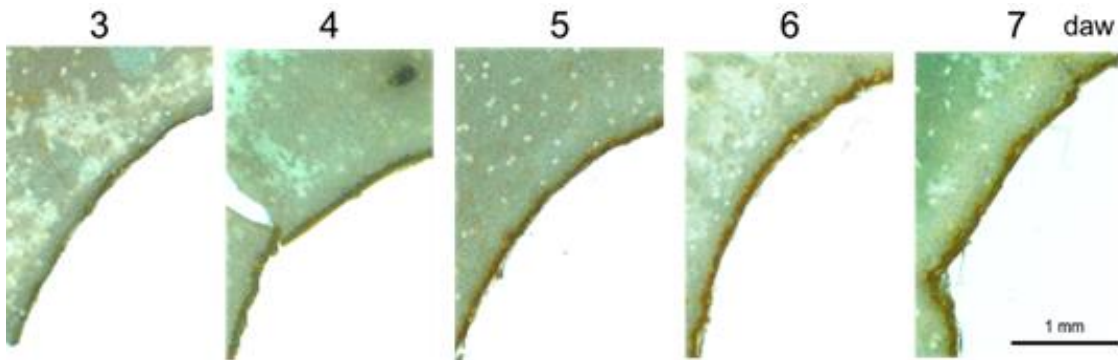


Figure 10: Suberin is completely formed 5 days after wounding in leaves of *S. tuberosum*. Leaves of wild-type potato plants were wounded with a 6 mm (Ø) cork borer. The wounded area was isolated using a 1 cm (Ø) cork borer, stained for suberin with SudanIII and subjected to bright light microscopy up to 7 days after wounding (daw). Bar = 1 mm.

3.2. Suberin biosynthetic genes are induced after Pep13 infiltration in *Solanum tuberosum* leaves (RNAseq data)

To identify genes possibly involved in suberin formation in potato plants, RNA from wild-type *S. tuberosum* leaves infiltrated with either the PAMP Pep13 or the nearly inactive peptide W2A was extracted at 4 and 12 hours after the treatment and submitted to RNA sequencing (RNAseq). Three biological replicates from each treatment were sent for RNAseq. RNAseq revealed at 4 and 12 h, respectively, a total of 641 and 3292 genes at least 3-fold differentially expressed after Pep13 infiltration in comparison to the W2A controls.

Among these genes, 12 hours after treatment showed high read counts of transcript levels from the transporter *StABCG1* (Fig. 11A), which is described to export suberin monomers (Landgraf et al., 2014), also from four genes possibly involved in the suberin pathway, including two fatty acyl-CoA reductases (*StFAR1* and *StFAR3*), the glycerol-3-phosphate acyltransferase 4 (*StGPAT4*) and the 3-ketoacyl-CoA 11 (*StKCS11*) (Fig. 11B), as well as two phenol oxidases (*StLAC14* and *StPPO* – Fig. 11C).

In contrast, the ketoacyl-CoA synthase 6 (*StKCS6*), responsible for the elongation of fatty acids in the suberin pathway in tubers (Serra et al., 2009a), showed a lower number of reads 12 hours after the treatment (Fig. 11A). Unfortunately, the cytochrome P450 *StCYP86A33* and the ω -hydroxyacid/fatty alcohol hydroxycinnamoyl transferase

StFHT, described to be essential for the aliphatic suberin formation and ferulate esters biosynthesis in tuber periderm, respectively, were not detected in the present RNAseq data.

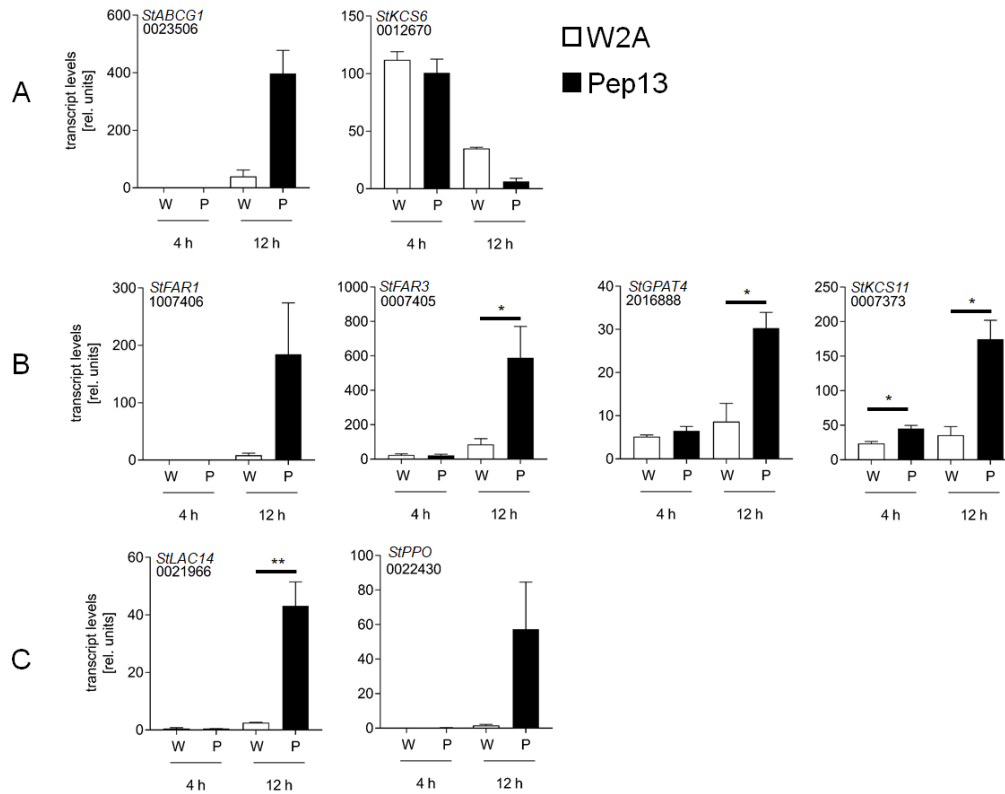


Figure 11: Genes putatively involved in suberin biosynthesis and phenol oxidases are activated by Pep13. RNA extracted from *S. tuberosum* leaves infiltrated with 100 μ M Pep13 (black bar) or 100 μ M of the nearly inactive peptide W2A (white bar) was isolated 4 and 12 hours after treatment and subjected to RNAsequencing. Data are derived from three independent experiments. Error bars represent SEM. Asterisks indicate statistically different values (t-test – Mann-Whitney - *, 0.01<p<0.05; **, 0.001<p<0.1). Numbers in italic indicates the Gene ID, which starts with PGSC0003DMG40. **A)** Genes described to be involved in the suberin pathway: *StABCG1* and *StKCS6*. **B)** Genes induced after Pep13 infiltration: *StFAR1*, *StFAR3*, *StGPAT4* and *StKCS11*. **C)** Phenol oxidases: *StLAC14* and *StPPO*.

3.3. Suberin-related genes are differentially expressed after Pep13 infiltration

To corroborate the transcriptome data, the gene expression levels of the targets *StABCG1*, *StFHT*, *StCYP86A33*, *StKCS6*, *StFAR1*, *StFAR3*, *StLAC14* and *StPPO* was evaluated by RT-qPCR. Three-week-old leaves of wild-type *S. tuberosum* plants were infiltrated with Pep13 and the transcript levels of these targets were evaluated daily up to

7 days and compared with a 12 hours post inoculation time point (0.5 dai), in two independent experiments. The nearly inactive analog W2A was used as a control for the infiltration.

Infiltration of Pep13 generated an accumulation of *StABCG1* transcript levels 1 day after infiltration, 12 hours for *StFHT* and 2 days after infiltration for *StCYP86A33*, maintaining significantly high levels until the 7th day (Fig. 12A, B and C). On the other hand, *StKCS6* had a statistically significant reduced level of transcripts, starting after 12 hours, returning to normal levels after the 2nd day (Fig. 12D). *StFAR1* and *StFAR3* transcript levels accumulated 12 hours after the treatment, increasing significantly after the 1st day, staying high until the 7th day (Fig. 12E and F). Both phenol oxidases showed an accumulation of transcript levels 12 hours after treatment, showing a significantly higher level of transcript up to the 4th and 2nd day, respectively for *StLAC14* and *StPPO* (Fig. 12G and H). These data show that all genes analyzed were differentially expressed at early time points after Pep13 infiltration.

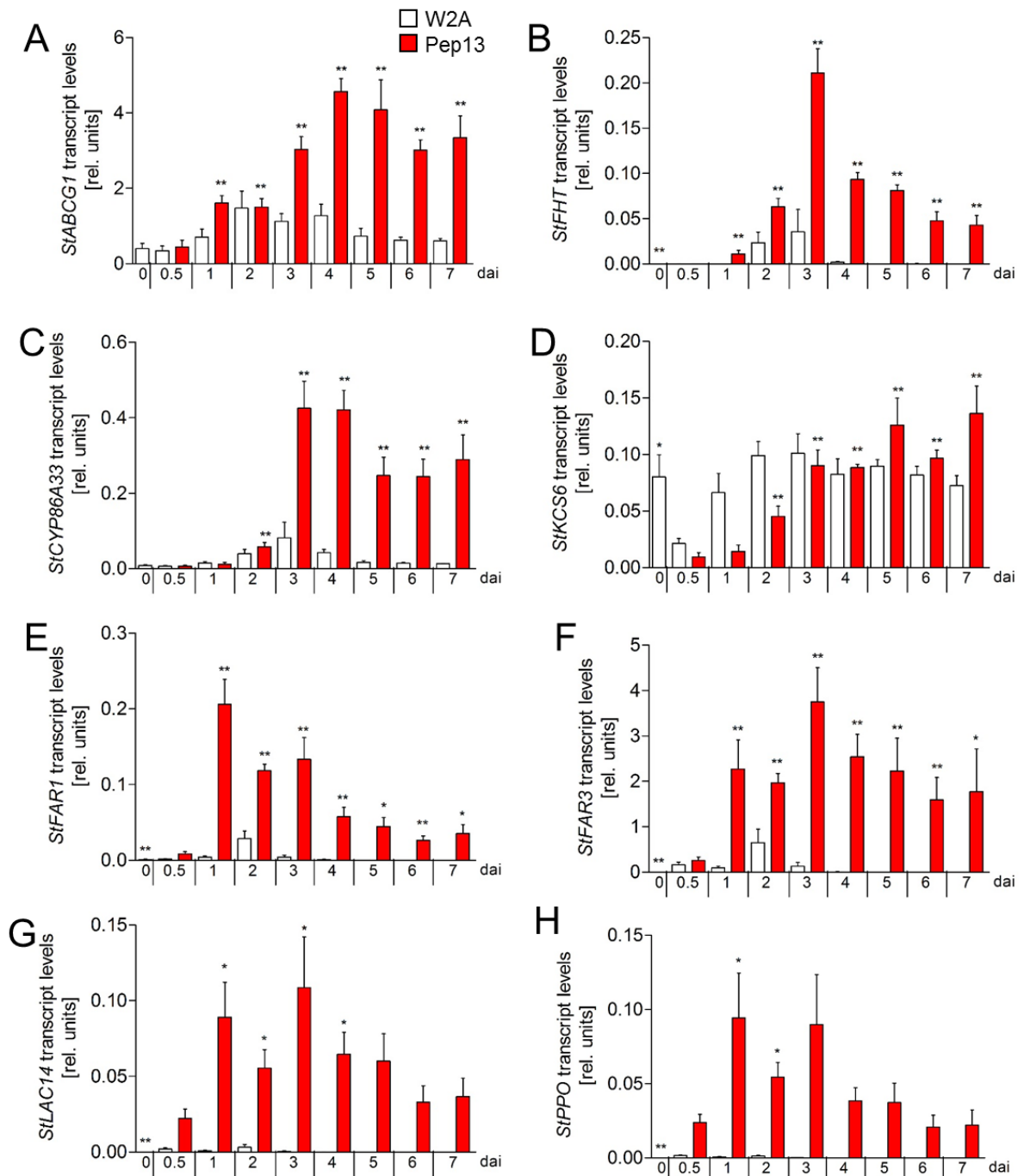


Figure 12: Pep13 infiltration induces expression of genes related to suberin. RNA was extracted from infiltrated leaves of 3-week-old wild-type *S. tuberosum* plants grown in a phytochamber, reverse transcribed and subjected to RT-qPCR. Gene expression of *StABCG1* (A), *StFHT* (B), *StKCS6* (C), *StCYP86A33* (D), *StFAR1* (E), *StFAR3* (F), *StLAC14* (G) and *StPPO* (H) was determined up to 7 days after Pep13 or the nearly inactive analog W2A infiltration (dai). Expression of *StEF1 α* was used as a reference. Data are derived from two independent experiments (n = 6). Error bars represent SEM. Asterisks indicate statistically different values in comparison to the 0.5 dai value (t-test - Mann-Whitney - *, 0.01 < p < 0.05; **, 0.001 < p < 0.1).

3.4. Suberin-related genes are differentially expressed after wounding

The transcript levels of the genes identified in the RNAseq experiment from Pep13-treated leaves were also analyzed by RT-qPCR in wounded *S. tuberosum* leaves. The expression of *StABCG1*, *StFHT*, *StCYP86A33*, *StKCS6*, *StFAR1*, *StFAR3*, *StKCS11*, *StGPAT4*, *StLAC14* and *StPPO* was determined daily for up to 7 days and compared with the 12 hours after wounding time point, unless stated otherwise.

Transcript levels of *StABCG1* and *StFHT* increased in response to wounding 12 hours after the treatment, those of *StCYP86A33* 2 days after wounding (Fig. 13A, B and C). These genes maintained a statistically significant higher level of transcripts up to 7 days after wounding. On the other hand, *StKCS6* showed a reduction in the transcript levels after treatment, returning to normal levels 1 days after wounding (Fig. 13D). *StFAR1* and *StFAR3* had an accumulation of transcript levels 12 hours after treatment, maintaining high levels until the 7th day, while *StKCS11* showed a slight accumulation 3 to 5 days after wounding (Fig. 13E, F and G), and *StGPAT4* did not show any statistically significant difference in expression (Fig. 13H). For that reason, *StKCS11* and *StGPAT4* were not included in further analyses. For both phenol oxidases (*StLAC14* and *StPPO*) 0 days after wounding (no treatment) was used as control. Both showed an accumulation of transcript levels 12 hours after treatment, staying high until the 6th and 7th day, respectively for *StLAC14* and *StPPO* (Fig. 13I and J). Variation in transcript levels of the genes analyzed, except for *StKCS11* and *StGPAT4*, occurs very early after leaves are wounded.

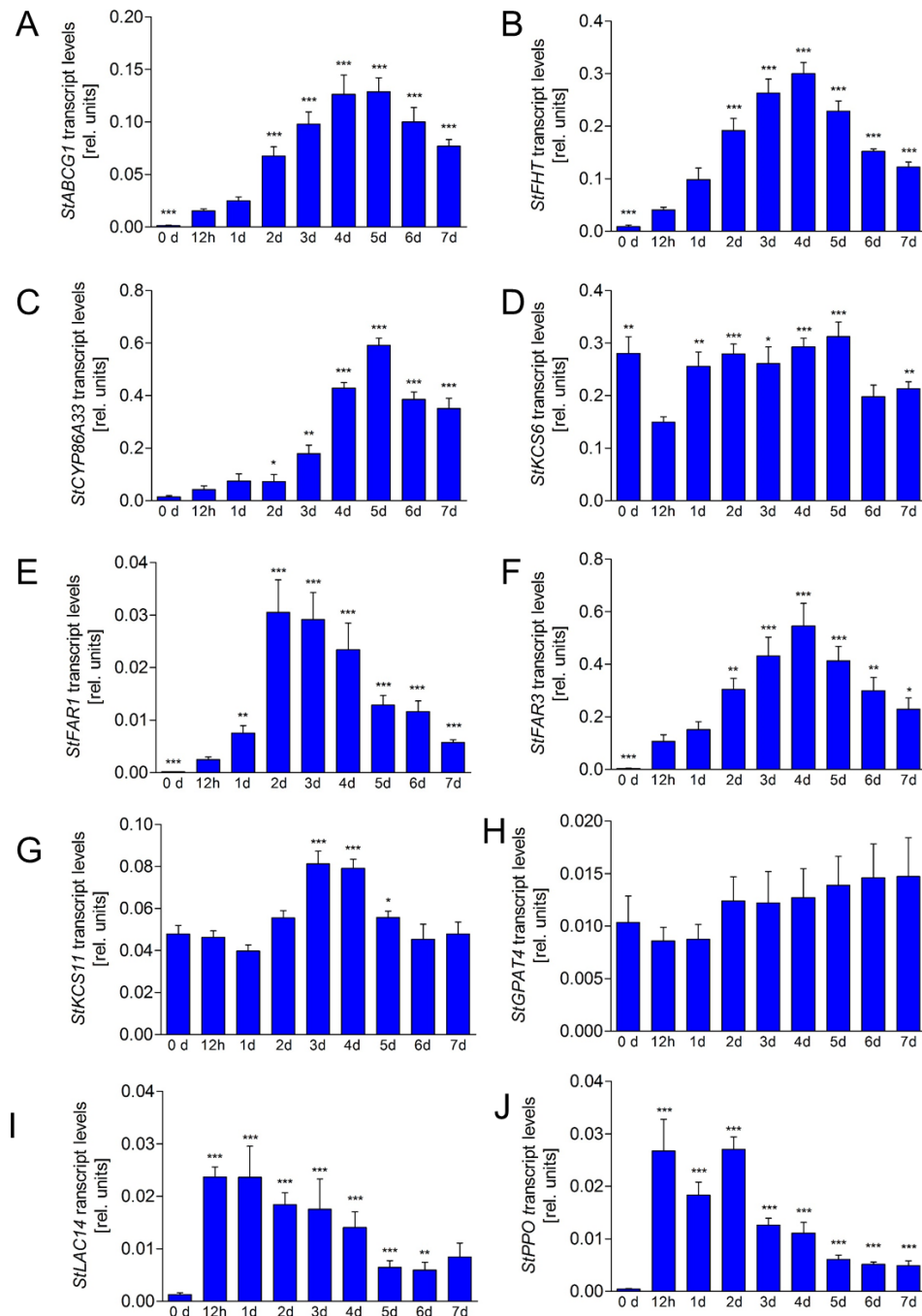


Figure 13: Wounding leaves induces genes related to suberin. RNA was extracted from wounded leaves of 3-week-old wild-type *S. tuberosum* plants grown in a phytochamber, reverse transcribed and subjected to RT-qPCR. Gene expression of *StABCG1* (A), *StFHT* (B), *StKCS6* (C), *StCYP86A33* (D), *StFAR1* (E), *StFAR3* (F), *StKCS11* (G), *StGPAT4* (H), *StLAC14* (I) and *StPPO* (J) was analyzed up to 7 days after wounding (d). Expression of *StEF1 α* was used as a reference. Data are derived from at least two independent experiments (n = 11), the figures are representative for a third experiment. Error bars represent SEM. Asterisks indicate statistically different values in comparison to the 12 hours after wounding (h) values for *StABCG1*, *StFHT*, *StKCS6*, *StCYP86A33*, *StFAR1*, *StFAR3*, *StKCS11* and *StGPAT4* and 0 d (no treatment) values for *StLAC14* and *StPPO* (t-test - Mann-Whitney - *, 0.01 < p < 0.05; **, 0.001 < p < 0.1; ***, p < 0.001).

3.5. Suberin-related genes are differentially expressed after *Phytophthora infestans* inoculation

The expression of the genes related to suberin formation was also evaluated after *P. infestans* infection. Transcript levels were measured for the targets *StKCS6*, *StCYP86A33*, *StFHT*, *StABCG1*, *StFAR1*, *StFAR3*, *StLAC14* and *StPPO* daily for up to 7 days after inoculation. The expression levels of these genes were compared to a mock inoculation at 0 h (no treatment).

P. infestans infection induced a statistically significant accumulation of transcripts 6 days after inoculation for *StABCG1*, after 5 days for *StFHT* and 7 days for *StCYP86A33* (Fig. 14A, B and C). *StFHT* maintained a higher level of transcripts up to 7 days after the treatment. On the other hand, *StKCS6* showed a significantly reduced level of transcripts at the 1st day (Fig. 14D). Similar to the suberin-related genes, *StFAR1* and *StFAR3* had a statistically significant accumulation of transcripts after 6 days, decreasing thereafter (Fig. 14E and F). Both phenol oxidases showed an accumulation of transcripts at the 6th and 5th day, respectively for *StLAC14* and *StPPO*, declining subsequently (Fig. 14G and H). In response to *P. infestans*, all genes studied showed a high expression between 5 and 7 days after inoculation, except *StKCS6*.

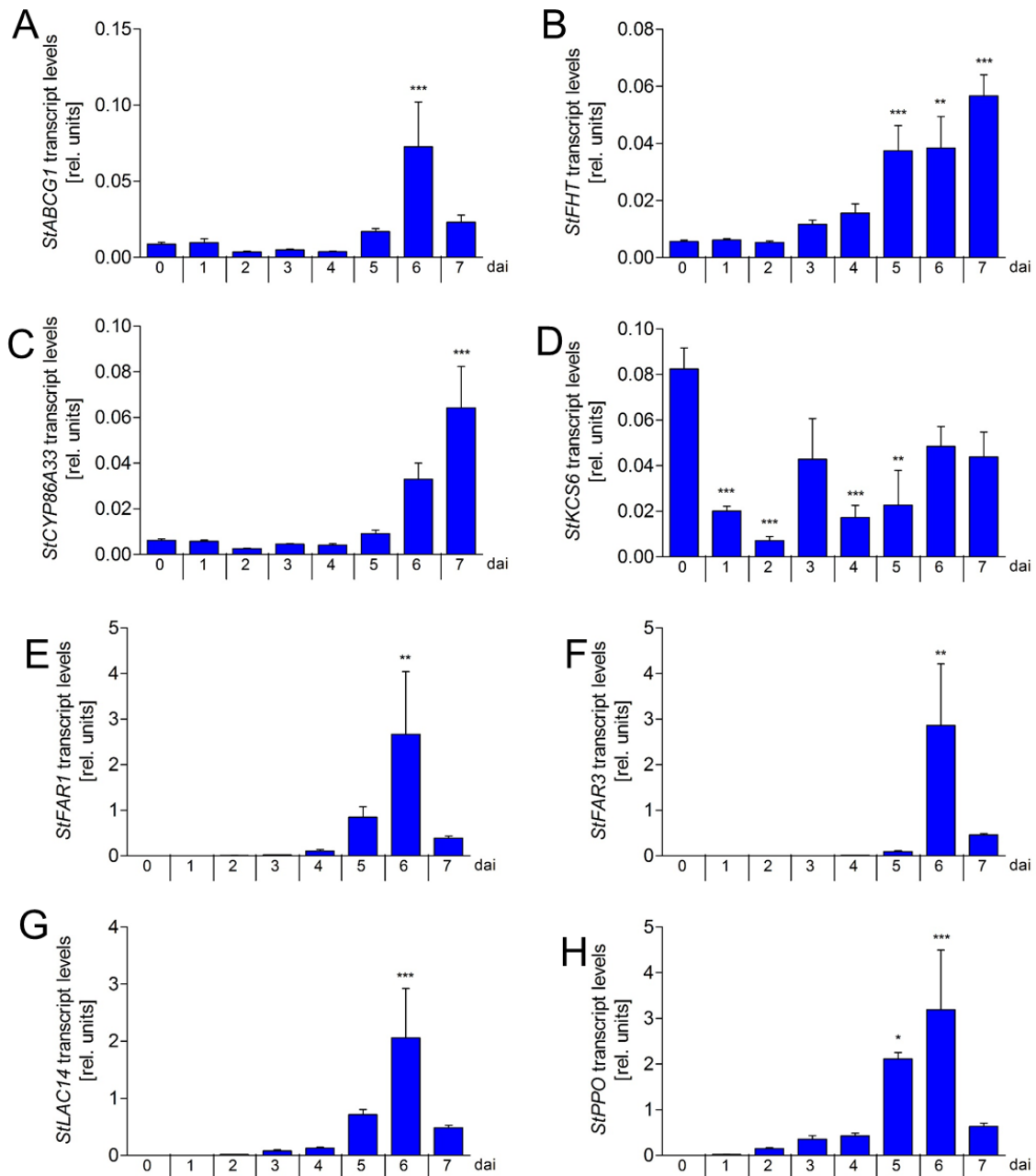


Figure 14: *P. infestans* infection induces genes related to suberin. RNA was extracted from inoculated leaves (1×10^5 zoospores/mL) of 3-week-old wild-type *S. tuberosum* plants grown in a phytochamber, reverse transcribed and subjected to RT-qPCR. Gene expression of *StABCG1* (A), *StFHT* (B), *StKCS6* (C), *StCYP86A33* (D), *StFAR1* (E), *StFAR3* (F), *StLAC14* (G) and *StPPO* (H) was determined up to 7 days after *P. infestans* inoculation (dai). Expression of *StEF1a* was used as a reference. Data are derived from three independent experiments ($n = 6$). Error bars represent SEM. Asterisks indicate statistically different values in comparison to the 0 h (no treatment) value (ANOVA – Dunnett test - *, $0.01 < p < 0.05$; **, $0.001 < p < 0.1$; ***, $p < 0.001$).

3.6. The suberin transporter *StABCG1* was edited with CRISPR/Cas9

To generate loss of function in potato plants, transgenic plants expressing the Cas9 and one sgRNA targeted at *AtABCG1* were generated. In an effort to select the *StABCG1*-CrisprCas plants with edited alleles, a PCR product from the region around the selected gRNA (see section 2.8.4) was submitted to an *in vitro* cleavage with Cas9 and the specific gRNA was performed. The target sequence is located asymmetrically within the amplicon, leading to different sized fragments when cut. Wild-type alleles are recognized by the gRNA/Cas9 complex and cleaved, whereas, if indels are present in the allele at the target site, the complex is unable to cleave the site and the PCR product stays intact.

This approach demonstrated that plants #132, #143 and #149 are chimeric for the *StABCG1* alleles since different tissues of the same plant showed different results (Fig.15). The plant #142 is fully edited for all performed analyses and the plant #155 has at least one WT allele, but also at least one edited allele (Fig.15). As expected, WT and EV have all *StABCG1* alleles as WT. All transformed plants showed leaves, roots and tubers similar to the WT when they were not treated.

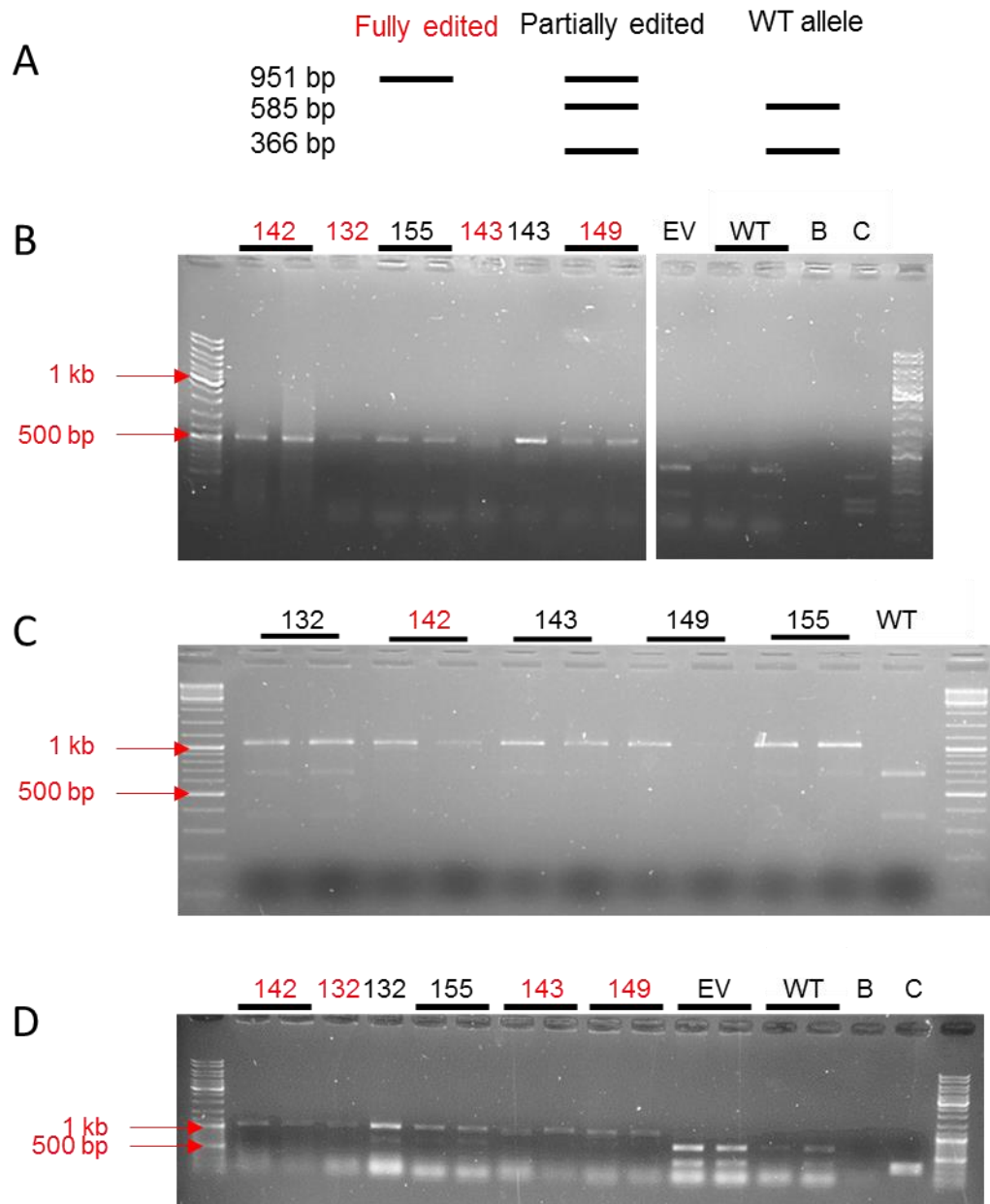


Figure 15: *StABCG1*-CrisprCas plants have chimeric tissue for *StABCG1*. Screening of transformants by CRISPR/Cas9 system with analysis of the target site. The target region was amplified by PCR from genomic DNA extracted from leaves from wild-type (WT), empty vector (EV) and *StABCG1*-CrisprCas plants (#132, #142, #143, #149, #155). The PCR product was purified and cut *in vitro* with the Guide-it™ Genotype Confirmation Kit. (A) Expected fragment sizes after the *in vitro* CRISPR/Cas9 cut. (B) PCR products used for digestion were derived from different tubers of wild-type and *StABCG1*-CrisprCas plants. (C) and (D) PCR products used for digestion were derived from different leaves of wild-type, EV and *StABCG1*-CrisprCas plants. Digestion products were visualized on 1 % agarose gel electrophoresis with Midori Green under UV-light. Names in red denote fully edited samples. B denotes blank (no DNA used in the reaction), C denotes control (DNA and gRNA from the TAKARA Bio kit).

3.6.1. *StABCG1* knockout mutants were identified by Illumina sequencing

Given that the *StABCG1*-CrisprCas plants might have chimeric tissues, PCR products from the region around the gRNA of the plants #132, #142, #143, #149, #155 and WT were sent for Illumina sequencing so that the alleles could be determined. A total of 1,004,589 reliable reads were obtained by Illumina sequencing of the *StABCG1*-CrisprCas and WT plants. Considering possible mutations, errors of extraction, PCRs or readings, the sequence of 92.53 % of the reads from the WT plant was identical to the 20 bp gRNA. On the other hand, the 5 transformed plants showed between 92.69 % and 99.49 % reads with indels mutations. All the transformed plants can be considered fully edited, for the reason that all of them contain less than 1 % of WT alleles, with the exception of plant #155 (7.31 %). However, plants #142 and #149 showed a high number of reads from alleles containing an in-frame deletion, which leads to a missing valine and leucine, respectively, in the protein (Table 2 and Fig.16).

Table 2: *StABCG1*-CrisprCas allele analysis. Total number of reads, wild-type alleles and percentage of alleles containing indels (insertion and deletion), which are in frame found in the five different *StABCG1*-CrisprCas (#132, #142, #143, #149 and #155) and WT plants. The sequences were obtained by Next-generation Illumina sequencing.

	Total reads	WT alleles	in frame indels
WT	72,674	92.53 %	0.44 %
#132	94,126	0.51 %	2.40 %
#142	757,373	0.77 %	30.40 %
#143	22,687	0.36 %	0.23 %
#149	32,556	0.59 %	10.38 %
#155	25,173	7.31 %	0.23 %

WT	<u>GACGGCGAGATAGTCGCCCTCTGGGTGCATCAGGGTCGG</u>	
#132	GACGGCGAGATAGTCGCC--CCTGGGTGCATCAGGGTCGG	31%
	GACGGCGAGATAGTCGCC-----CAGGGTCGG	16%
	GACGGCGAGATAGTCGC--TCCTGGGTGCATCAGGGTCGG	15%
	GACGGCGAGATAGTCGCC-TCCTGGGTGCATCAGGGTCGG	15%
	GACGGCGAGATAGTCGCC-----GCATCAGGGTCGG	7%
	GACGGCGAGATAGTCGCC CT TCCTGGGTGCATCAGGGTCG	5%
	GACGGCGAGATAGTCGCC---CTGGGTGCATCAGGGTCGG	2% V missing
#142	GACGGCGAGATAGTCGCC--CCTGGGTGCATCAGGGTCGG	29%
	GACGGCGAGATAGTCGCC---CTGGGTGCATCAGGGTCGG	28% V missing
	GACGGCGAGATAGTCGCC-TCCTGGGTGCATCAGGGTCGG	25%
	GACGGCGAGATAGTCGC--TCCTGGGTGCATCAGGGTCGG	8%
#143	GACGGCGAGATAGTCGCC-TCCTGGGTGCATCAGGGTCGG	57%
	GACGGCGAGATAGTCGCC--CCTGGGTGCATCAGGGTCGG	27%
	GACGGCGAGATAGTCGCCG-CCTGGGTGCATCAGGGTCGG	6%
#149	GACGGCGAGATAGTCGCC--CCTGGGTGCATCAGGGTCGG	43%
	GACGGCGAGATAGTCGCC-TCCTGGGTGCATCAGGGTCGG	20%
	GACGGCGAGATAGTCGCCGT---GGGTGCATCAGGGTCGG	9% L missing
	GACGGCGAGATAGTCGCCG-CCTGGGTGCATCAGGGTCGG	8%
	GACGGCGAGATAGTCGCC----TGGGTGCATCAGGGTCGG	5%
	GA-----	5%
#155	GACGGCGAGATAGTCGCC-TCCTGGGTGCATCAGGGTCGG	43%
	GACGGCGAGATAGTCGCCG-CCTGGGTGCATCAGGGTCGG	39%
	GACGGCGAGATAGTCGCCCTCTGGGTGCATCAGGGTCGG	7% wt

Figure 16: *StABCG1*-CrisprCas alleles. Main alleles found in the five different *StABCG1*-CrisprCas (#132, #142, #143, #149 and #155) and WT plants. Hyphen denotes deletions; Bold letters denotes insertions; The 20 bp gRNA is underlined in red; and the PAM sequence is underlined in blue.

By Illumina sequencing, the plants #132 and #143 were identified as fully edited plants, since they have the lowest number of reads from WT alleles, and also a low number of in-frame indels. Nevertheless, each transformed plant revealed to have more than 92 % of the *StABCG1* alleles edited and they might contain chimeric tissue.

3.6.2. Pep13-infiltrated *StABCG1*-CrisprCas plants have defective suberin formation

To understand whether the edited *StABCG1*-CrisprCas plants have affected suberin formation, the PAMP Pep13 was infiltrated in 3-week-old wild-type *S. tuberosum* plants. First, the expression of the *StABCG1* was measured by RT-qPCR and showed a

significantly reduced expression of the *StABCG1* gene 1 day after Pep13 infiltration in all transformed lines (Fig.17).

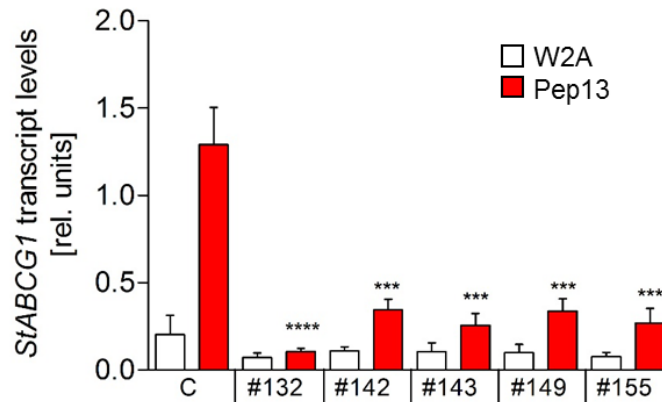


Figure 17: Reduced expression of *StABCG1* in *StABCG1*-CrisprCas plants after Pep13 infiltration. RNA was extracted from infiltrated leaves of 3-week-old wild-type *S. tuberosum* plants grown in a phytochamber, reverse transcribed and subjected to RT-qPCR. *StABCG1* expression was analyzed for controls (C - WT and EV) and five different *StABCG1*-CrisprCas (#132, #142, #143, #149 and #155) plants 24 hours after infiltration of 100 μ M Pep13 (red bars) and 100 μ M of the nearly inactive analog W2A (white bars). *StABCG1* expression was normalized to that of *StEF1 α* . Data are derived from two independent experiments (n = 8). Error bars represent SEM. Statistical differences between the controls were calculated using Mann Whitney U test (***0.0001<p<0.001; ****p<0.0001).

The formation of suberin in the same *StABCG1*-CrisprCas plants was then evaluated. The necrotic lesions induced by Pep13 were analyzed daily up to 10 days. SudanIII-stained lesions were visualized and it was possible to observe a red layer in 100 % of the controls (WT and EV) 7 days after wounding, but none of the lesions from the transformed plants indicated suberin formation (Fig.18).

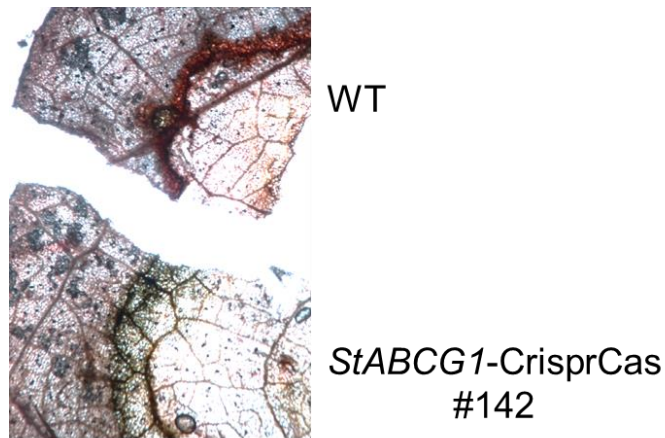


Figure 18: Loss of suberin in *StABCG1-CrisprCas* plants in response to Pep13 infiltration. Microscopy of suberin staining of lesions after Pep13 infiltration of wild-type (WT – top) and *StABCG1-CrisprCas* #142 (bottom) plants. The phenotype is representative to the other *StABCG1-CrisprCas* lines. Leaves of 3-week-old plants grown in a phytochamber from wild-type, empty vector and *StABCG1-CrisprCas* plants were infiltrated with 100 μ M Pep13. Seven days later, the infiltrated area was isolated, stained with SudanIII and subjected to bright light microscopy. Bars = 1 mm.

In addition to the lack of suberin, tissue browning around the lesions was observed in all 5 transformed plants at 6 days after infiltration, but not in the controls (WT and EV) (Fig.19).

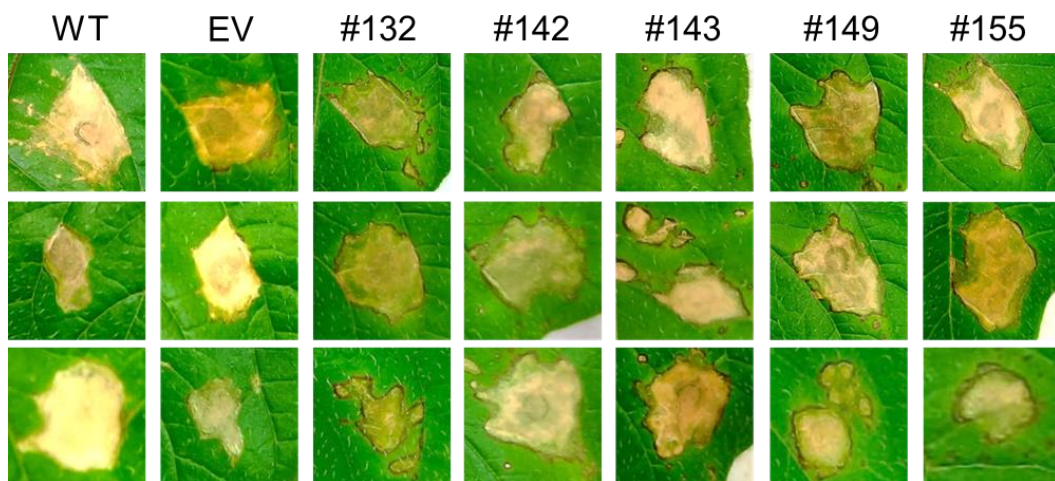


Figure 19: *StABCG1-CrisprCas* leaves develop tissue browning after Pep13-induced lesions. Phenotype of wild-type (WT), empty vector (EV) and five different *StABCG1-CrisprCas* (#132, #142, #143, #149 and #155) plants 10 days after Pep13 infiltration. Leaves of wild-type (WT), empty vector and *StABCG1-CrisprCas* plants were infiltrated with 100 μ M Pep13. Ten days later, the lesions were photographed.

The low level of *StABCG1* transcripts on *StABCG1*-CrisprCas plants affects the suberin formation and the lesion formed after Pep13 infiltration, leading to a browning of the tissue around the lesion.

3.6.3. Wounded leaves of *StABCG1*-CrisprCas plants have defective suberin formation

Following the reduced levels of *StABCG1* transcripts in response to Pep13 infiltration on the *StABCG1*-CrisprCas plants, the expression of this gene in response to wounding was also investigated by RT-qPCR in wounded leaves from 3-week-old wild-type *S. tuberosum* plants. Figure 20 shows the comparison between expression levels of *StABCG1* at 0 and 3 days after wounding (daw) and highlights that even plants not fully edited have reduced levels of these transcripts 3 days after wounding.

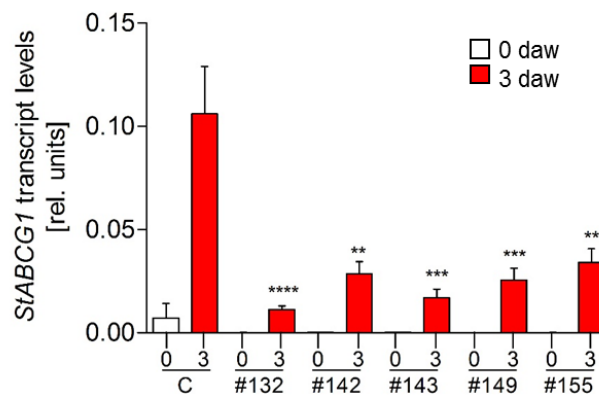


Figure 20: Reduced expression of *StABCG1* in *StABCG1*-CrisprCas plants after wounding. RNA was extracted from wounded leaves of 3-week-old wild-type *S. tuberosum* plants grown in a phytochamber, reverse transcribed and subjected to RT-qPCR. *StABCG1* expression of controls (C - WT and EV) and five different *StABCG1*-CrisprCas (#132, #142, #143, #149 and #155) plants 0 and 3 days after wounding (daw). *StABCG1* expression was normalized to *StEF1α*. Data are derived from two independent experiments (n = 8). Error bars represent SEM. Statistical differences between the controls were calculated using Mann Whitney U test (**, 0.001 < p < 0.1; ***, 0.0001 < p < 0.001; ****, p < 0.0001).

To check whether the reduced levels of *StABCG1* transcripts correlate with reduced suberin formation, wounded leaves were analyzed daily for up to 10 days. SudanIII-stained lesions showed a red layer in 100 % of the controls (WT and EV) at 5

days after wounding, indicating suberin formation. On the other hand, the majority of lesions from the transformed plants did not show the typical red layer, indicating a defect in suberin formation (Fig. 21). To quantify suberin formation, the wounded sites were divided into 4 fragments and assessed for the presence or absence of suberin with SudanIII. The quantification of suberin formation was performed 3, 4, 5, 6 and 7 days after wounding, from at least 46 wounding sites. Suberin started to form on the 4th day in about 65 % of the WT samples, and less than 20 % of the EV and #149 samples. No suberin was observed in the samples of #132, #142, #143 and #155 plants. On the 5th day up to the 7th day, all samples from WT and EV showed suberin formation, while the transformed plants never showed more than 40 % of the samples with suberin (Fig. 22). Although these results were previously observed in all other wounding/staining experiments, the quantitative data presented here derived from one experiment, and should be substantiated with more repetitions.

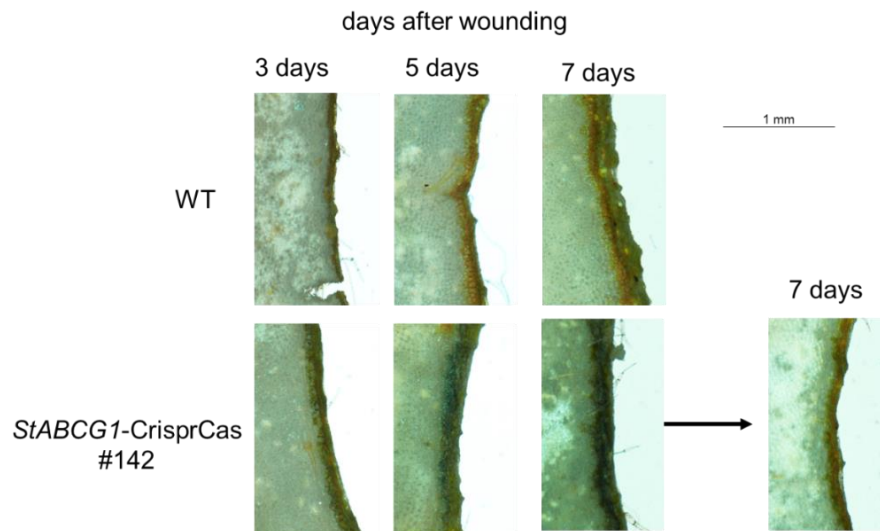


Figure 21: *StABCG1*-CrisprCas wounded leaves showed defective suberin formation. Leaves of wild-type (WT - upper panel) and *StABCG1*-CrisprCas #142 (bottom panel) plants were wounded with a 6 mm (\emptyset) cork borer. The wounded area was isolated using a 1 cm (\emptyset) cork borer, stained for suberin with SudanIII and subjected to bright light microscopy 3, 5 and 7 days after wounding. Pictures of plant #142 are representative for all five *StABCG1*-CrisprCas lines. Bar = 1 mm.

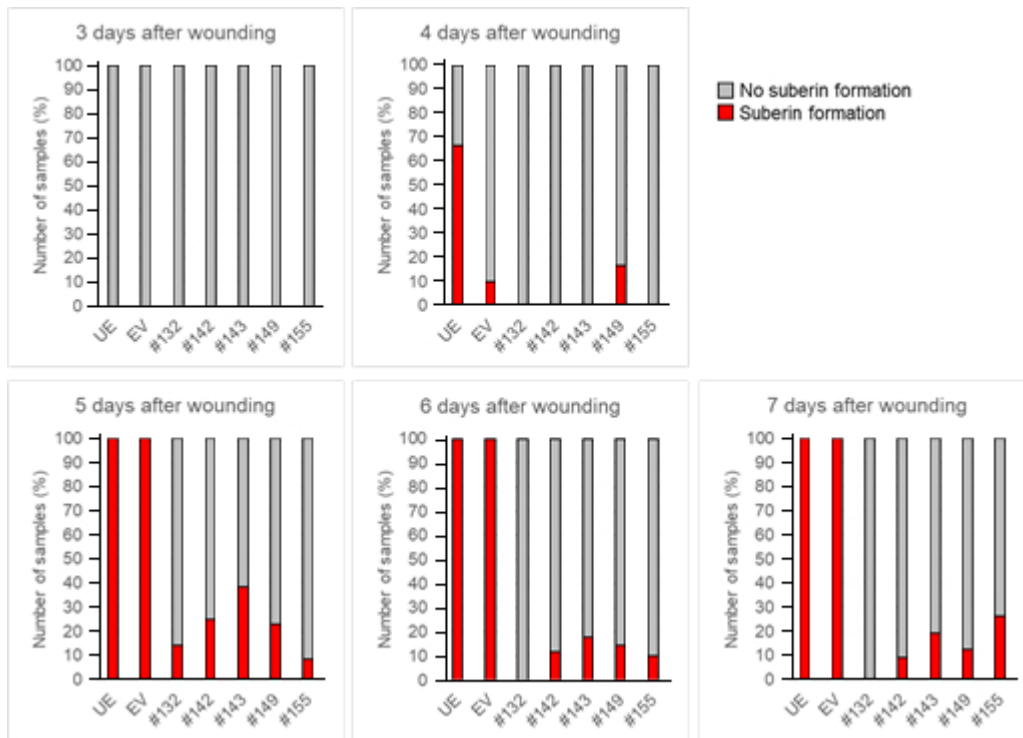


Figure 22: *StABCG1*-CrisprCas leaves showed defective suberin formation. Leaves of wild-type (WT), empty vector and five different *StABCG1*-CrisprCas plants (#132, #142, #143, #149 and #155) were wounded with a 6 mm (\varnothing) cork borer. The wounded area was isolated using a 1 cm (\varnothing) cork borer and samples were taken up to 7 days after wounding. Samples were stained with SudanIII and subjected to bright light microscopy. Staining was quantified in at least 46 wounded sites. Red bars denote the number of samples with suberin formation, and grey bars, number of samples with no suberin formation. Data are derived from 1 experiment.

After Pep13 infiltration, in addition to the lack of suberin, tissue browning around the lesions was observed in all 5 transformed plants 6 days after wounding, but not in the controls (WT and EV). Photos were taken after 10 days (Fig. 23).

Editing of *StABCG1* leads to at least partial loss of gene function. The *StABCG1*-CrisprCas plants had reduced *StABCG1* transcript levels, which correlates with reduced suberin formation and tissue browning around the lesions.

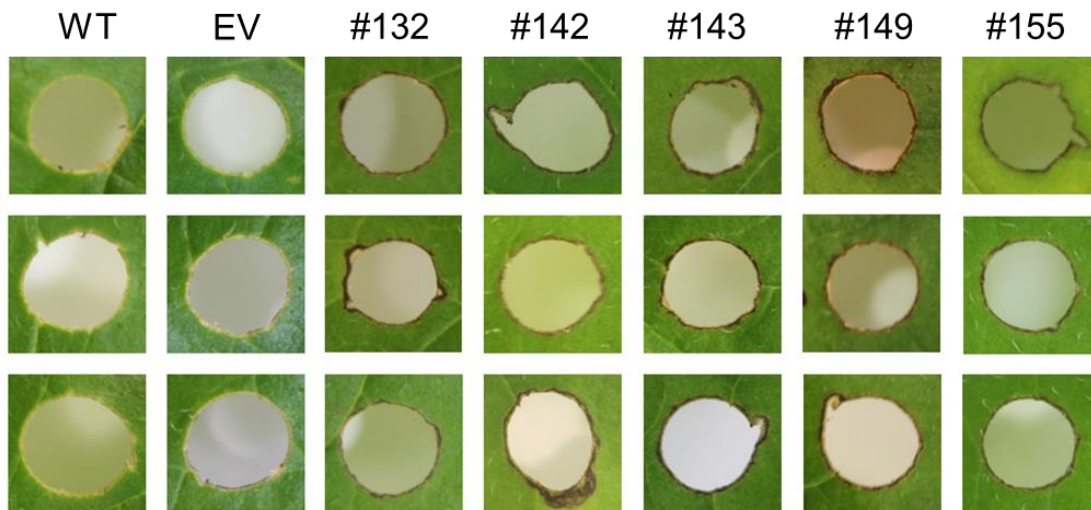


Figure 23: *StABCG1*-CrisprCas leaves tissue browning after wounding. Phenotype of wild-type (WT), empty vector (EV) and five different *StABCG1*-CrisprCas (#132, #142, #143, #149 and #155) plants 10 days after wounding. Leaves of wild-type (WT), empty vector and *StABCG1*-CrisprCas plants were wounded with a 6 mm (\emptyset) cork borer. Ten days later, the wounded area was photographed.

3.6.4. Wounded *StABCG1*-CrisprCas leaves show dramatic changes in metabolites profile

To identify compounds differentially occurring in the wounded leaves from WT and *StABCG1*-CrisprCas, untargeted metabolite profiling was performed via ultra-high performance liquid chromatography coupled with electrospray ionization quadrupole time-of-flight mass spectrometry by Dr. Karin Gorzolka. The untargeted metabolite profiling revealed a total of 220 features, which showed at least 20-fold higher abundance and 289 features, which showed at least 20-fold lower abundance in comparison to the wounded WT leaves (total of 1150 analyzed features). Among these features, some hydroxycinnamic acid amides (HCAAs), which are described to have antimicrobial activity and serve as cell wall reinforcement compounds (Dobritzsch et al., 2016), were identified to have an enhanced abundance in the *StABCG1*-CrisprCas wounded leaves, like caffeoyl noradrenaline (CafNor), caffeoyl putrescine (CafPut), coumaroyl agmatine (CA), coumaroyl noradrenaline (CouNor), coumaroyl octopamine (CO), feruloyl agmatine (FA), feruloyl noradrenaline (FNor), feruloyl octopamine (FO) and feruloyl tyramine (Fig. 24). Although, coumaroyl tyramine (CT) did not show significant differences in peak area from

the wounded WT leaves in ANOVA (Fig. 24), Mann Whitney U test (t-test) with both samples showed statistical differences of **** ($p < 0.0001$).

In addition to the lack of suberin observed in the *StABCG1*-CrisprCas plants, a dramatic change of metabolites of the wounded tissue was found.

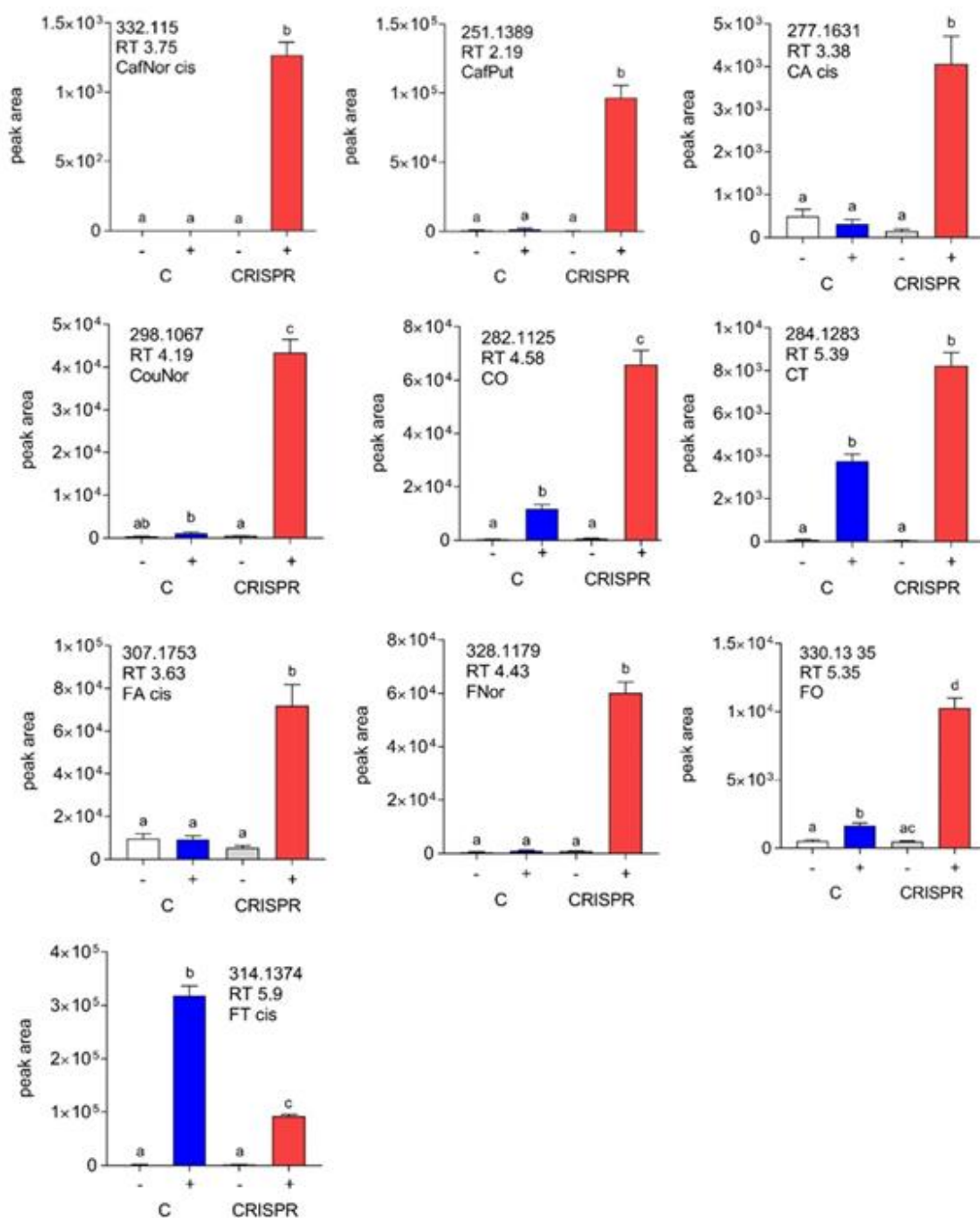


Figure 24: HCAAs accumulate preferentially in wounded *StABCG1*-CrisprCas. Leaves of wild-type and five different *StABCG1*-CrisprCas plants (#132, #142, #143, #149 and #155) were wounded with a 6 mm (\emptyset) cork borer. Ten days later, the wounded area was isolated using a 1 cm (\emptyset) cork borer. A methanol extraction from the samples was performed and subjected to UPLC-MS analysis. Caffeoyl noradrenaline (CafNor), caffeoyl putrescine (CafPut), coumaroyl agmatine (CA), coumaroyl octopamine (CO), coumaroyl noradrenalin (CouNor), coumaroyl tyramine (CT), feruloyl agmatine (FA), feruloyl noradrenaline (FNor), feruloyl octopamine (FO), and feruloyl tyramine (FT). Data from three independent experiments are shown from non-wounded (white/grey, -) and 10 days wounded tissue (blue/red, +). Statistical differences were calculated using one-way ANOVA. Different letters indicate significant differences ($n = 9$).

3.6.5. *StABCG1*-CrisprCas plants have defective suberin formation after *Phytophthora infestans* infection

To analyze whether *StABCG1* expression is also reduced after *P. infestans* infection, RT-qPCR was employed to measure the transcript levels of *StABCG1* in infected wild-type *S. tuberosum* plants. A preliminary experiment suggested that the transformed plants had a reduced expression of the *StABCG1* gene 3 days after *P. infestans* inoculation (Fig. 25) and reduced suberin formation 7 days after inoculation (Fig. 26).

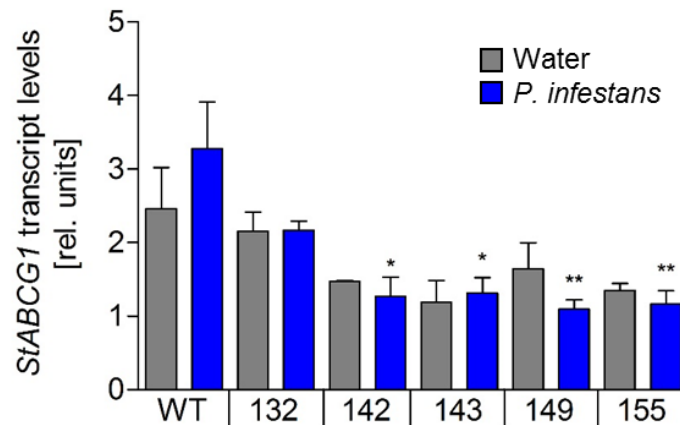


Figure 25: Reduced expression of *StABCG1* in *StABCG1*-CrisprCas plants after *P. infestans* inoculation. RNA was extracted from inoculated leaves (1×10^5 zoospores/mL) of 3-week-old wild-type *S. tuberosum* plants grown in a phytochamber, reverse transcribed and subjected to RT-qPCR. *StABCG1* expression was analyzed for wild-type (WT) and five different *StABCG1*-CrisprCas (#132, #142, #143, #149 and #155) plants 3 days after *P. infestans* (blue bars) and water (grey bars) inoculation. *StABCG1* expression was normalized to that of *StEF1 α* . Data are derived from one experiment ($n = 6$). Error bars represent SEM. Statistical differences between the WT were calculated using t-test – Mann-Whitney (*, $0.01 < p < 0.05$; **, $0.001 < p < 0.1$).



Figure 26: Defective suberin formation in *StABCG1*-CrisprCas plants in response to *P. infestans*. Microscopy of suberin staining with SudanIII of lesions 7 days after *P. infestans* inoculation of wild-type (WT – left panel) and *StABCG1*-CrisprCas #142 (right panel) plants. Phenotype is representative for the other *StABCG1*-CrisprCas lines. Leaves of WT, empty vector and *StABCG1*-CrisprCas were inoculated with a 1×10^5 zoospores/mL suspension. Seven days later, the infection area was isolated. Samples were stained with SudanIII and subjected to bright light microscopy. Bar = 1 cm.

With the purpose of investigating the resistance or susceptibility of the *StABCG1*-CrisprCas plants against *P. infestans*, inoculations were performed in the abaxial side of leaves from wild-type and transformed *S. tuberosum* plants. Biomass of the oomycete was evaluated 2 days after inoculation by qPCR (Fig. 27) and 3 days after inoculation by qPCR (Fig. 28) and by fluorescence (Fig. 29). Due to the high variability, these analyses were repeated several times and using different methods (qPCR and fluorescence) and all experiments that were performed are shown. In addition, Ulrike Smolka (IPB/Halle, Germany) performed four more repetitions including two *StABCG1*-CrisprCas lines (#132 and #143; Supplementary figure 1). It is possible to observe that the infection 2 days after inoculation (Fig. 27) and once at 3 days after inoculation (Fig. 28D) was very weak since the inoculum showed a significantly higher amount of *P. infestans* DNA in comparison to the WT. Similarly, no infection was found once in the analysis performed by Ulrike Smolka, since no significant difference was found between the WT and the inoculum (Supplementary figure 1A). The plant #142 was the only one to show a significantly higher amount of *P. infestans* DNA 2 days after inoculation in comparison to the WT. For figures 28D and 29, most of the *StABCG1*-CrisprCas showed a higher amount of *P. infestans* DNA in comparison to the controls. In the repetitions

performed by Ulrike Smolka, a significantly higher amounts of *P. infestans* biomass was found in the plant #143 once (Supplementary figure 1B) and a significantly lower *P. infestans* biomass was found in the plant #132 (Supplementary figure 1D). In all other repetitions there was no significant difference between the *StABCG1*-CrisprCas plants and the WT (Supplementary figure 1).

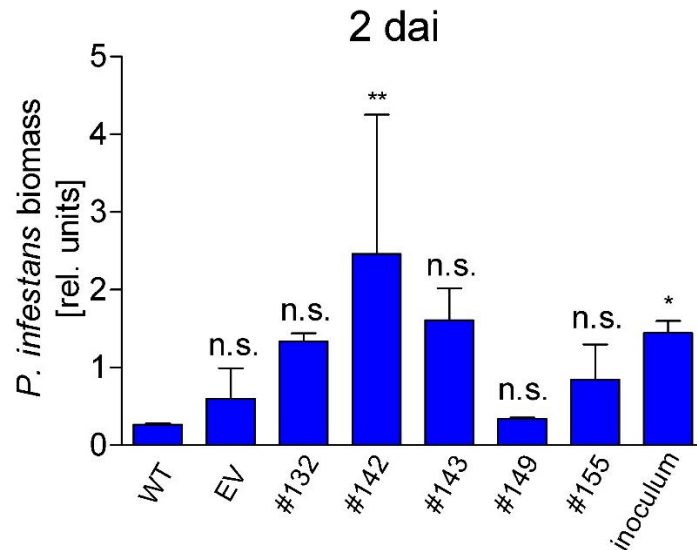


Figure 27: *P. infestans* biomass 2 days after inoculation (dai). *P. infestans* DNA was determined by qPCR in leaf disks 2 days after inoculation of wild-type (WT), empty vector (EV) and five different *StABCG1*-CrisprCas (#132, #142, #143, #149 and #155) plants. DNA was isolated from inoculated leaves (1×10^5 zoospores/mL) of 3-week-old plants grown in a phytochamber. Error bars represent SEM. Data are derived from one experiment ($n = 2$). Statistical differences between growth on WT and other plants were determined by t-test – Mann-Whitney (*, $0.01 < p < 0.05$; **, $0.001 < p < 0.1$; n.s., not significant).

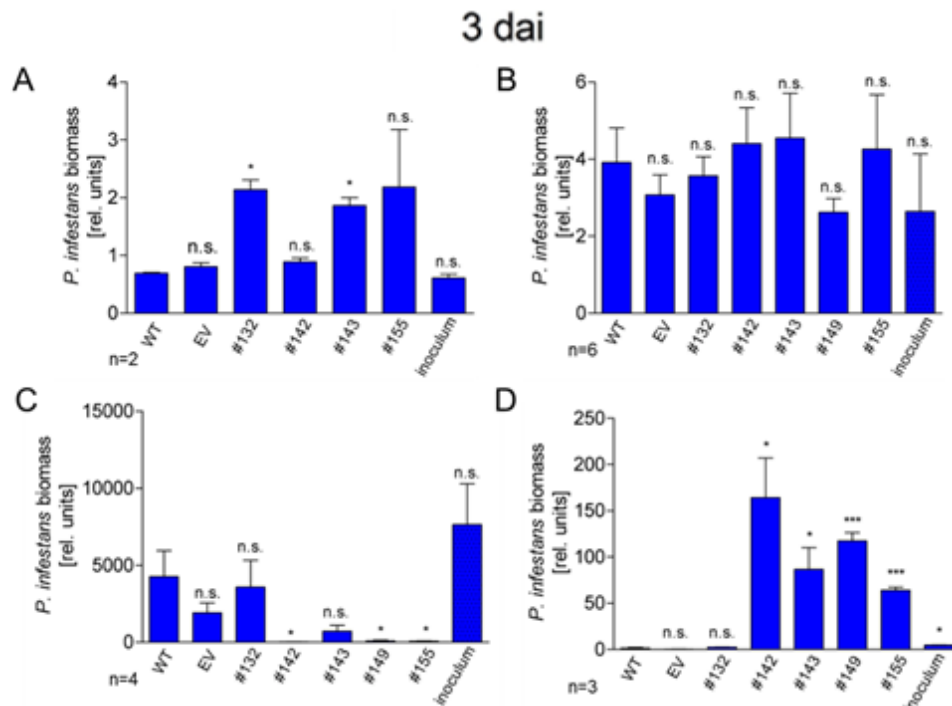


Figure 28: *P. infestans* biomass 3 days after inoculation (dai). *P. infestans* DNA was determined by qPCR in leaf disks 3 days after inoculation of wild-type (WT), empty vector (EV) and five different *StABCG1*-CrisprCas (#132, #142, #143, #149 and #155) plants. A, B, C and D represent independent experiments. DNA was isolated from inoculated leaves (1×10^5 zoospores/mL) of 3-week-old plants grown in a phytochamber. Error bars represent SEM. For each graph, data are derived from one independent experiment (n is described for each graph in the figure). Statistical differences between growth on WT and other plants were determined by t-test – Mann-Whitney (*, $0.01 < p < 0.05$; **, $0.001 < p < 0.1$; ***, $p < 0.001$; n.s., not significant).

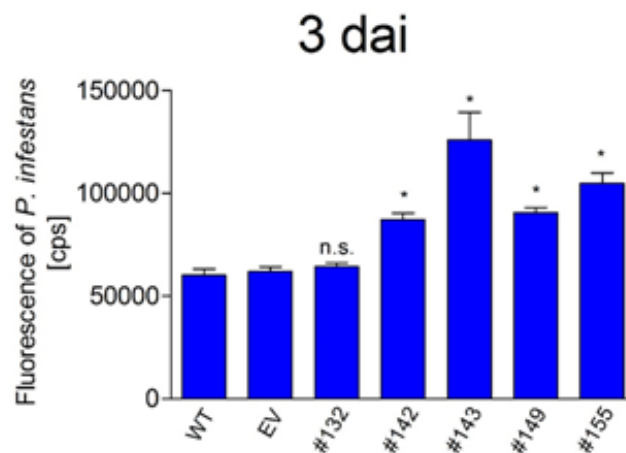


Figure 29: *P. infestans* growth 3 days after inoculation (dai). *P. infestans* fluorescence was determined GFP expression on NightShade in leaves 3 days after inoculation of wild-type (WT), empty vector (EV) and five different *StABCG1*-CrisprCas (#132, #142, #143, #149 and #155) plants. Error bars represent SEM. Data are derived from two independent experiments (n = 12). Statistical differences between growth on WT and other plants were determined by t-test – Mann-Whitney (*, $0.01 < p < 0.05$; n.s., not significant).

The reduction of *StABCG1* transcription levels is very minor, maybe due to the fact that the highest expression of *StABCG1* happened 6 days after *P. infestans* inoculation (Fig. 14), but it still correlates with the suberin formation after *P. infestans* infection. However, due to the inconsistency of the results and because the gene expression was verified just once, it is not possible to conclude if the *StABCG1*-CrisprCas plants are resistant or susceptible to *P. infestans*.

3.6.6. Tubers from *StABCG1*-CrisprCas plants have defective suberin formation

In an attempt to verify that editing of the *StABCG1* gene affects not just leaves but also other tissues from the transformed plants, tubers of *StABCG1*-CrisprCas plants were harvested and analyzed. To check if suberin is formed in the *StABCG1*-CrisprCas plants, tubers of *StABCG1*-CrisprCas and controls (WT and EV) plants were harvested from the greenhouse. Tuber disks were stored at room temperature, and stained for suberin with SudanIII 7 days after wounding. All controls showed a red layer around the wounding site, while the transformed tubers had a defect in the suberin formation, since the red layer was not present in all samples (Fig. 30).

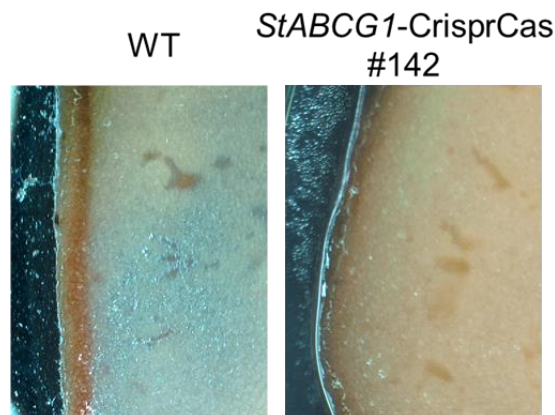


Figure 30: Defective suberin in *StABCG1*-CrisprCas tubers. Tubers of Wild-type (WT – left panel) and *StABCG1*-CrisprCas #142 (right panel) plants were harvested from greenhouse-grown, stored at room temperature, wounded with a sterile scalpel, stained for suberin with SudanIII 7 days after wounding and submitted to microscopy. Picture of plant #142 is representative for the other *StABCG1*-CrisprCas lines. Bar = 0.5 mm.

To analyze if the defective suberin formation in *StABCG1*-CrisprCas tubers correlates to weight loss, tubers were harvested and analyzed. The *StABCG1*-CrisprCas tubers had a 3.6 % higher weight loss in comparison to the tubers used as controls (WT and EV) 7 days after harvesting. This difference reached 7.9 % at 35 days after harvesting (Fig. 31).

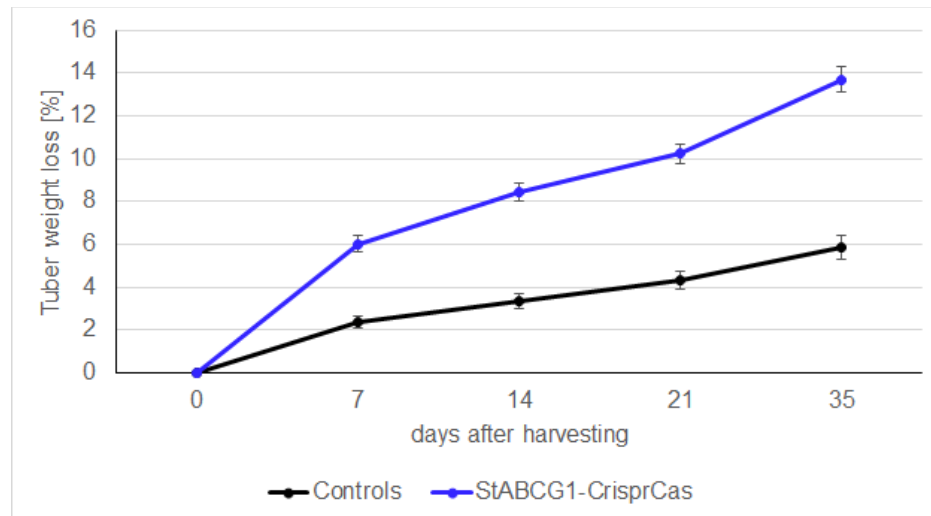


Figure 31: Weight loss from *StABCG1*-CrisprCas tubers. Tubers of *StABCG1*-CrisprCas (blue bar) and controls (WT and EV - black bar) plants were harvested from greenhouse, stored at room temperature and weighed at the indicated time points (Controls, n = 216, *StABCG1*-CrisprCas, n = 462). Three independent experiments were performed with at least four independent plants for each line (WT, EV, *StABCG1*-CrisprCas: #132, #142, #143, #149 and #155). Error bars represent SEM. Statistical differences between the controls were calculated using t-test Mann-Whitney (***, p<0.001).

With the purpose of determining loss of water through wounded lesions, greenhouse-grown tubers of *StABCG1*-CrisprCas and controls (WT and EV) plants were harvested, cut into two different-sized fractions with a sterile scalpel and stored at room temperature. The bigger and smaller fractions were weighed up to 10 days after wounding. Both fractions of the transformed tubers together showed a significant difference in weight loss from the 1st day onwards after wounding in comparison to the controls (Fig. 32). The fractions together of the transformed tubers lost 2.14 % more weight over the controls 1 day after wounding, reaching a difference of 7.37 % on the 10th day after wounding.

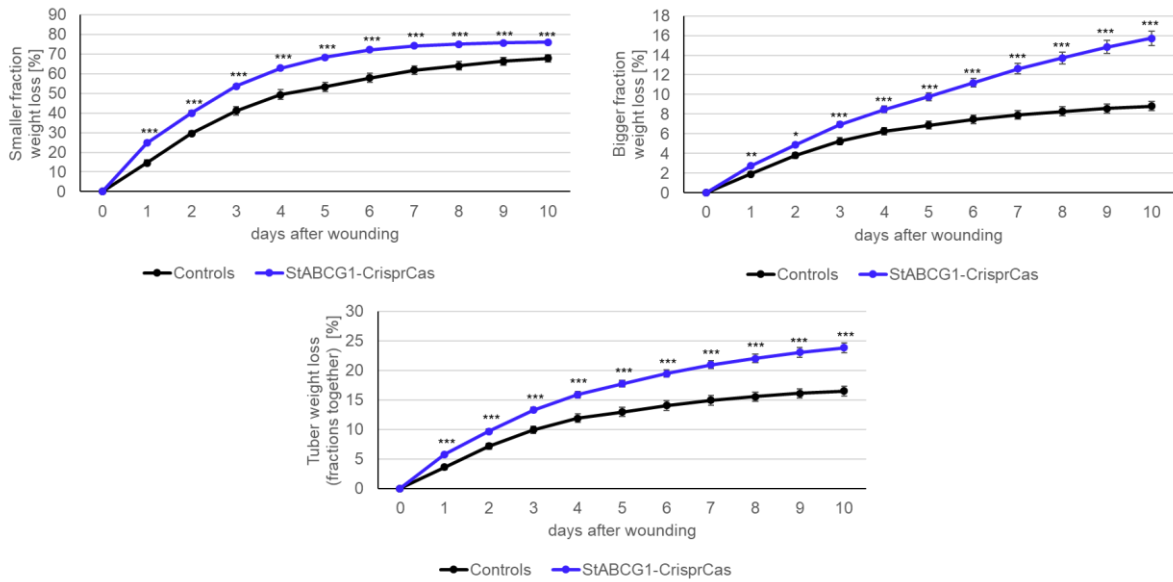


Figure 32: Weight loss of wounded tubers of *StABCG1-CrisprCas*. Tubers of *StABCG1-CrisprCas* (blue bar) and controls (WT and EV - black bar) plants were harvested from greenhouse, stored at room temperature, divided into two different-sized fractions with a sterile scalpel and weighed at the indicated time points (Controls, n = 18, *StABCG1-CrisprCas*, n = 47), two independent experiments were performed with at least six independent plants for each line (WT, EV, *StABCG1-CrisprCas*: #132, #142, #143, #149 and #155). Error bars represent SEM. Statistical differences between the controls were calculated using t-test Mann-Whitney (*, 0.01 < p < 0.05; **, 0.001 < p < 0.1; ***, p < 0.001).

In order to understand how suberin is involved in water loss and plant defense, tubers from WT and *StABCG1-CrisprCas* plants were wounded with a peeler and analyzed up to 14 days. In contrast to the controls, the transformed tubers produced a darker tissue 2 days after wounding. They also dried and shriveled 14 days after wounding, while the WT tubers were still intact, apart from the wounding (Fig. 33A). Transformed peeled tubers stored in a non-sterile box started rotting and molding 3 days after peeling, and after 7 days, they were completely covered by mycelium of undefined fungi, while the wild-type peeled tubers were still dry and did not show and macroscopic contamination (Fig. 33B). The white formation around the WT tubers shown in Fig. 33B is dried starch.

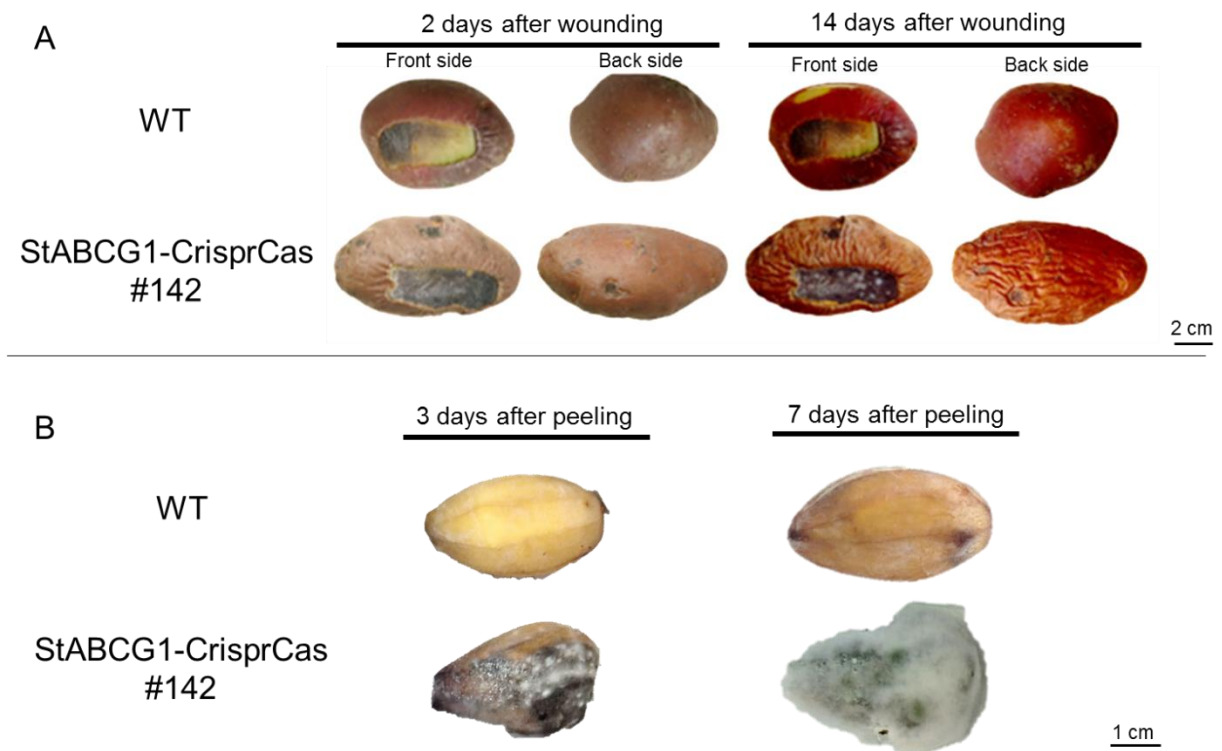


Figure 33: *StABCG1*-CrisprCas tubers dried and shriveled after wounding. Tubers of *StABCG1*-CrisprCas #142 and Wild-type (WT) plants were harvested from greenhouse-grown plants and stored at room temperature for further analysis. Picture shown are representative for the other *StABCG1*-CrisprCas lines. (A) Tubers were wounded with a sterile potato peeler, stored at a non-sterile paper bag and analyzed for up to 14 days after wounding; (B) Tubers were totally peeled with a sterile potato peeler, stored in a non-sterile paper box at room temperature and analyzed up to 7 days.

The significant difference in water loss and the change of color of the wounded tissue on the transformed tubers suggests that the suberin barrier acts as a water barrier. Due to water loss, the transformed tubers formed a microenvironment, which has high humidity and is appropriate for undefined growth of microorganisms.

3.6.7. Tubers of *StABCG1*-CrisprCas plants showed acquired resistance after *Phytophthora infestans* inoculation

Given that unidentified fungi were able to grow in wounded tubers, due to the water loss, *P. infestans* was used to determine resistance or susceptibility in tubers. *P. infestans* constitutively expressing GFP was inoculated onto wounded tubers at 0, 3, 7 and 14 days

after wounding. The fluorescence was determined 4 and 7 days after inoculation for each treatment. The quantification of *P. infestans* growth by fluorescence indicates a reduced growth of the oomycete on the *ABCG1*-CrisprCas #142 tubers 0 days after wounding/7 days after inoculation in comparison to the WT tuber at the same conditions and time point (Fig. 34). It is also possible to observe a wound-induced resistance in both lines on the 3rd day after wounding.

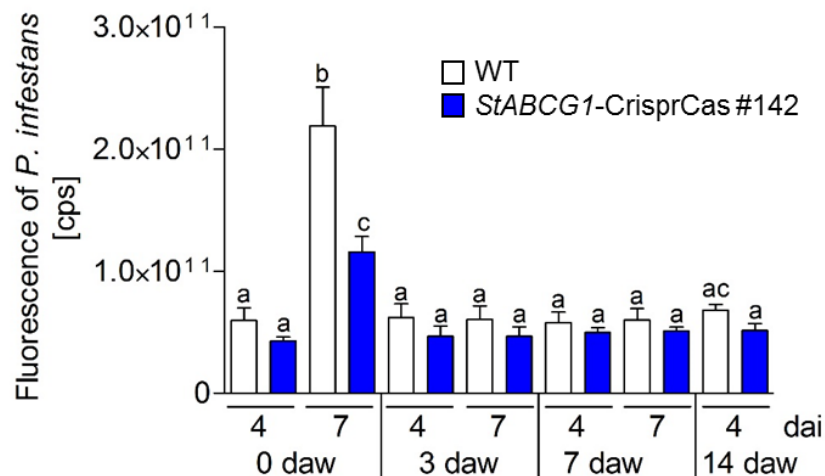


Figure 34: *StABCG1*-CrisprCas tuber are resistant against *P. infestans* 7 days after inoculation after wounding. Tubers of *StABCG1*-CrisprCas #142 and Wild-type (WT) plants were harvested from greenhouse-grown and stored at room temperature cut in cylinders with a sterile cork borer and a scalpel, let in a 12-wells petri dish with wet paper-filter. *P. infestans* constitutively expressing GFP was inoculated (1×10^5 zoospores/mL) and fluorescence was determined on NightShade in tubers 0, 3, 7 and 14 days after wounding (daw), 4 and 7 days after inoculation (dai). Error bars represent SEM. Data are derived from two independent experiments (WT, $n = 7$; *StABCG1*-CrisprCas, $n = 11$). Statistical differences were calculated using one-way ANOVA. Different letters indicate significant differences.

Wild-type and transformed tubers had an acquired resistance after wounding from 0 days after wounding/7 days after inoculation onwards, but *StABCG1*-CrisprCas tubers did not allow growth (Fig. 24).

3.7. Activation of suberin biosynthetic genes

In a second part of this work, different approaches were used to obtain plants with enhanced suberin formation. First, we targeted the activation of the suberin biosynthetic

genes described by Serra et al. (2010; 2009a; 2009b) and Landgraf et al. (2014). And later, the transcription factor *AtMYB39* was transferred to potato plants.

3.7.1. Expression of the betalain pathway via TALE triggers necrosis in *Solanum tuberosum*

To see if the TAL-effector can be expressed in potato the system of Grützner et al. (2021) was chosen. They described that betalain can generate red spots when its biosynthetic genes are expressed in *N. benthamiana* (Fig. 35), therefore it can be used as reporter genes to check the effect of TALE in different plants. The constructs containing the betalain biosynthesis genes under control of TALE and three different promoters were kindly provided by Dr. Marillonnet (IPB/Halle, Germany), pAGM50344, pAGM26035, pAGM24071 (Fig. 36).

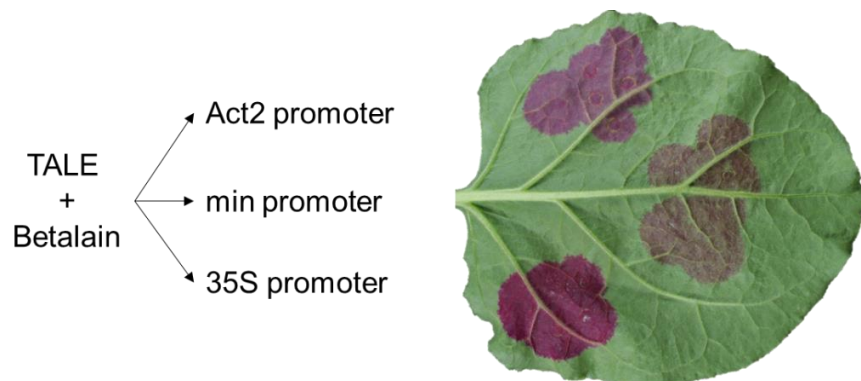


Figure 35: Transient expression of betalain under control of TALE constructs. Betalain biosynthesis genes under control of Act2 promoter (pAGM50344), min promoter (pAGM26035) and 35S promoter (pAGM24071) were infiltrated in *N. benthamiana* leaves. The pictures were taken 5 days after infiltration. Figure provided by Dr. Marillonnet.

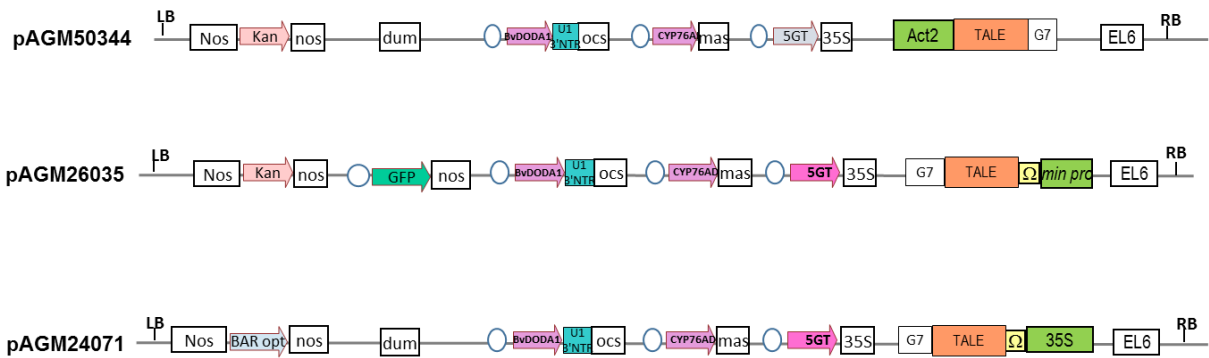


Figure 36: Recombinant plasmids carrying betalain biosynthesis genes under control of TALE provided by Dr. Marillonnet. Nos, nopaline synthase promoter/terminator; Kan, kanamycin resistance gene; dum, dummy position (empty); Blue circles, TAL effector binding site; BvDODA1, 3,4-dihydroxyphenylalanine 4,5-dioxygenase 1 from *Beta vulgaris*; U1 3'NTR, 3' untranslated sequences from TMV U1 viral genome; Ocs, octopine synthase terminator; CYP76AD1, cytochrome P450 76AD1 from *B. vulgaris*; mas, mannopine synthase terminator; 5GT, glucosyltransferase from *Dorotheanthus bellidiformis*; 35S, CaMV 35S promoter (green) and terminator (white); Act2, actin 2 promoter from *Arabidopsis thaliana*; TALE, Transcription activator-like effector; G7, *Agrobacterium tumefaciens* g7 terminator; EL6, linkers; LB and RB, left and right T-DNA borders; GFP, green fluorescent protein reporter gene; min pro, minimal promoter; BAR opt, BASTA resistance gene. Golden Gate assembled for the constructs pAGM50344, pAGM26035 and pAGM24071.

In order to check if TALE can be used as an overexpression regulator for the suberin pathway genes, pAGM50344, pAGM26035 and pAGM24071 constructs were used for transient expression in *S. tuberosum*.

After infiltration of *A. tumefaciens* containing the constructs separately, a red coloration formed on the leaves infiltrated containing pAGM50344 and pAGM24071. In addition, cell death occurred in all infiltrated leaves (Fig. 37). Infiltrated leaves showed a red coloration, suggesting that the TALE could be used as a regulator for the suberin pathway, but also can trigger cell death.

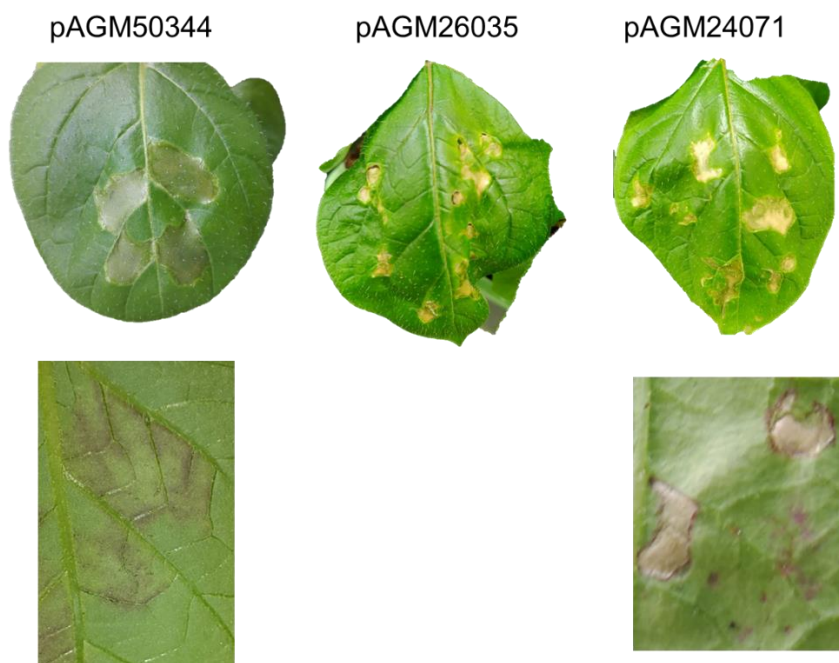


Figure 37: TALE triggers cell death in *S. tuberosum* cv. *Desirée*. Agrobacterium containing the constructs pAGM50344, pAGM26035 and pAGM24071, containing the betalain synthesis genes under control TALE on three different promoters, were infiltrated in leaves of 3-week-old wild-type *S. tuberosum* plants grown in a phytochamber. Two days later infiltrated leaves showed cell death and red coloration.

3.7.2. TAL-effector hinders stable transformation in *Solanum tuberosum*

To avoid cell death, an inducible promoter was used to limit the expression of the TALE. Yamamizo et al. (2016) showed that the expression of the PVS3 promoter occurs after pathogen infection and not under other conditions, like wounding. Unfortunately, Yamamizo et al. (2016) did not describe the variety of *S. tuberosum* used in their work. Two different constructs based on Yamamizo et al. (2016) were designed to verify if the promoter is active in *S. tuberosum* cv. *Desirée*. Potato plants were transformed with GFP or GUS genes under control of the PVS3 promoter. Pep13/W2A and *P. infestans* treatments were used in leaves of the transformed plants containing GFP or GUS under control of PVS3 promoter. GFP-fluorescence or GUS staining was performed 24 hours after the treatment. The promoter PVS3 was activated by both constructs EP33 (pPVS3:GFP) and EP34 (pPVS3:GUS) 24 hours after *P. infestans* inoculation (Fig. 38A)

as well as 24 hours after Pep13 infiltration (Fig. 38B). In contrast, the control W2A infiltration did not activate the PVS3 promoter in any of the transformants (Fig. 38).

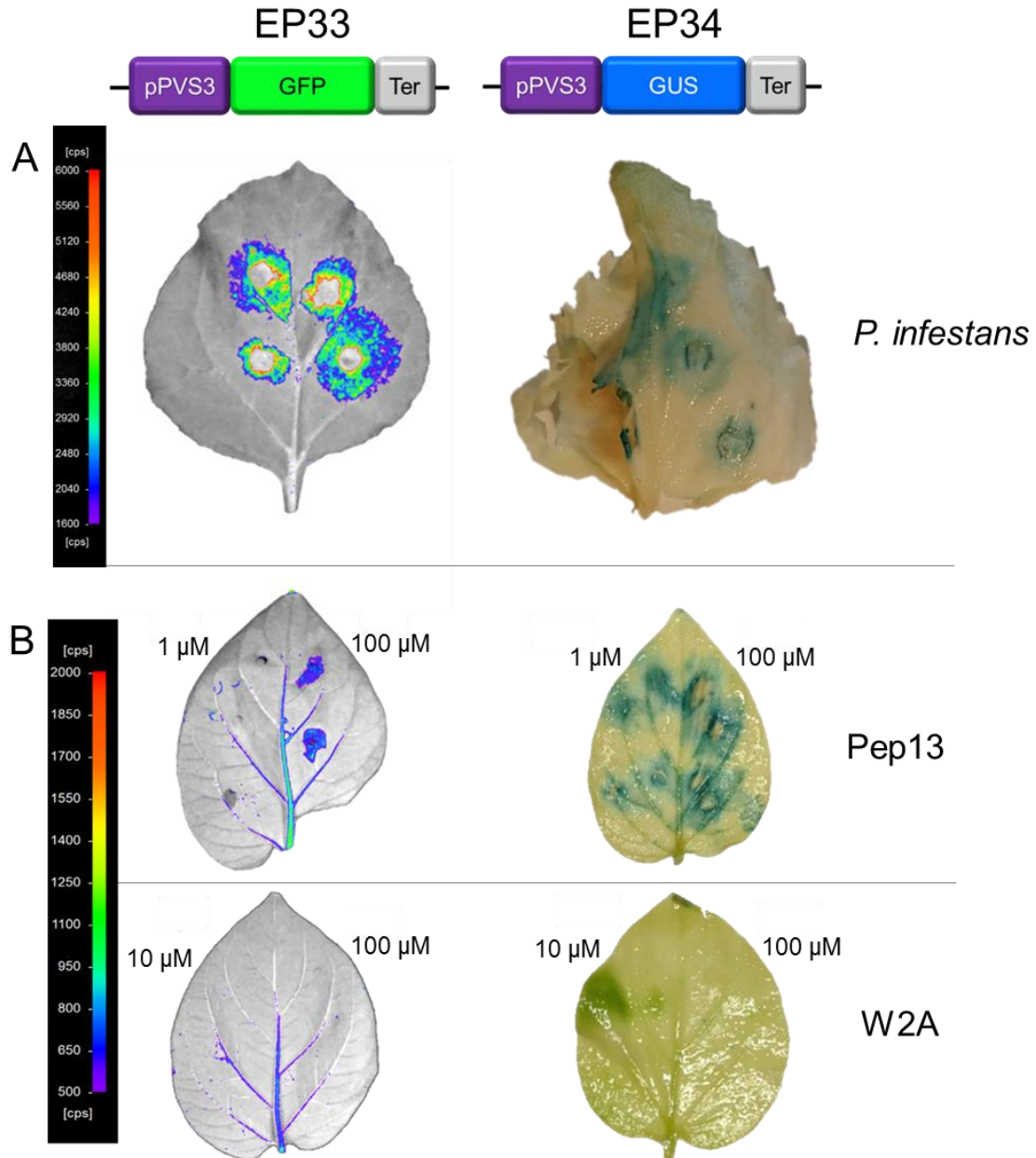


Figure 38: PVS3 promoter is activated after *P. infestans* and Pep13 treatments. Leaves of 3-week-old EP33 (pPVS3:GFP - **A** and **B**, left panels) and EP34 (pPVS3:GUS - **A** and **B**, right panels) plants grown in a phytochamber were inoculated with *P. infestans* (1×10^5 zoospores/mL) (**A**) and infiltrated with Pep13 (1 μM and 100 μM) and the nearly inactive analog W2A (10 μM and 100 μM) infiltration (**B**). GFP expression was determined on NightShade in leaves of EP33 plants 24 hours after treatment. EP34 leaves were destained with ethanol and stained for GUS with X-Gluc and analyzed 24 hours after treatment. Pictures are representative for the other lines.

The construct pAGR45 – containing *StABCG1*, *StFHT*, *StCYP86A33* and *StKCS6* under the control of TALE, which in turn is driven by the PVS3 promoter – and two empty vectors (controls pAGR44 – containing all genes, except of TALE and PVS3 promoter – and pAGR46 – containing just the TALE and PVS3 promoter) were used for stable transformation in *S. tuberosum*, generating the plants EP45, EP44 and EP46, respectively. The constructs used for the plants EP44 and EP45 were designed separately with two different *StFHT* alleles (A2 and A3).

Eight lines of EP44A2 and 4 EP44A3 were obtained. After three approaches to transform with pAGR45 and pAGR46 constructs, just 1 line of EP45A2 was obtained. The low rate of transformation with the EP45 construct and no lines obtained with the EP46 construct put forward the hypothesis that the PVS3 promoter has a residual activity, which is enough to trigger the TALE, which leads to cell death on *S. tuberosum cv. Desirée* and cannot be used as a regulator for the suberin biosynthesis genes in potato plants.

To solve this problem, a construct containing *StABCG1*, *StFHT*, *StCYP86A33* and *StKCS6* under control of PVS3 promoter was designed (pAGR51). Two different alleles of *StFHT* were used to design the construct, A2 and A3. Plants were generated by *A. tumefaciens* mediated transformation.

Conversely, the EP51A2 and EP51A3 plants did not show any overexpression of the analyzed genes 24 hours after Pep13 infiltration (Fig. 39A), nor after *P. infestans* inoculation (Fig. 39B), in comparison to the controls.

For that reason, no further analyses were performed with these plants.

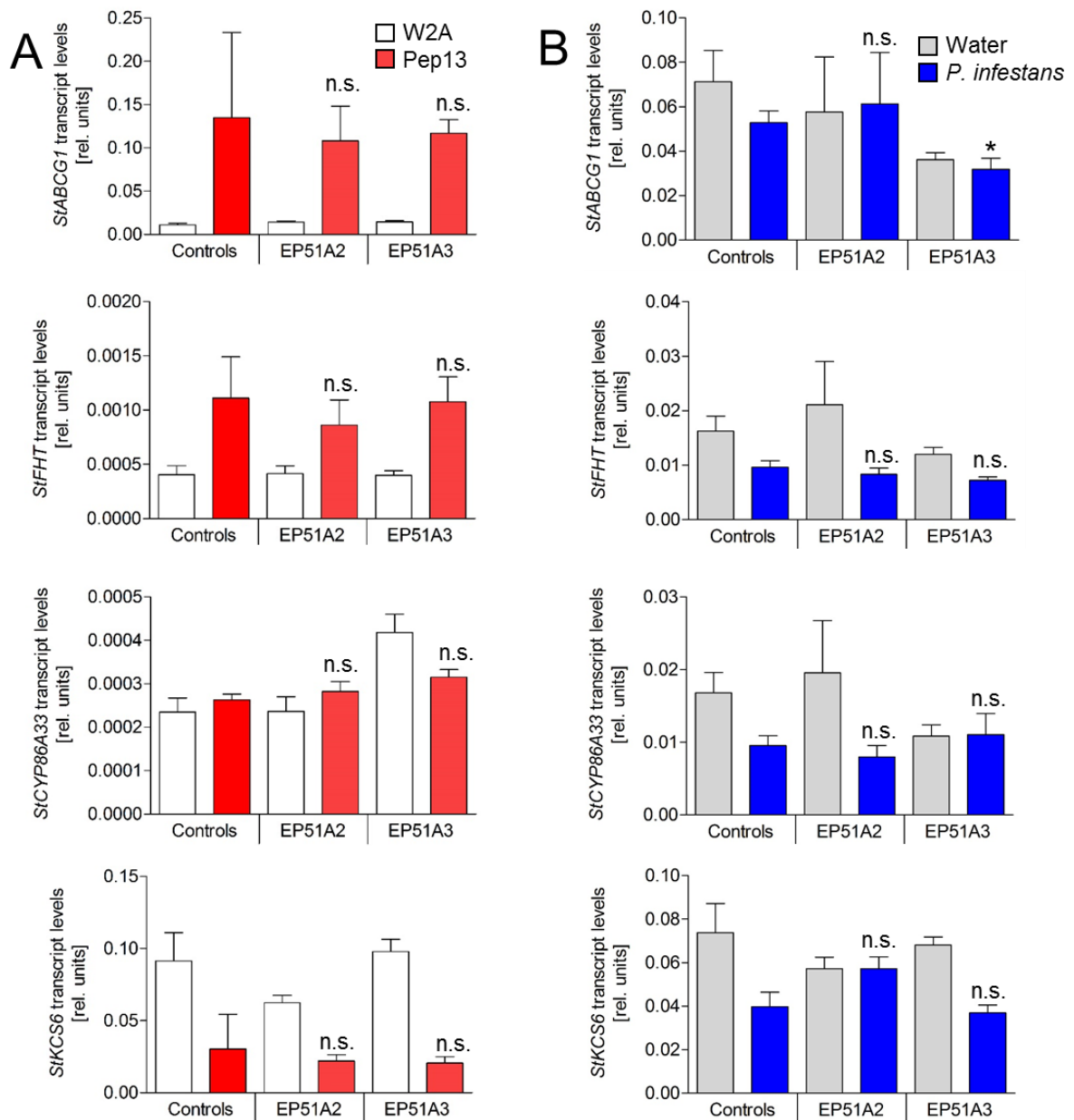


Figure 39: EP51 plants did not overexpress genes involved in the suberin pathway. *StABCG1*, *StFHT*, *StCYP86A33* and *StKCS6* expression of controls (WT and EV) and EP51 plants (genes involved in suberin pathway under control of pPVS3, a pathogen inducible promoter - A2E, A2W, A2F2, A2J2, A3B, A3D, A3F and A3G) 24 hours after (A) Pep13/W2A (100 μ M) and (B) *P. infestans* (1×10^5 zoospores/mL) or water inoculation. RNA was isolated from treated leaves of 3-week-old plants grown in a phytochamber and subjected to RT-qPCR. Gene expression was normalized to that of *StEF1 α* . Data are derived from one experiment (Pep13/W2A: Controls n = 2 and EP51A2 and EP51A3 n = 4; *P. infestans*/Water: Controls n = 8 and EP51A2 and EP51A3 n = 16). Error bars represent SEM. Statistical differences between the controls were calculated using t-test - Mann-Whitney (*, $0.01 < p < 0.05$; n.s., not significant values).

3.7.3. Expression of the transcription factor *AtMYB39* induces enhanced suberin formation in *Solanum tuberosum*

In a second approach, a construct was designed containing the transcription factor *AtMYB39* (Cohen et al., 2020) under control of the 35S promoter. This was named pAGR91 and used to generate potato plants via *A. tumefaciens* mediated transformation (EP91). As described before, *AtMYB39* was reported to induce suberin formation on leaves of *N. benthamiana* by transient expression.

To assess the gene expression levels of the target *AtMYB39*, RT-qPCR was employed to measure the transcript levels of *AtMYB39* in WT, EV and transgenic (EP91.1, EP91.7, EP91.10 and EP91.17) *S. tuberosum* plants. In addition, to analyze whether the expression of *AtMYB39* induces the expression of the studied genes, the transcript levels of *StABCG1*, *StFHT*, *StCYP86A33* and *StKCS6* were also measured by RT-qPCR. Samples were collected from three-week-old leaves of the controls and transgenic plants and the transcript levels of these targets were evaluated and compared with the controls, in two independent experiments. For technical reasons, the plant EP91.7 was included just in one experiment, yet it was included in the statistics.

The *AtMYB39* transcript levels found were statistically higher than the controls for all EP91 plants analyzed (Fig. 40A). The plant EP91.1 showed more differences in comparison to the controls, for example, it had significantly higher levels of transcript for *StABCG1* (Fig. 40B) and *StFHT* (Fig. 40C), and lower levels of transcript for *StKCS6* (Fig. 40E). In addition, the plant EP91.10 also had higher levels of transcript of *StFHT* (Fig. 40C). However, no differences were found in transcript levels of *StABCG1*, *StFHT* and *StKCS6* for the plants EP91.7 and EP91.17 in comparison to the controls. Also transcript levels of *StCYP86A33* was equivalent for all plants analyzed (Fig. 40D).

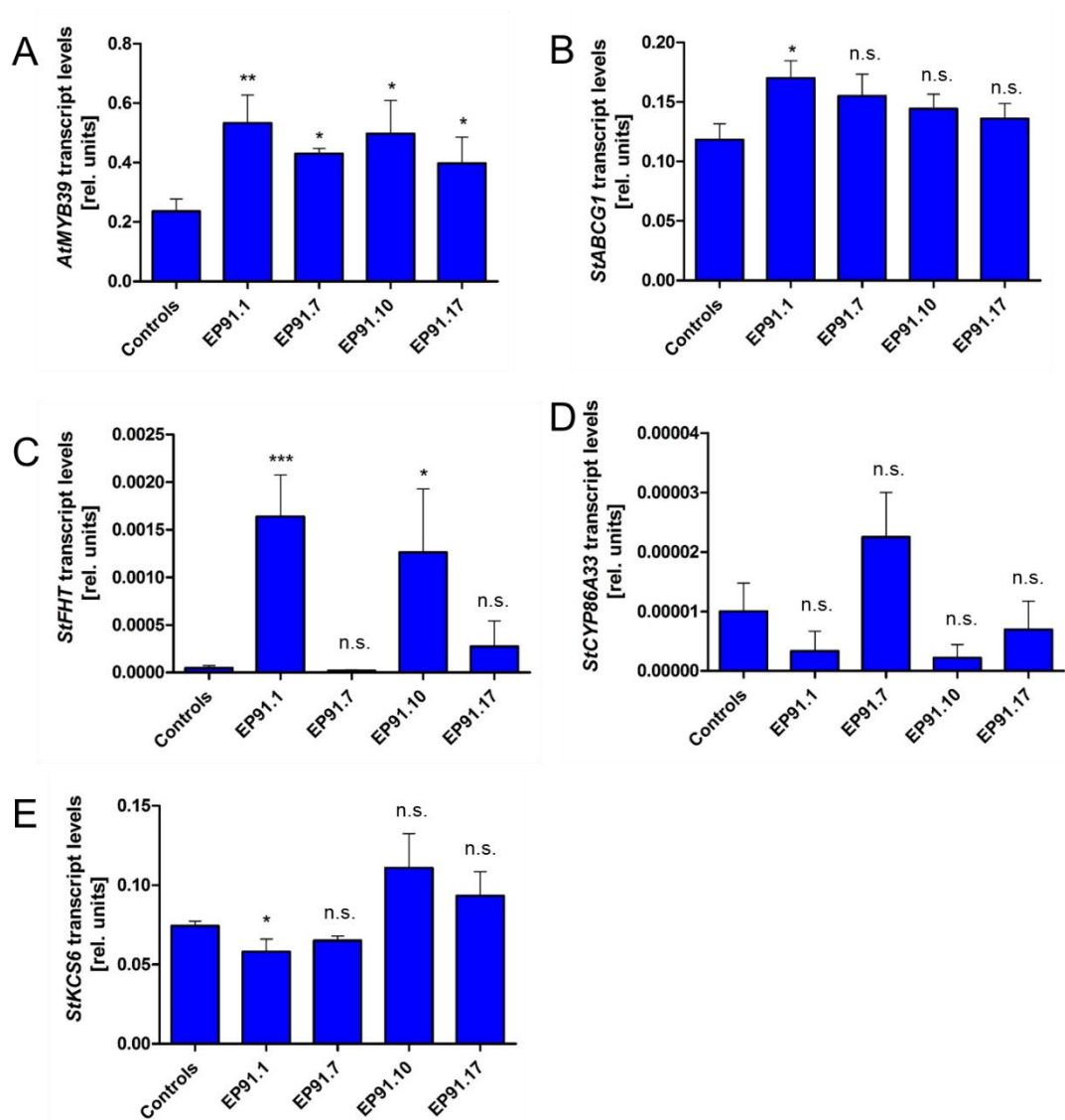


Figure 40: Gene expression of potato plants expressing *AtMYB39*. *AtMYB39*, *StABCG1*, *StFHT*, *StCYP86A33* and *StKCS6* expression of leaves from controls (WT and EV) and EP91 plants (*AtMYB39* under control of 35S) – EP91.1, EP91.7, EP91.10 and EP91.17. RNA was isolated from leaves of 3-week-old plants grown in a phytochamber and subjected to RT-qPCR. Gene expression was normalized to that of *StEF1α*. Data are derived from two experiment – The plant EP91.7 was included in just one experiment (Controls n = 24; EP91.1, EP91.10, EP91.17 n = 12 and EP91.7 n = 4). Error bars represent SEM. Statistical differences between the controls were calculated using t-test - Mann-Whitney (*, 0.01 < p < 0.05; **, 0.001 < p < 0.1; ***, p < 0.001; n.s., not significant values).

To check if the level of *AtMYB39* transcripts correlates with enhanced suberin formation, leaves from 3-week-old wild-type WT and EP91 plants grown in a phytochamber were wounded and analyzed after 3 days. After suberin staining by SudanIII, the samples were subjected to bright light microscopy and photographed. The

pictures were randomized and rated by at least two different people according to the amount of suberin presenting in the lesion (Fig. 41), in two independent experiments. Both experiment are showed in the figure 41. However, for technical reasons the plant EP91.7 was not included on the experiment 1 (Fig. 41A). All the plants analyzed had a higher rate of suberin formation in comparison to the controls in both experiments (Fig. 41), with the exception of plant EP91.7, which is included just in the second experiment. For this analysis, it is also important to highlight that the same phenotype was observed in other analyses, but not rated. In addition, statistics was not performed because the rating is separated in categories.

Thus, despite small or no changes in gene expression, suberin formation was enhanced in all 4 transformants expressing the *AtMYB39*, which was shown to induce some suberin related genes.

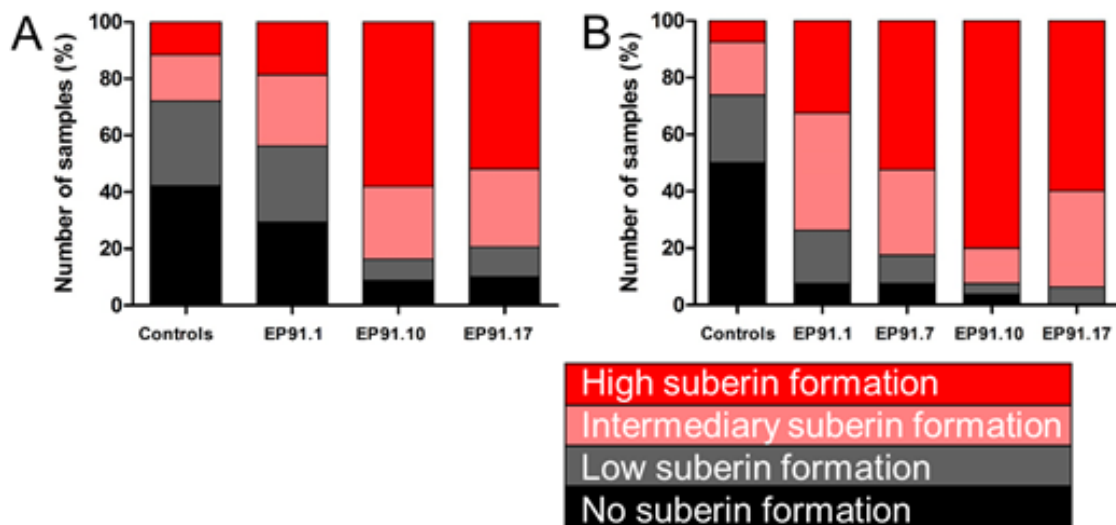


Figure 41: Rating of plants expressing *AtMYB39*. Leaves of controls (WT and EV) and three different EP91 plants (EP91.1, EP91.7, EP91.10 and EP91.17) were wounded with a 6 mm (\emptyset) cork borer. The wounded area was isolated using a 1 cm (\emptyset) cork borer 3 days after wounding. Samples were stained with SudanIII and subjected to bright light microscopy. Suberin staining was rated in 80 pictures of 20 wounded samples for each experiment. Bars denote number of samples with the respective level of suberin formation (Dark red, high suberin formation; light red, intermediary suberin formation; grey, low suberin formation; and black no suberin formation). Due to technical reasons the EP91.7 plant was evaluated only in one experiment.

4. DISCUSSION

In this work, suberin biosynthesis and its role in plant defense were studied in leaves and tubers of *S. tuberosum*. The genes previously described to be involved in the suberin pathway (*StABCG1*, *StFHT*, *StCYP86A33* and *StKCS6*) (Landgraf et al., 2014; Serra et al., 2010; Serra et al., 2009a; Serra et al., 2009b) have no constitutive or very low expression in leaves of *S. tuberosum*, low expression in roots and a high expression in tuber periderm (Haggitt, 2016; Landgraf et al., 2014; Boher et al., 2013; Serra et al., 2009a). The expression of these target genes was analyzed after different treatments. Also, plants with reduced suberin formation and plants with enhanced suberin formation were analyzed to understand the role the biopolymer in the defense.

4.1. Transcriptomic data revealed putative suberin biosynthesis genes

Proper development of the periderm is essential for tuber quality and storage, which has important economic implications for the potato commerce worldwide. Suberin accumulation is considered important for periderm formation, and may also act as part of the pathogen defense mechanism (Campilho et al., 2020, Barel and Ginzberg, 2008). Consequently, understanding the biosynthesis of suberin is critical to better understand this protective layer in plant defense and also possibly improving tuber storage life. The first enzymes involved in the suberin metabolic pathway in plants have only been recently discovered, but there are still many others to be studied (Nomberg et al., 2022). Suberization of cell walls can be formed after different stresses. For example, wounding and pathogen infection can activate the genes related to the pathway, leading to suberin formation on the periderm (Campilho et al., 2020; Schreiber et al., 2005; Lulai and Corsini, 1998).

In this work a series of genetic transformations was performed to investigate the role of suberin in plant defense, either by inducing the simultaneous expression of important genes of the suberin biosynthetic pathway via a suberin-related transcription factor, or by editing the suberin transporter. Mutants were thoroughly investigated for their

response to artificial- and pathogen-induced symptoms. By employing different techniques, we analyzed the effect of the *AtMYB39* and *StABCG1* on suberin production and side effects of the absence of suberin, respectively, as well as the quality and conservation of tubers.

The suberin transporter *StABCG1* has a high expression in roots and tuber periderm, as well as in leaves after wounding (Landgraf et al., 2014). In leaves of *S. tuberosum* c.v. Desirée, a significantly higher expression of the *StABCG1* gene was found very early after wounding (12 hours after the treatment – Fig. 13A), 1 day after Pep13 infiltration (Fig. 12A) and 5 days after *P. infestans* inoculation (Fig. 14A). These data are in agreement with Landgraf et al. (2014), who reported high amounts of *StABCG1* transcripts in leaves after wounding, showing an increase between 8 and 12 hours after wounding. In addition, our data show even higher expression on later days. In contrast, Landgraf et al. (2014) reported a higher expression of *StABCG1* gene 12 hours after Pep13 infiltration in leaves. Yet, it is possible to observe an increase of transcript levels from 1 up to 7 days after infiltration on our analysis. Up to now, between the genes related to suberin biosynthesis, data after Pep13 infiltration were available only for *StABCG1*, nevertheless, transcript levels of all genes studied were analyzed and compared to different approaches. Landgraf (2016) described an accumulation of *StABCG1* transcript levels 4 days after *P. infestans* inoculation, while our data show this accumulation after 6 days. However, this could be explained by the highly variable interaction between *S. tuberosum* and *P. infestans*. Minor changes may affect the interaction and the infection processes. For example, small alterations in humidity or temperature have direct influence on the oomycete germination (Minogue and Fry, 1981; Glendinning and Macdonald, 1963). This effect was also observed in the *StABCG1*-CrisprCas inoculation (Fig. 28, 29 and supplementary figure 1).

Gou et al. (2009) reported a very low constitutive expression of the *FHT* homologous gene (*AtASFT1*) in Arabidopsis stems, however, its expression is about 20-fold higher 1 day after wounding in stems (Vishwanath, 2013b). When kiwifruits (*Actinidia chinensis*) are wounded, an increase of transcript levels of *FHT* can be found until 6 days after wounding (Welimii et al., 2020). These facts suggest that the expression of *FHT* can be highly induced in plants after wounding. *StFHT* had similar expression as

StABCG1 after wounding (Fig. 13A and B), but showed a significantly higher expression 12 hours after Pep13 infiltration (Fig. 12B) and 5 days after *P. infestans* (Fig. 14B). Boher et al. (2013) reported high amounts of *StFHT* protein between 1 and 3 days after wounding in leaves, and this might correlate with the increased transcript levels of *StFHT* found in our data, assuming that the protein accumulation depends on higher transcript abundance. Despite being different in patho-systems, potato plants after inoculation of *P. infestans* (Kelley et al., 2010) and tomato plants inoculated with the pathogenic bacteria *Ralstonia solanacearum* (Swanson et al., 2004) show symptoms between 3 and 4 days after inoculation. *StFHT* expression after *P. infestans* inoculation is consistent with Kashyap et al. (2021), who described an accumulation of transcript levels of the homologous *SIFHT* (tomato) between 4 and 9 days after inoculation of *R. solanacearum*. Consistently, *StFHT* had a significantly higher expression starting 12 hours after Pep13 infiltration in leaves, but still lower in comparison to the expression after wounding (Fig. 42).

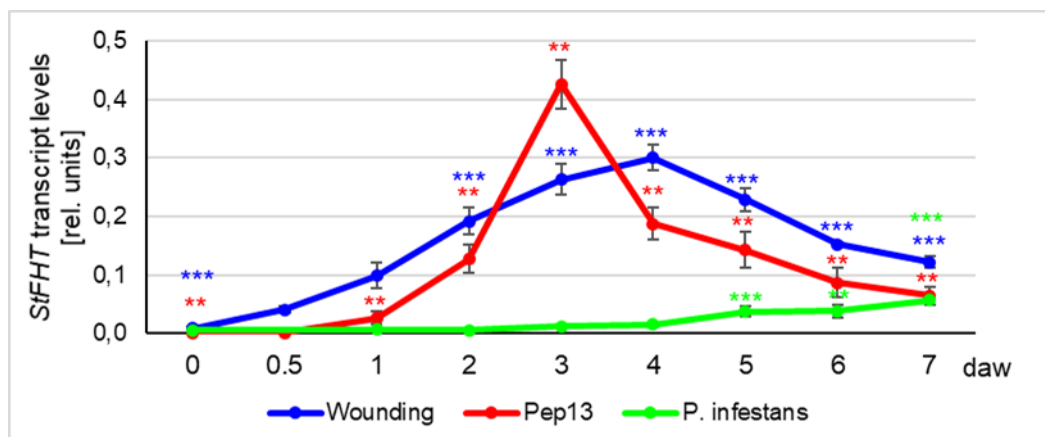


Figure 42: Induced expression of *StFHT* after wounding, Pep13 infiltration and *P. infestans* inoculation. Data derived from figures 12, 13 and 14. Gene expression of *StFHT* was analyzed up to 7 days after wounding (blue), after Pep13 infiltration (red) and after *P. infestans* inoculation (green).

Findings regarding *StCYP86A33* revealed very low constitutive expression in roots and none in stems, leaves, tubers parenchyma and flowers (Bjelica et al., 2016; Haggitt, 2016; Serra et al., 2009b). On the other hand, very high levels of transcripts can be found in tuber periderm between 2 and 14 days after wounding (Wahrenburg et al., 2021;

Woolfson et al., 2018; Lulai and Neubauer, 2014; Serra et al., 2009b). In contrast, the Arabidopsis homologous gene (*AtCYP86A1*) has constitutively high transcript levels only in roots, yet, stems can accumulate transcripts 1 day after wounding (Vishwanath, 2013b; Höfer et al., 2008; Duan and Schuler, 2005). So far, no data were published about *StCYP86A33* in wounded potato leaves. However, Wei et al. (2020) reported high levels of transcripts in shoots and leaves of *AchnCYP86A1* in kiwifruit, which is homologous to *StCYP86A33*. The same study showed an accumulation of transcript levels until 6 days after wounding. Our data show higher expression of *StCYP86A33* at later time points in comparison to the other genes involved in the suberin pathway, like *StABCG1* and *StFHT*, after each treatment (wounding – Fig. 13; Pep13 infiltration – Fig. 12; and *P. infestans* inoculation – Fig. 14).

In contrast to the other genes studied, *StKCS6* had a significant decrease of transcript levels 12 hours after wounding (Fig. 13D) and Pep13 infiltration (Fig. 12D), and 1 day after *P. infestans* inoculation (Fig. 14D). Serra et al. (2009a) reported very low constitutive expression of *StKCS6* in stems, roots and leaves and no expression in the tuber parenchyma. However, *StKCS6* is highly expressed in tuber periderm, like *StCYP86A33*. In contrast, the homologous *HaKCS2* gene in sunflower has a highly constitutive expression in stems, roots, and leaves (González-Mellado et al., 2019). Our analysis showed that *StKCS6* transcript levels are reduced 12 hours after wounding, returning to normal levels 1 day after wounding. However, we analyzed until 7 days, and as demonstrated in the literature, this gene could have an accumulation of transcript levels in leaves at much later time points. For example, Fogelman et al. (2014) showed a strong expression of *StKCS6* 10 days after wounding in tubers and Holbein et al. (2019) also reported, although there are differences in the approaches, very high expression of the homologous *AtKCS2* gene in Arabidopsis 10 days after inoculation of the parasitic nematode *Heterodera schachtii* in roots.

StABCG1, *StFHT* and *StCYP86A33* have a similar pattern of expression after wounding, Pep13 infiltration and *P. infestans* inoculation, indicating a co-regulation of these genes after the lesion is formed in leaves of *S. tuberosum*. The expression pattern of the genes studied suggest that there is a correlation of the gene expression and the cell death/lesion after each treatment in most of the genes. This is clearly visible for *StFHT*

expression (Fig. 42). For example, *StABCG1*, *StFHT*, *StKCS6*, *StFAR1*, *StFAR3*, *StLAC14* and *StPPO* had a very rapid response in transcript levels after wounding, which causes an instantaneous lesion on the leaf surface. On the other hand, leaves infiltrated with Pep13 had a slightly slower increase of transcript levels, as observed by Pep13 causing a hypersensitive response 24 hours after infiltration. In a laboratory-controlled experimental setup, *P. infestans* starts its necrotrophic phase 3 days after inoculation (Kelley et al., 2010). In this plant-pathogen interaction, cell death occurs later in comparison to the other treatments, triggering a significantly higher expression on these suberin-related genes much later (Fig. 14).

As the main focus of this study was the suberin production in leaves, gene expression for all genes was analyzed in leaves after different treatments. Given that these genes were already described in tubers of *S. tuberosum* (Landgraf et al., 2014; Serra et al., 2010; Serra et al., 2009a; Serra et al., 2009b), it is possible that the genes controlling suberin formation in tubers might be different from the ones in leaves. Furthermore, there are more genes involved in the suberin pathway, which are yet to be described in potato. In addition, the *StKCS6* is downregulated after each treatment performed in leaves, but it is still involved in the suberin pathway in tubers. Or yet, *StGPAT5* and *StGPAT6* were suggested to be involved in the metabolism of acyl chains and glycerol for the suberin biosynthesis (Woolfson et al., 2018).

As previously described, FAR genes encode Fatty acyl-CoA Reductases and they are responsible for the reduction of acyl chains to primary alcohols (Domergue et al., 2010). Analyzing the amino acid sequence of *StFAR1* and *StFAR3*, it was possible to find the respective homologous genes *AtFAR4* (54 % identity) and *AtG7/AtCER3/FAR3* (63 % identity) in Arabidopsis. Domergue et al. (2010) reported that *AtFAR4* is constitutively expressed in roots, but not in leaves, and it is also wounding-induced in stems. Furthermore, *StFAR1* is also upregulated, similarly to the genes involved in suberin biosynthesis in potato (*StABCG1*, *StFHT* and *StCYP86A33*) after the treatments analyzed (Fig. 12, 13 and 14), suggesting a role in suberin formation. Nonetheless, functional analyses must be performed, such as gene knockout and assessment for suberin formation. On the other hand, although *StFAR3* was also upregulated after each treatment (Fig. 12, 13 and 14), the expression of its homologous gene in Arabidopsis might be

considered dubious, since Domergue et al. (2010) and Rowland et al. (2006) reported different patterns of expression in the same tissues. In addition, Kamigaki et al. (2009) described that the RNAi-plants targeting the Peroxisome Biogenesis Factor 10 (*AtPEX10*) reduced cuticular wax accumulation and these plants also present low *AtFAR3* transcript levels. Rowland et al. (2006) also showed that *AtFAR3* plays a role in cuticular wax biosynthesis. Supporting this data, Kosma et al. (2014) reported that the overexpression of the transcription factor *AtMYB41* leads to the accumulation of suberin biosynthesis gene transcripts, resulting in a 22-fold increase in suberin-type in relation to cutin-type aliphatic monomers in leaves. *AtFAR4* is 1762-fold change higher in *AtMYB41* overexpressing plants in comparison to the wild-type, while *AtFAR3* had a 0.1-fold change higher (Kosma et al., 2014), implying that *AtFAR4* and its homologous *StFAR1* are more likely to be involved in suberin biosynthesis and *FAR3* in cutin biosynthesis in Arabidopsis and potato.

In contrast to the other genes, *StKCS6* is not induced after any of the treatments analyzed in leaves. In addition, it has a constitutive expression in leaves, what might be sufficient for its enzymatic activity in the suberin pathway. A second hypothesis is that there is another KCS gene is responsible for the elongation of fatty acids in potato leaves. Moreover, *StKCS11* and *StGPAT4* transcript levels were significantly high in the RNAseq data of Pep13-infiltrated leaves (Fig. 11). This results that were not consistent with RT-qPCR data of wounded leaves (Fig. 13), and so these genes were not analyzed after Pep13 infiltration and *P. infestans* inoculation.

4.2. Use of CrisprCas9 technology in *Solanum tuberosum*

In the last decade, the use of CRISPR/Cas9 technology was a big step in targeted genome editing in eukaryotes. CRISPR/Cas9 allows deletions/insertions into selected genes, by breaking both DNA strands, which triggers repair mechanisms, resulting in the knockout or modification of the gene of interest (Makarova et al., 2018).

Generally, many crops are polyploid. For example, wheat can be tetraploid or hexaploid, depending on the variety, rice is tetraploid, sugarcane is octoploid, and the cultivated potato is a tetraploid crop. The use of the CRISPR/Cas9 technology does not

require changes for polyploid plants (Makarova et al., 2018). A key problem regarding editing polyploid plants is the need to prove that all alleles have been successfully edited, since multiple allele mutations occur less frequently in comparison to that in single alleles, while other plants used for research are less heterozygous or sometimes homozygote. Still, Wang et al. (2014) reported the successful use of CRISPR/Cas technology for editing of all three genomes of hexaploid bread wheat, with a mutation frequency of 5.6 %. On the other hand, very few works have reported gene editing by CRISPR/Cas9 in potato plants. Usually, they have a low efficiency as they mostly employ generation of protoplasts and subsequently regeneration of plant shoots. Andersson et al. (2018), for example, used PEG-mediated protoplast transformation of potato plants. All four alleles of the Granule-bound Starch Synthase gene (*StGBSS1*) were edited with an efficiency of 2-3 %. More recently, the same group reported that, by changing the Cas9 promoter, it was possible to obtain an improvement with 35 % full allelic gene editing (Johansen et al., 2019). The use of protoplasts to transform potato plants seems to be very convenient, but it was previously described to cause more aneuploidy or structural chromosomal changes in *S. tuberosum* than *Agrobacterium tumefaciens*-mediated transformation (ATMT) (Fossi et al., 2016). Kieu et al. (2021), for instance, reported the use of ATMT to insert the CRISPR/Cas9 machinery in potato plants, targeting 7 different susceptibility genes, including *StDND1* (Defense, no death), *StbHLH7* (Basic helix-loop-helix protein) and *StDMR6-1* (Downy mildew resistance 6-1), which leads to *P. infestans* resistance. They had different efficiency for 4-alleles mutations for each gene, ranging from 0 % to 18 %. However, they did not check single nucleotide indels, suggesting that the efficiency might be even higher. In addition, the 0 % efficiency is regarding the *StHDS* (1-hydroxy-2-methyl-2-(E)-butenyl-4-diphosphate Synthase), which its knockout results in a seedling-lethal phenotype in Arabidopsis and *N. benthamiana* (Zhang et al., 2019b). Furthermore, Butler et al. (2015) reported a transformation of tetraploid potato plants via ATMT, using a geminivirus-based DNA replicon to increase the copy number of CRISPR/Cas9, reaching an efficiency of 32 %. A recent report had compared the efficiency of both methods, ATMT and PEG-mediated protoplast transformation, targeting genes encoding Starch-Branching Enzymes (*StSBR1* and *StSBE2*) in tetraploid potato (Tuncel et al., 2019). Although, in their work, 3 different constructs were used, and the number of

approaches were different for each method, through ATMT, 12 % of the calli generated plants with mutations in at least one of the targeted genes, and through PEG-treated protoplasts, 1.5 %. In the protoplast approach, 7 out of 10 plants did not present the Cas9 integrated in the genome, in such a way that the editing of the SBE genes were induced by transient expression of the sgRNA/Cas9 complex. The low rate of transgenic plants might be due to the absence of selection pressure, since the cassette was not present in the genome. Even if this genotype is still not commercially allowed in Europe, this represents a big step in genetic engineering, since the absence of the Cas9 reduces one breeding step to remove the cassette from the genome and it also avoids the disruption of other genes, since the integration in the genome is random.

4.3. StABCG1-CrisprCas plants have defective suberin formation

In order to prevent or reduce suberin formation, CRISPR/Cas9 technology was used to knockout the *StABCG1* gene via ATMT. PCR products derived from the region around the gRNA cut with Cas9/gRNA complex (Fig. 15) and the Illumina sequencing (Table 2 and Fig. 16) revealed that the plants obtained had possibly chimeric tissue. According to the sequencing results, four of the five plants analyzed had a very low (< 1 %) number of reads corresponding to WT alleles (Table 2), which can be considered as insignificant due to possible mutations, errors of DNA extraction, PCRs and/or readings. In addition, the number of reads containing *in frame* indels found in the plants #132 and #143 was less than 2.5 %, identifying both plants as fully knocked out plants (Table 2). It has not been determined whether all alleles of the *StABCG1* gene contribute equally to protein activity in potato plants. Still, all five *StABCG1*-CrisprCas plants had similar phenotypes. Only few readings of the Illumina sequencing had just a single amino acid missing (mainly in plant #142 and #149 – Fig. 16). Most of the mutations found in the *StABCG1*-CrisprCas plants results in a frame shift.

The use of CRISPR/Cas9 technology for editing a gene, does not necessarily reduce its respective transcript levels. For example, Jia et al. (2016) reported no changes in transcript levels of *CBF1* (C-repeat binding factor 1) in *Arabidopsis cbf1,3-1* CRISPR/Cas9 double mutant, even though the *CBF1* allele presented an 11 bp deletion,

leading to a frame shift with earlier stop codon in the predicted amino acid sequence. On the other hand, Zhang et al. (2019b) described a dramatic reduction of transcript levels in maize after use of CRISPR/Cas9 technology. Here, all *StABCG1*-CrisprCas plants had a significantly reduced expression of *StABCG1* after Pep13 infiltration and after wounding (Fig. 17 and 20). The frameshift leads to an earlier stop codon formation, which is located downstream of the homologous sequences of the primers used for RT-qPCR in the alleles with most reads. This suggests either a reduction of transcript levels due to the out-of-target primers or that the transcripts formed might lead to a nonsense-mediated mRNA decay.

The *StABCG1*-CrisprCas plants also had a defective suberin formation in leaves (Fig. 18 and 21) and in tubers (Fig. 30), supporting the hypothesis that *StABCG1* transporter is necessary to export the suberin monomers, as described by Landgraf et al. (2014). Nonetheless, a small number of wounded samples in leaves and tubers of the *StABCG1*-CrisprCas plants were able to produce suberin, indicating a possible gene redundancy. In the literature, a surprising number of ABC genes are described. For instance, Banasiak and Jasinski (2021) had reported around 130 ABC transporters in *Arabidopsis*, 43 of which belong to family G. No other plant in this review contained more ABC genes than potato, which contains 250 ABC transporters, wherein 130 have its place in the family G. Recently, the homologous gene *AtABCG1* of *Arabidopsis* was reported to be involved in the transport of suberin precursors (Shanmugarajah et al., 2019) in roots and *in vitro*. Nevertheless, a variety of ABC transporters are identified to have the same role in roots, suggesting functional redundancy (Xin and Herburger, 2021). In *Arabidopsis*, for example, *AtABCG1* is described to be involved in suberin formation in roots and *AtABCG2*, *AtABCG6* and *AtABCG20*, in roots, coats and seeds (Nomberg et al., 2022). Yadav et al. (2014) reported that the triple-mutant *atabcg2atabcg6atabcg20* displayed defective suberin formation and higher permeability in roots. This redundancy appears to be normal for ABC transporters. For example, three different reports showed that a defective pollen wall was found in *Arabidopsis* when both *AtABCG1* and *AtABCG16* were knocked out together, the same does not happen in single mutants (Liu et al., 2020; Yim et al., 2016; Yadav et al., 2014). Also, in *N. benthamiana*, *NbABCG2* is described to be functionally redundant to *NbABCG1*, which are related to pre- and postinvasion defense

against *P. infestans* (Shibata et al., 2016). These facts suggest, that even with the completely knocked out *StABCG1*, there may still be other genes with similar functions in *S. tuberosum*.

4.3.1. Browning in the *StABCG1*-CrisprCas plants

Leaves from *StABCG1*-CrisprCas had developed a brown ring around the lesion after Pep13 infiltration and after wounding (Fig. 19 and 23). Also, the transformed tubers turned brown faster than the WT after wounding (Fig. 33A). Wounding and mechanical damage, for example, were already described to induce overproduction of reactive oxygen species (ROS - Chen et al., 2017; Zhang et al., 2018), suggesting that the tissue browning might be derived from enzymatic and/or non-enzymatic reactions. Upon tissue disruption, substrates encounter proteins (enzymatic tissue-browning), such as polyphenol oxidases (peroxidases – PRXs; polyphenol oxidases – PPOs; Laccases – LAC) or reactive oxygen species (non-enzymatic tissue browning). Browning tissue indicates oxidation of phenolic compounds to quinones, causing a dark tissue formation, as described in fruits and vegetables (González et al., 2020; Jukant, 2017; Llorente et al., 2011). Quinones are effective oxidizing agents, tending to react with different compounds, such as proteins, nucleic acids and lipids (Zhu et al., 2020; Loomis, 1974). The lack of suberin observed in the *StABCG1*-CrisprCas plants implies that the gas barrier is absent, promoting the entrance of oxygen, which leads to induce ROS and consequently tissue browning.

In this work, the general term polyphenol oxidases is abbreviated as PPOs to cover the specific terms PPOs and LAC. PPOs can be found in different plant tissues and are involved in different pathways (Jukant, 2017), as well as in plant defense responses (González et al., 2020). In the literature, there are several examples of the usage from genetic engineering to reduce enzymatic browning in plants. Just in potato, different studies had shown that the downregulation (Llorente et al., 2011; Coetzer et al., 2001; Bachem et al., 1994) or knockout (González et al., 2020) of PPOs leads to reduction of the enzymatic browning. Also, silencing of *StPPO* has been reported to enhance resistance against bruise (Rommens et al., 2006; Bachem et al., 1994).

The brown tissue formed after wounding in the *StABCG1*-CrisprCas plants was analyzed by untargeted metabolite profiling via ultra-high performance liquid chromatography coupled with electrospray ionization quadrupole time-of-flight mass spectrometry, with help of Dr. Karin Gorzolka (IPB, Halle, Germany). This brown tissue revealed a variety of hydroxycinnamic acid amides (HCAAs) in a larger quantity in comparison to the controls (Fig. 24). Some of these compounds, such as ferulic acid and occasionally caffeic acid, can be found covalently-linked to suberin, as well as in the non-polymeric suberin waxes, being an important part of the suberin structure (Graça, 2010). In addition, at least for feruloyl derivatives compounds, for example, it is possible to correlate that the more oxidized amines found in the HCAA, the greater the amount found in wounded leaves of the *StABCG1*-CrisprCas plants (Fig. 43). Although this fact is just a correlation, and it is not true for all HCAAs, it indicates that there might be more oxygen coming in the lesions in the absence of suberin.

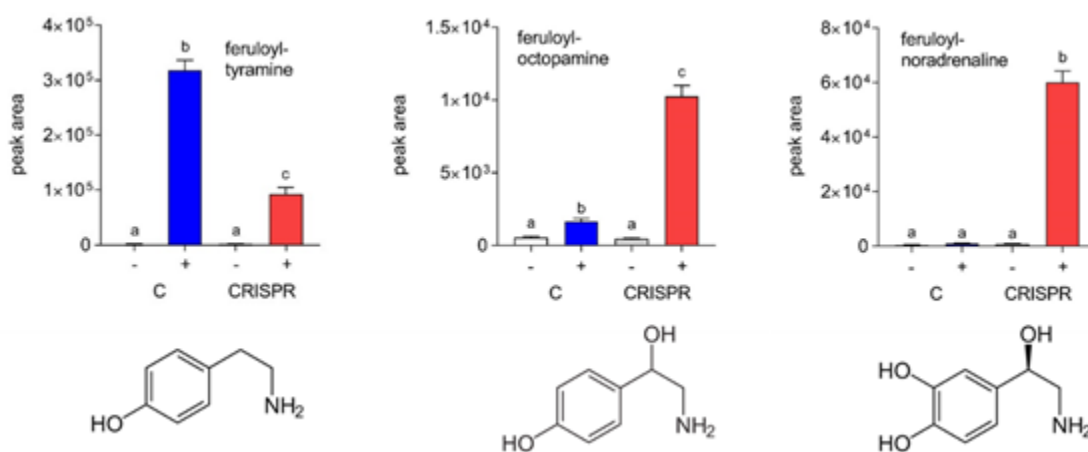


Figure 43: Feruloyl derivatives HCAAs accumulate in wounded *StABCG1*-CrisprCas. Data derived from figure 24. Ten-days-old wounded area from leaves of wild-type and *StABCG1*-CrisprCas plants was isolated and subjected to UPLC-MS analysis. Data from three independent experiments are shown from non-wounded (white/grey, -) and 10 days wounded tissue (blue/red, +). Chemical formulas correspond to the respective amine compound from the graph above.

HCAAs are described to have antimicrobial activity and also to contain pathogen infection by the formation of polymers reinforcing the secondary cell walls (Yogendra et al., 2015a; Yogendra et al., 2015b; Gunnaiah et al., 2012). For instance, in *Arabidopsis* plants, the expression of the agmatine coumaroyl transferase from wheat (*TaACT*) accumulates HCAAs, such as coumaroylagmatine and coumaroylputrescine, leading to

Fusarium head blight resistance (Kage et al., 2017). In *Solanum* species, overexpressing Tyramine N-hydroxycinnamoyl transferase in tomato plants lead to an accumulation of HCAAs, which leads to enhanced tolerance against *Pseudomonas syringae* (Campos et al., 2014). More specifically, Dobritsch et al. (2016) reported that *S. tuberosum* plants expressing the p-coumaroyl-CoA:agmatine N4-p-coumaroyl transferase gene *AtACT* and the gene *AtDTX18*, encoding a MATE transporter, were able to secrete high levels of coumaroylagmatine and putrescine conjugates. The same study also correlated the high amounts of the compound with reduced biomass of *P. infestans* on these plants, suggesting an antimicrobial activity for coumaroylagmatine.

In the absence of suberin, wounded *StABCG1*-CrisprCas tubers are also possibly exporting different compounds, which might prevent growth of pathogens, as already seen in wounded leaves. Unfortunately, we were not able to perform metabolomics in tubers as it has been done in leaves. However, the accumulation of HCAAs in leaves from *StABCG1*-CrisprCas plants put forward the hypothesis that the same is happening in the transformed tubers. For example, Landgraf et al. (2014) reported accumulation of some HCAAs in *StABCG1*-RNAi tuber periderm, like caffeoyl- and feruloylputrescine. Ginzberg (2008) suggests that accumulation of HCAA is happening very early after wounding in the periderm of tubers and these compounds act as a primary phenolic barrier against pathogen attack, due to their antimicrobial activity, and cell wall reinforcement. Together with the suberin polyaromatic domain, formed later, they will serve as a permanent barrier. Very few reports have described suberin formation though temporal changes across wound-healing in tubers of *S. tuberosum*, which still need to be well-studied in timescales. However, an old report has described that the deposition of the suberin phenolic domain slowly starts to form 1 day after wounding in tubers, and it extends to radial walls of the lesion after 4 days, and it is completely formed after the 5th day (Lulai and Corsini, 1998). The same report described that suberin aliphatic domain starts slowly 1 day after wounding and it extends to radial walls of the lesion after 6 days (Lulai and Corsini, 1998). In our analyses, it was possible to observe an acquired resistance 7 days after *P. infestans* inoculation (Fig. 34), when the oomycete was inoculated directly into the *StABCG1*-CrisprCas tubers after the wounding. Considering that at this time point, suberin is not formed, the oomycete is able to grow on the wild-type tubers 0 days after wounding.

Possibly due to different compounds formed after wounding in the *StABCG1*-CrisprCas tubers, growth of *P. infestans* was significantly reduced in comparison to the controls at 0 day after wounding/7 days after inoculation. As described by Lulai and Corsini (1998), at 3 days after wounding, suberin phenolic deposition can be found in the first layer of cells around the lesion and the suberin aliphatic domain is still not totally developed. For this reason, the beginning of suberin formation on the lesion could be holding the oomycete to grow in the wild-type tubers 3 days after wounding onwards, since no significant difference of *P. infestans* fluorescence was found at 3, 7 or 14 days after wounding (Fig. 34). Yet, further analyses are needed to understand what is exactly inducing the resistance in *StABCG1*-CrisprCas tubers after wounding.

4.4. *AtMYB39* expressing potato plants had enhanced suberin formation

In order to enhanced suberin formation in *S. tuberosum*, different constructs were tested. Although the betalain constructs, which contain the betalain biosynthesis genes under control of TALE, had generated a red coloration in potato leaves, it also triggered necrosis in potato plants (Fig. 37). In addition, insufficient number of plants could be generated with the EP45 constructs, which contain the putative suberin biosynthetic genes under control of TALE and the pathogen inducible promoter *pPVS3*, indicating that cell death triggered by the TALE inhibit plant growth. For example, similar cell death has been described in tomato plants after transient expression of TALE (Schornack et al., 2005). To bypass these difficulties, a cassette containing each putative gene involved in the suberin pathway under control of the 35S promoter was used. However, none of the target genes had an overexpression in the transgenic plants in comparison to the controls (Fig. 39), despite the fact that the promoters and terminators chosen being already proven to work in potato plants.

As cited before, a number of transcription factors was described to induce suberin formation in Arabidopsis (Shukla et al., 2021; Cohen et al., 2020; Mahmood et al., 2019; Lashbrooke et al., 2016; Kosma et al., 2014). For instance, Cohen et al. (2020) had described that overexpression of the *AtMYB39* in Arabidopsis activated the suberin-

related genes and enhanced suberin deposition in *Arabidopsis* roots. In addition, it leads to formation of a suberin-like lamellae in *N. benthamiana* leaves after transient expression.

To achieve enhanced suberin formation in *S. tuberosum* leaves, a construct containing the *AtMYB39* under control of the 35S promoter was designed and used to generate transgenic potato plants. Indeed, the expression of *AtMYB39* in *S. tuberosum* changed the expression of some suberin-related genes. Unfortunately, this observation is not true for all lines (Fig. 40). Despite all EP91 plants showing identical edition patterns and response to wounding, the plant EP91.1, for example, showed a significant differential expression for *StABCG1*, *StFHT* and *StKCS6*. However, the transcript levels of the transgenic lines EP91.7 and EP91.17 were equivalent to the controls for all genes studied (Fig. 40). Although Cohen et al. (2020) had reported significant overexpression of CYP86A1, homologous to *StCYP86A33*, in *AtMYB39* expressing *N. benthamiana* leaves, all EP91 lines had an equivalent expression of this gene in comparison to the controls (Fig. 40). In addition, the homologous gene *KCS2* was also overexpressed after *AtMYB39*, while *StKCS6* transcript levels were significantly reduced in the EP91.1 plant. This fact correlates with the previously mentioned hypotheses (see section 4.1), that *StKCS6* has a constitutive expression in leaves and that is enough for its enzymatic activity in the suberin pathway or it is not involved in the suberin formation in potato leaves. Even though not all plants had shown a significant change on transcript levels of the studied genes, all plants analyzed were able to produce more suberin 3 days after wounding in comparison to the controls (Fig. 41).

As Cohen et al. (2020) had described, *AtMYB39* not only activates the genes involved in suberin formation, but also those needed in the assembly and deposition of the suberin components at their pertinent subcellular sites. For a better analysis, the expression of other genes should be evaluated in *S. tuberosum*. However, not many genes are described to be related to the suberin formation in potato. In addition, the enhanced suberin formation in the *AtMYB39* expressing plants indicates that the transcription factor in fact regulates the suberin biosynthesis also in *S. tuberosum*.

To correlate the suberin role in the plant defense, it is still necessary to analyze the *P. infestans* biomass on these plants. However, due to technical reasons and time issues,

this analysis could not be performed. Yet, these plants can be used in future studies as a resource to identify the target genes of *AtMYB39* in potato.

5. SUMMARY

Potato (*Solanum tuberosum*) is one of the most important food crop worldwide with a production of 359 million tonnes per year. Germany is responsible for an annual production of 11 million tonnes, behind China, India, Ukraine, Russia and USA. One of the main causes of potato yield loss is late blight, a disease caused by the oomycete *Phytophthora infestans*. Due to reduced potato production and increased use of fungicides, late blight causes approximately US\$ 10 billion in losses worldwide each year, making late blight economically the most important foliar disease.

Plants have different ways to protect themselves in response to pathogens and insect attacks. For example, they can produce metabolites, signaling molecules or induce formation of physical barriers, such as cutin and suberin. Suberin is a heteropolymer composed of polyaliphatic linked with polyphenolic components. The polyaliphatic domain is mostly composed of a mixture of long chain fatty acids, primary alcohols, and glycerol, while the polyphenolic domain contains hydroxycinnamic acid derivatives, with ferulate being the major aromatic constituent of suberin in Arabidopsis, potato, and many other plants. This lipophilic barrier is presumed to contribute to successful defense against pathogens, such as *P. infestans*, and to be important for wound healing.

To date, several publications have proposed a correlation between suberin formation and plant defense, nevertheless very few show actual functional data. A number of studies have shown plants lacking suberin, but few have investigated their interactions with pathogens and wounding. Therefore, a concise description of the defense responses of plants either containing suberin or not is of significant interest.

To this end, potato plants were generated with reduced or enhanced suberin formation. Loss-of-function was obtained by gene editing using CRISPR/Cas9 targeting of the suberin transporter gene *StABCG1*. Gain of function was obtained by expressing the transcription factor *AtMYB39* from Arabidopsis in potato plants.

StABCG1 edited plants were analyzed to investigate suberin formation in leaves after infiltration of the *Phytophthora*-specific pathogen-associated molecular pattern Pep13, and in leaves and tubers after wounding and inoculation of *P. infestans*. These

analyses revealed the importance of suberin deposition in lesions occurring in *S. tuberosum*. While editing *StABCG1* had no consistent effect on *P. infestans* infection, wounding of leaves and tubers resulted in extensive tissue browning, correlating with a profound difference in the metabolite pattern. These plants revealed an accumulation of hydroxycinnamic acid amides, which are described to have an antimicrobial activity and also to contain pathogen infections, by reinforcing the secondary cell walls. These results suggest that the loss of suberin formation around disrupted cells prevents wound healing and allows oxygen diffusion into the cells, providing evidence that suberin deposition acts as a gas barrier.

The expression of the Arabidopsis transcription factor *MYB39* in potato plants resulted in enhanced suberin formation around wound sites in leaves, suggesting that *AtMYB39* induces expression of potato genes involved in suberin formation. However, not all genes identified as important for suberin formation in potato tubers were activated in *AtMYB39* expressing plants, suggesting that yet unidentified genes are required for suberin biosynthesis in leaves. The *AtMYB39* expressing plants are thus available for further studies to identify leaf-specific suberin biosynthesis genes.

This work presents functional evidence that suberin plays a pivotal role in wound healing of both leaves and tubers of potato.

6. ZUSAMMENFASSUNG

Die Kartoffel (*Solanum tuberosum*) ist, mit einer Produktion von 359 Millionen Tonnen pro Jahr, eine der wichtigsten Nahrungsmittelpflanzen weltweit. Deutschland liegt mit einer Jahresproduktion von 11 Millionen Tonnen hinter China, Indien, der Ukraine, Russland und den USA. Eine der Hauptursachen für Ertragseinbußen bei Kartoffeln ist die Kraut- und Knollenfäule. Sie ist auch bekannt als Kartoffelmehltau und wird durch den Oomyceten *Phytophthora infestans* verursacht. Aufgrund der verringerten Kartoffelproduktion und des verstärkten Einsatzes von Fungiziden verursacht die Kraut- und Knollenfäule jedes Jahr weltweit Verluste in Höhe von etwa 10 Milliarden US-Dollar und ist damit die wirtschaftlich wichtigste Blattkrankheit.

Pflanzen haben verschiedene Möglichkeiten, sich gegen Krankheitserreger und Insektenbefall zu schützen. Sie können beispielsweise Stoffwechselprodukte und Signalmoleküle produzieren oder die Bildung physikalischer Barrieren wie Cutin und Suberin veranlassen. Suberin ist ein Heteropolymer, das aus polyaliphatischen Bestandteilen in Verbindung mit polyphenolischen Komponenten besteht. Die polyaliphatische Domäne besteht hauptsächlich aus einer Mischung langkettiger Fettsäuren, primärer Alkohole und Glycerin, während die polyphenolische Domäne Hydroxyzimtsäurederivate enthält, wobei in Arabidopsis, Kartoffeln und vielen anderen Pflanzen Ferulasäure der wichtigste aromatische Bestandteil des Suberins ist. Es wird angenommen, dass diese lipophile Barriere zur erfolgreichen Abwehr von Krankheitserregern wie *P. infestans* beiträgt und wichtig für die Wundheilung ist.

Bisher wurde in mehreren Veröffentlichungen ein Zusammenhang zwischen der Bildung von Suberin und der pflanzlichen Verteidigung angenommen, doch nur sehr wenige zeigen tatsächliche funktionelle Daten. Eine Reihe von Studien haben Pflanzen mit fehlendem Suberin gezeigt, aber nur wenige haben ihre Wechselwirkungen mit Krankheitserregern und Verwundungen untersucht. Daher ist eine präzise Beschreibung der Abwehrreaktionen von Pflanzen, die entweder Suberin aufweisen oder nicht, von großem Interesse.

Zu diesem Zweck wurden Kartoffelpflanzen mit reduzierter oder erhöhter Suberinbildung erzeugt. Dieser Funktionsverlust wurde durch Gen-Editierung mittels CRISPR/Cas9-Targeting des Suberin-Transporter-Gens *StABCG1* erreicht. Ein Funktionsgewinn wurde durch die Expression des Transkriptionsfaktors *AtMYB39* aus Arabidopsis in Kartoffelpflanzen erreicht.

Um die Suberinbildung in Blättern nach Infiltration des Phytophthora-spezifischen pathogen-assoziierten molekularen Musters Pep13 zu untersuchen, wurden *StABCG1*-editierte Pflanzen analysiert. Außerdem wurde die Suberinbildung in Blättern und Knollen nach Verwundung und Inokulation von *P. infestans* analysiert. Diese Analysen zeigten die Bedeutung der Suberinablagerung bei Läsionen in *S. tuberosum*. Während die Editierung von *StABCG1* keine einheitliche Auswirkung auf die Infektion mit *P. infestans* hatte, führte die Verwundung von Blättern und Knollen zu einer ausgedehnten Bräunung des Gewebes, was mit einem tiefgreifenden Unterschied im Metabolitenmuster korrelierte. Diese Pflanzen wiesen eine Anhäufung von Hydroxyzimtsäureamiden auf, denen eine antimikrobielle Wirkung und eine Hemmung von Pathogeninfektionen durch Verstärkung der sekundären Zellwände beschrieben wurde. Daraus lässt sich schließen, dass der Verlust der Suberinbildung rund um die zerstörten Zellen die Wundheilung verhindert und die Sauerstoffdiffusion in die Zellen ermöglicht, was darauf hindeutet, dass die Suberinablagerungen als Gasbarriere wirken.

Die Expression des Arabidopsis-Transkriptionsfaktors *MYB39* in Kartoffelpflanzen führte zu einer verstärkten Suberinbildung rund um Wundstellen in den Blättern, was darauf schließen lässt, dass *AtMYB39* die Expression von Kartoffelgenen induziert, die an der Suberinbildung beteiligt sind. Allerdings wurden nicht alle Gene, die als wichtig für die Suberinbildung in Kartoffelknollen identifiziert wurden, in *AtMYB39*-exprimierenden Pflanzen aktiviert, was darauf schließen lässt, dass noch weitere nicht-identifizierte Gene für die Biosynthese von Suberin in Blättern notwendig sind. Die *AtMYB39*-exprimierenden Pflanzen stehen somit für weitere Studien zur Identifizierung blattspezifischer Gene für die Suberinbiosynthese zur Verfügung.

Diese Arbeit liefert funktionelle Beweise dafür, dass Suberin eine zentrale Rolle in der Wundheilung sowohl von Blättern als auch von Knollen der Kartoffel spielt.

7. REFERENCES

- Altmann, S. (2009). Dissertation: Funktionelle Analyse von 13-Lipoxygenaseabgeleiteten Oxylipinen in der Pathogenabwehr von *Solanum tuberosum* L. Available in <<http://dx.doi.org/10.25673/72>>. Accessed 08 December 2021.
- Andersson, M., Turesson, H., Olsson, N., Fält, A. S., Ohlsson, P., Gonzalez, M. N., ... & Hofvander, P. (2018). Genome editing in potato via CRISPR-Cas9 ribonucleoprotein delivery. *Physiologia Plantarum*, 164(4), 378-384.
- Andersson, M., Turesson, H., Nicolia, A., Fält, A. S., Samuelsson, M., & Hofvander, P. (2017). Efficient targeted multiallelic mutagenesis in tetraploid potato (*Solanum tuberosum*) by transient CRISPR-Cas9 expression in protoplasts. *Plant Cell Reports*, 36, 117-128.
- Andolfo, G., Ruocco, M., Di Donato, A., Frusciante, L., Lorito, M., Scala, F., & Ercolano, M. R. (2015). Genetic variability and evolutionary diversification of membrane ABC transporters in plants. *BMC Plant Biology*, 15(1), 1-15.
- Bachem, C. W., Speckmann, G. J., van der Linde, P. C., Verheggen, F. T., Hunt, M. D., Steffens, J. C., & Zabeau, M. (1994). Antisense expression of polyphenol oxidase genes inhibits enzymatic browning in potato tubers. *Bio/technology*, 12(11), 1101-1105.
- Bachmann-Pfabe, S., Hammann, T., Kruse, J., & Dehmer, K. J. (2019). Screening of wild potato genetic resources for combined resistance to late blight on tubers and pale potato cyst nematodes. *Euphytica*, 215(3), 48.
- Banasiak, J., & Jasiński, M. (2022). ATP-binding cassette transporters in nonmodel plants. *New Phytologist*, 233(4), 1597-1612. Barberon, M.; Vermeer, J. E. M.; De Bellis, D.; Wang, P.; Naseer, S.; et al. (2016). Adaptation of root function by nutrient-induced plasticity of endodermal differentiation. *Cell*. Vol. 164. 447-459.
- Barberon, M., Vermeer, J. E. M., De Bellis, D., Wang, P., Naseer, S., Andersen, T. G., ... & Geldner, N. (2016). Adaptation of root function by nutrient-induced plasticity of endodermal differentiation. *Cell*, 164(3), 447-459.
- Barel, G., & Ginzberg, I. (2008). Potato skin proteome is enriched with plant defence components. *Journal of Experimental Botany*, 59(12), 3347-3357.
- Barrell, P. J., Meiyalaghan, S., Jacobs, J. M., & Conner, A. J. (2013). Applications of biotechnology and genomics in potato improvement. *Plant Biotechnology Journal*, 11(8), 907-920.
- BASF. (2011). Application for authorization of *Phytophthora* resistant potato PH05-026-0048 for food and feed uses, processing and cultivation according to Regulation (EC) No 1829/2003. Available in <http://www.transgen.de/pdf/zulassung/Kartoffel/PH05-026-0048_application.pdf>. Accessed 08 December 2021.
- Beisson, F., Li-Beisson, Y., & Pollard, M. (2012). Solving the puzzles of cutin and suberin polymer biosynthesis. *Current opinion in Plant Biology*, 15(3), 329-337.
- Beisson, F., Li, Y., Bonaventure, G., Pollard, M., & Ohlrogge, J. B. (2007). The acyltransferase GPAT5 is required for the synthesis of suberin in seed coat and root of *Arabidopsis*. *The Plant Cell*, 19(1), 351-368.
- Bernards, M. A. (2002). Demystifying suberin. *Canadian Journal of Botany*, 80(3), 227-240.
- Bernards, M. A., & Razem, F. A. (2001). The poly (phenolic) domain of potato suberin: a non-lignin cell wall bio-polymer. *Phytochemistry*, 57(7), 1115-1122.
- Bernards, M. A., Fleming, W. D., Llewellyn, D. B., Priefer, R., Yang, X., Sabatino, A., & Plourde, G. L. (1999). Biochemical characterization of the suberization-associated anionic peroxidase of potato. *Plant Physiology*, 121(1), 135-146.

- Bernards, M. A., Lopez, M. L., Zajicek, J., & Lewis, N. G. (1995). Hydroxycinnamic Acid-derived Polymers Constitute the Polyaromatic Domain of Suberin (*). *Journal of Biological Chemistry*, 270(13), 7382-7386.
- Bjelica, A., Haggitt, M. L., Woolfson, K. N., Lee, D. P., Makhzoum, A. B., & Bernards, M. A. (2016). Fatty acid ω -hydroxylases from *Solanum tuberosum*. *Plant Cell Reports*, 35, 2435-2448.
- Blume, B., & Grierson, D. (1997). Expression of ACC oxidase promoter—GUS fusions in tomato and *Nicotiana plumbaginifolia* regulated by developmental and environmental stimuli. *The Plant Journal*, 12(4), 731-746.
- BMEL. (2021). Bundesministerium für Ernährung und Landwirtschaft. <<https://www.bmel-statistik.de>> Accessed in 11.05.2022.
- Boch, J., Scholze, H., Schornack, S., Landgraf, A., Hahn, S., Kay, S., ... & Bonas, U. (2009). Breaking the code of DNA binding specificity of TAL-type III effectors. *Science*, 326(5959), 1509-1512.
- Boher, P., Serra, O., Soler, M., Molinas, M., & Figueras, M. (2013). The potato suberin feruloyl transferase FHT which accumulates in the phellogen is induced by wounding and regulated by abscisic and salicylic acids. *Journal of Experimental Botany*, 64(11), 3225-3236.
- Bradeen, J. M., & Kole, C. (Eds.). (2016). *Genetics, genomics and breeding of potato*. CRC Press.
- Britt, A. B. (1999). Molecular genetics of DNA repair in higher plants. *Trends in Plant Science*, 4(1), 20-25.
- Brunner, F., Rosahl, S., Lee, J., Rudd, J. J., Geiler, C., Kauppinen, S., ... & Nürnberger, T. (2002). Pep-13, a plant defense-inducing pathogen-associated pattern from *Phytophthora* transglutaminases. *The EMBO Journal*, 21(24), 6681-6688.
- Buskila, Y., Tsrur, L., Sharon, M., Teper-Bamnolker, P., Holczer-Erich, O., Warshavsky, S., ... & Eshel, D. (2011). Postharvest dark skin spots in potato tubers are an oversubering response to *Rhizoctonia solani* infection. *Phytopathology*, 101(4), 436-444.
- Butler, N. M., Baltés, N. J., Voytas, D. F., & Douches, D. S. (2016). Geminivirus-mediated genome editing in potato (*Solanum tuberosum* L.) using sequence-specific nucleases. *Frontiers in Plant Science*, 7, 1045.
- Butler, N. M., Atkins, P. A., Voytas, D. F., & Douches, D. S. (2015). Generation and inheritance of targeted mutations in potato (*Solanum tuberosum* L.) using the CRISPR/Cas system. *PLoS one*, 10(12), e0144591.
- Campilho, A., Nieminen, K., & Ragni, L. (2020). The development of the periderm: the final frontier between a plant and its environment. *Current Opinion in Plant Biology*, 53, 10-14.
- Campos, L., Lison, P., López-Gresa, M. P., Rodrigo, I., Zacares, L., Conejero, V., & Bellés, J. M. (2014). Transgenic tomato plants overexpressing tyramine N-hydroxycinnamoyltransferase exhibit elevated hydroxycinnamic acid amide levels and enhanced resistance to *Pseudomonas syringae*. *Molecular Plant-Microbe Interactions*, 27(10), 1159-1169.
- Capote, T., Barbosa, P., Usié, A., Ramos, A. M., Inácio, V., Ordás, R., ... & Morais-Cecílio, L. (2018). ChIP-Seq reveals that QsMYB1 directly targets genes involved in lignin and suberin biosynthesis pathways in cork oak (*Quercus suber*). *BMC Plant Biology*, 18, 1-19.
- Chen, X., Ren, L., Li, M., Qian, J., Fan, J., & Du, B. (2017). Effects of clove essential oil and eugenol on quality and browning control of fresh-cut lettuce. *Food Chemistry*, 214, 432-439.
- Clasen, B. M., Stoddard, T. J., Luo, S., Demorest, Z. L., Li, J., Cedrone, F., ... & Zhang, F. (2016). Improving cold storage and processing traits in potato through targeted gene knockout. *Plant Biotechnology Journal*, 14(1), 169-176.
- Coetzer, C., Corsini, D., Love, S., Pavek, J., & Tumer, N. (2001). Control of enzymatic browning in potato (*Solanum tuberosum* L.) by sense and antisense RNA from tomato polyphenol oxidase. *Journal of Agricultural and Food Chemistry*, 49(2), 652-657.
- Cohen, H., Fedyuk, V., Wang, C., Wu, S., & Aharoni, A. (2020). SUBERMAN regulates developmental suberization of the Arabidopsis root endodermis. *The Plant Journal*, 102(3), 431-447.

- Cohen, H., Szymanski, J., & Aharoni, A. (2017). Assimilation of 'omics' strategies to study the cuticle layer and suberin lamellae in plants. *Journal of Experimental Botany*, 68(19), 5389-5400.
- Compagnon, V., Diehl, P., Benveniste, I., Meyer, D., Schaller, H., Schreiber, L., ... & Pinot, F. (2009). CYP86B1 is required for very long chain ω -hydroxyacid and α , ω -dicarboxylic acid synthesis in root and seed suberin polyester. *Plant Physiology*, 150(4), 1831-1843.
- Cooke, D. E. L., & Lees, A. K. (2004). Markers, old and new, for examining *Phytophthora infestans* diversity. *Plant Pathology*, 53(6), 692-704.
- Cornu, T. I., Thibodeau-Beganny, S., Guhl, E., Alwin, S., Eichtinger, M., Joung, J. K., & Cathomen, T. (2008). DNA-binding specificity is a major determinant of the activity and toxicity of zinc-finger nucleases. *Molecular Therapy*, 16(2), 352-358.
- Degenhardt, B., & Gimmler, H. (2000). Cell wall adaptations to multiple environmental stresses in maize roots. *Journal of Experimental Botany*, 51(344), 595-603.
- Diambra, L. A. (2011). Genome sequence and analysis of the tuber crop potato. *Nature*, 475.
- Diémé, A., Sambe, M. A. N., Agbangba, E. C., & Sy, M. O. (2013). Residual effects of sucrose and hormonal treatments of the tuberization medium on in vitro germination of potato (*Solanum tuberosum* L.) microtubers. *American Journal of Plant Sciences*, 4(09), 1872.
- Dobritzsch, M., Lübken, T., Eschen-Lippold, L., Gorzolka, K., Blum, E., Matern, A., ... & Rosahl, S. (2016). MATE transporter-dependent export of hydroxycinnamic acid amides. *The Plant Cell*, 28(2), 583-596.
- Domergue, F., Vishwanath, S. J., Joubès, J., Ono, J., Lee, J. A., Bourdon, M., ... & Rowland, O. (2010). Three Arabidopsis fatty acyl-coenzyme A reductases, FAR1, FAR4, and FAR5, generate primary fatty alcohols associated with suberin deposition. *Plant Physiology*, 153(4), 1539-1554.
- Duan, H., & Schuler, M. A. (2005). Differential expression and evolution of the Arabidopsis CYP86A subfamily. *Plant Physiology*, 137(3), 1067-1081.
- Eck, J. V. (2018). Genome editing and plant transformation of solanaceous food crops. *Current Opinion in Biotechnology*, 49, 35-41.
- Enciso-Maldonado, G. A., Lozoya-Saldaña, H., Colinas-Leon, M. T., Cuevas-Sanchez, J. A., Sanabria-Velázquez, A. D., Bamberg, J., & Raman, K. V. (2022). Assessment of wild *Solanum* species for resistance to *Phytophthora infestans* (Mont.) de Bary in the Toluca valley, Mexico. *American Journal of Potato Research*, 99(1), 25-39.
- Engler, C., & Marillonnet, S. (2014). Golden gate cloning. *DNA cloning and assembly methods*, 119-131.
- Engler, C., Gruetzner, R., Kandzia, R., & Marillonnet, S. (2009). Golden gate shuffling: a one-pot DNA shuffling method based on type II restriction enzymes. *PloS one*, 4(5), e5553.
- Engler, C., Kandzia, R., & Marillonnet, S. (2008). A one pot, one step, precision cloning method with high throughput capability. *PloS one*, 3(11), e3647.
- Enstone, D. E., Peterson, C. A., & Ma, F. (2002). Root endodermis and exodermis: structure, function, and responses to the environment. *Journal of Plant Growth Regulation*, 21, 335-351.
- Eschen-Lippold, L., Rothe, G., Stumpe, M., Göbel, C., Feussner, I., & Rosahl, S. (2007). Reduction of divinyl ether-containing polyunsaturated fatty acids in transgenic potato plants. *Phytochemistry*, 68(6), 797-801.
- FAO. (2021). Food and Agriculture Organization Corporate Statistical Database. <<http://www.fao.org>> Accessed in 30.07.2021.
- Feltkamp, D., Baumann, E., Schmalenbach, W., Masterson, R., & Rosahl, S. (1995). Expression of the mannopine synthase promoter in roots is dependent on the mas elements and correlates with high transcript levels of mas-binding factor. *Plant Science*, 109(1), 57-65.
- Fogelman, E., Oren-Shamir, M., Hirschberg, J., Mandolino, G., Parisi, B., Ovadia, R., ... & Ginzberg, I. (2019). Nutritional value of potato (*Solanum tuberosum*) in hot climates: anthocyanins, carotenoids, and steroidal glycoalkaloids. *Planta*, 249, 1143-1155.

- Fogelman, E., Tanami, S., & Ginzberg, I. (2015). Anthocyanin synthesis in native and wound periderms of potato. *Physiologia Plantarum*, 153(4), 616-626.
- Fossi, M., Amundson, K., Kuppu, S., Britt, A., & Comai, L. (2019). Regeneration of *Solanum tuberosum* plants from protoplasts induces widespread genome instability. *Plant Physiology*, 180(1), 78-86.
- Franke, R., Höfer, R., Briesen, I., Emsermann, M., Efremova, N., Yephremov, A., & Schreiber, L. (2009). The DAISY gene from *Arabidopsis* encodes a fatty acid elongase condensing enzyme involved in the biosynthesis of aliphatic suberin in roots and the chalaza-micropyle region of seeds. *The Plant Journal*, 57(1), 80-95.
- Franke, R., Briesen, I., Wojciechowski, T., Faust, A., Yephremov, A., Nawrath, C., & Schreiber, L. (2005). Apoplastic polyesters in *Arabidopsis* surface tissues—a typical suberin and a particular cutin. *Phytochemistry*, 66(22), 2643-2658.
- Franke, R., & Schreiber, L. (2007). Suberin—a biopolyester forming apoplastic plant interfaces. *Current Opinion in Plant Biology*, 10(3), 252-259.
- Gillund, F. T., Nordgaard, L., Bøhn, T., Wikmark, O. G., Konestabo, H. S., & Hilbeck, A. (2013). Selection of nontarget testing organisms for ERA of GM potato with increased resistance to late blight. *Potato Research*, 56, 293-324.
- Ginzberg, I. (2008). Wound-periderm formation. Induced plant resistance to Herbivory, 131-146.
- Gisi, U., Walder, F., Resheat-Eini, Z., Edel, D., & Sierotzki, H. (2011). Changes of genotype, sensitivity and aggressiveness in *Phytophthora infestans* isolates collected in European countries in 1997, 2006 and 2007. *Journal of Phytopathology*, 159(4), 223-232.
- Gisi, U., & Cohen, Y. (1996). Resistance to phenylamide fungicides: a case study with *Phytophthora infestans* involving mating type and race structure. *Annual Review of Phytopathology*, 34(1), 549-572.
- Glendinning, D., MacDonald, J. A., & Grainger, J. (1963). Factors affecting the germination of sporangia in *Phytophthora infestans*. *Transactions of the British Mycological Society*, 46(4), 595-603.
- González, M. N., Massa, G. A., Andersson, M., Turesson, H., Olsson, N., Fält, A. S., ... & Feingold, S. E. (2020). Reduced enzymatic browning in potato tubers by specific editing of a polyphenol oxidase gene via ribonucleoprotein complexes delivery of the CRISPR/Cas9 system. *Frontiers in Plant Science*, 10, 1649.
- González-Mellado, D., Salas, J. J., Venegas-Calderón, M., Moreno-Pérez, A. J., Garcés, R., & Martínez-Force, E. (2019). Functional characterization and structural modelling of *Helianthus annuus* (sunflower) ketoacyl-CoA synthases and their role in seed oil composition. *Planta*, 249, 1823-1836.
- Gorzolka, K., Perino, E. H. B., Lederer, S., Smolka, U., & Rosahl, S. (2021). Lysophosphatidylcholine 17: 1 from the Leaf Surface of the Wild Potato Species *Solanum bulbocastanum* Inhibits *Phytophthora infestans*. *Journal of Agricultural and Food Chemistry*, 69(20), 5607-5617.
- Gou, J. Y., Yu, X. H., & Liu, C. J. (2009). A hydroxycinnamoyltransferase responsible for synthesizing suberin aromatics in *Arabidopsis*. *Proceedings of the National Academy of Sciences*, 106(44), 18855-18860.
- Graça, J. (2010). Hydroxycinnamates in suberin formation. *Phytochemistry Reviews*, 9, 85-91.
- Graça, J., & Pereira, H. (2000). Suberin structure in potato periderm: glycerol, long-chain monomers, and glyceryl and feruloyl dimers. *Journal of Agricultural and Food Chemistry*, 48(11), 5476-5483.
- Grützner, R., Schubert, R., Horn, C., Yang, C., Vogt, T., & Marillonnet, S. (2021). Engineering betalain biosynthesis in tomato for high level betanin production in fruits. *Frontiers in Plant Science*, 12, 682443.
- Gunnaiyah, R., Kushalappa, A. C., Duggavathi, R., Fox, S., & Somers, D. J. (2012). Integrated metabolo-proteomic approach to decipher the mechanisms by which wheat QTL (Fhb1) contributes to resistance against *Fusarium graminearum*. *PloS one*, 7(7), e40695.

- Haggitt, M. (2016). Dissertation: Role of Fatty Acid omega-hydroxylase 1 and abscisic acid in potato tuber suberin formation. Available in <<https://ir.lib.uwo.ca/etd/4074>>. Accessed 17.01.2021.
- Halim, V. A., Altmann, S., Ellinger, D., Eschen-Lippold, L., Miersch, O., Scheel, D., & Rosahl, S. (2009). PAMP-induced defense responses in potato require both salicylic acid and jasmonic acid. *The Plant Journal*, 57(2), 230-242.
- Halim, V. A. (2006). Dissertation: The Role of Salicylic Acid and Octadecanoids for Pathogen Defense in Potato. Available in <<https://sundoc.bibliothek.uni-halle.de/diss-online/06/06H120/index.htm>>. Accessed 09 December 2021.
- Halim, V. A., Hunger, A., Macioszek, V., Landgraf, P., Nürnberger, T., Scheel, D., & Rosahl, S. (2004). The oligopeptide elicitor Pep-13 induces salicylic acid-dependent and-independent defense reactions in potato. *Physiological and Molecular Plant Pathology*, 64(6), 311-318.
- Hatsugai, N., Igarashi, D., Mase, K., Lu, Y., Tsuda, Y., Chakravarthy, S., ... & Katagiri, F. (2017). A plant effector-triggered immunity signaling sector is inhibited by pattern-triggered immunity. *The EMBO Journal*, 36(18), 2758-2769.
- Haverkort, A. J., Struik, P. C., Visser, R. G. F., & Jacobsen, E. J. P. R. (2009). Applied biotechnology to combat late blight in potato caused by *Phytophthora infestans*. *Potato Research*, 52, 249-264.
- Higgins, C. F. (2001). ABC transporters: physiology, structure and mechanism—an overview. *Research in Microbiology*, 152(3-4), 205-210.
- Höfer, R., Briesen, I., Beck, M., Pinot, F., Schreiber, L., & Franke, R. (2008). The Arabidopsis cytochrome P450 CYP86A1 encodes a fatty acid ω -hydroxylase involved in suberin monomer biosynthesis. *Journal of Experimental Botany*, 59(9), 2347-2360.
- Höfgen, R., & Willmitzer, L. (1988). Storage of competent cells for Agrobacterium transformation. *Nucleic Acids Research*, 16(20), 9877.
- Holbein, J., Franke, R. B., Marhavý, P., Fujita, S., Górecka, M., Sobczak, M., ... & Siddique, S. (2019). Root endodermal barrier system contributes to defence against plant-parasitic cyst and root-knot nematodes. *The Plant Journal*, 100(2), 221-236.
- Holsters, M., Silva, B., Van Vliet, F., Genetello, C., De Block, M., Dhaese, P., ... & Schell, J. (1980). The functional organization of the nopaline A. tumefaciens plasmid pTiC58. *Plasmid*, 3(2), 212-230.
- Hufford, M. B., Berny Mier y Teran, J. C., & Gepts, P. (2019). Crop biodiversity: an unfinished magnum opus of nature. *Annual Review of Plant Biology*, 70, 727-751.
- Jefferson, R. A., Kavanagh, T. A., & Bevan, M. W. (1987). GUS fusions: beta-glucuronidase as a sensitive and versatile gene fusion marker in higher plants. *The EMBO Journal*, 6(13), 3901-3907.
- Jia, Y., Ding, Y., Shi, Y., Zhang, X., Gong, Z., & Yang, S. (2016). The cbfs triple mutants reveal the essential functions of CBF s in cold acclimation and allow the definition of CBF regulons in Arabidopsis. *New Phytologist*, 212(2), 345-353.
- Jinek, M., Chylinski, K., Fonfara, I., Hauer, M., Doudna, J. A., & Charpentier, E. (2012). A programmable dual-RNA-guided DNA endonuclease in adaptive bacterial immunity. *Science*, 337(6096), 816-821.
- Johansen, I. E., Liu, Y., Jørgensen, B., Bennett, E. P., Andreasson, E., Nielsen, K. L., ... & Petersen, B. L. (2019). High efficacy full allelic CRISPR/Cas9 gene editing in tetraploid potato. *Scientific Reports*, 9(1), 1-7.
- Joubès, J., Raffaele, S., Bourdenx, B., Garcia, C., Laroche-Traineau, J., Moreau, P., ... & Lessire, R. (2008). The VLCFA elongase gene family in *Arabidopsis thaliana*: phylogenetic analysis, 3D modelling and expression profiling. *Plant Molecular Biology*, 67, 547-566.
- Jones, J. D., & Dangl, J. L. (2006). The plant immune system. *Nature*, 444(7117), 323-329.
- Judelson, H. S., & Blanco, F. A. (2005). The spores of *Phytophthora*: weapons of the plant destroyer. *Nature Reviews Microbiology*, 3(1), 47-58.

- Judelson, H. S., & Tooley, P. W. (2000). Enhanced polymerase chain reaction methods for detecting and quantifying *Phytophthora infestans* in plants. *Phytopathology*, 90(10), 1112-1119.
- Jukanti, A. (2017). Polyphenol oxidases (PPOs) in plants. Springer Singapore.
- Kage, U., Karre, S., Kushalappa, A. C., & McCartney, C. (2017). Identification and characterization of a fusarium head blight resistance gene Ta ACT in wheat QTL-2 DL. *Plant Biotechnology Journal*, 15(4), 447-457.
- Kamigaki, A., Kondo, M., Mano, S., Hayashi, M., & Nishimura, M. (2009). Suppression of peroxisome biogenesis factor 10 reduces cuticular wax accumulation by disrupting the ER network in *Arabidopsis thaliana*. *Plant and Cell Physiology*, 50(12), 2034-2046.
- Kandel, S., Morant, M., Benveniste, I., Blée, E., Werck-Reichhart, D., & Pinot, F. (2005). Cloning, functional expression, and characterization of CYP709C1, the first sub-terminal hydroxylase of long chain fatty acid in plants: induction by chemicals and methyl jasmonate. *Journal of Biological Chemistry*, 280(43), 35881-35889.
- Karki, H. S., Jansky, S. H., & Halterman, D. A. (2021). Screening of wild potatoes identifies new sources of late blight resistance. *Plant Disease*, 105(2), 368-376.
- Kashyap, A., Jiménez-Jiménez, Á. L., Zhang, W., Capellades, M., Srinivasan, S., Laromaine, A., ... & Coll, N. S. (2022). Induced ligno-suberin vascular coating and tyramine-derived hydroxycinnamic acid amides restrict *Ralstonia solanacearum* colonization in resistant tomato. *New Phytologist*, 234(4), 1411-1429.
- Kelley, B. S., Lee, S. J., Damasceno, C. M., Chakravarthy, S., Kim, B. D., Martin, G. B., & Rose, J. K. (2010). A secreted effector protein (SNE1) from *Phytophthora infestans* is a broadly acting suppressor of programmed cell death. *The Plant Journal*, 62(3), 357-366.
- Kieu, N. P., Lenman, M., Wang, E. S., Petersen, B. L., & Andreasson, E. (2021). Mutations introduced in susceptibility genes through CRISPR/Cas9 genome editing confer increased late blight resistance in potatoes. *Scientific Reports*, 11(1), 1-12.
- Krishnamurthy, P., Ranathunge, K., Franke, R., Prakash, H. S., Schreiber, L., & Mathew, M. K. (2009). The role of root apoplastic transport barriers in salt tolerance of rice (*Oryza sativa* L.). *Planta*, 230, 119-134.
- Kolattukudy, P. T. (1981). Structure, biosynthesis, and biodegradation of cutin and suberin. *Annual Review of Plant Physiology*, 32(1), 539-567.
- Kotula, L., Schreiber, L., Colmer, T. D., & Nakazono, M. (2017). Anatomical and biochemical characterisation of a barrier to radial O₂ loss in adventitious roots of two contrasting *Hordeum marinum* accessions. *Functional Plant Biology*, 44(9), 845-857.
- Kosma, D. K., Murmu, J., Razeq, F. M., Santos, P., Bourgault, R., Molina, I., & Rowland, O. (2014). At MYB 41 activates ectopic suberin synthesis and assembly in multiple plant species and cell types. *The Plant Journal*, 80(2), 216-229.
- Landgraf, R. (2016). Dissertation: Charakterisierung des Pamp-induzierbaren Transporters *ABCG1* aus *Solanum tuberosum*. Available in <<http://dx.doi.org/10.25673/1874>>. Accessed 08 December 2021.
- Landgraf, R., Smolka, U., Altmann, S., Eschen-Lippold, L., Senning, M., Sonnewald, S., ... & Rosahl, S. (2014). The ABC transporter ABCG1 is required for suberin formation in potato tuber periderm. *The Plant Cell*, 26(8), 3403-3415.
- Lanoue, A., Burlat, V., Henkes, G. J., Koch, I., Schurr, U., & Röse, U. S. (2010). De novo biosynthesis of defense root exudates in response to Fusarium attack in barley. *New Phytologist*, 185(2), 577-588.
- Lashbrooke, J., Cohen, H., Levy-Samocho, D., Tzfadia, O., Panizel, I., Zeisler, V., ... & Aharoni, A. (2016). MYB107 and MYB9 homologs regulate suberin deposition in angiosperms. *The Plant Cell*, 28(9), 2097-2116.
- Lazo, G. R., Stein, P. A., & Ludwig, R. A. (1991). A DNA transformation-competent *Arabidopsis* genomic library in *Agrobacterium*. *Bio/technology*, 9(10), 963-967.

- Lee, S. B., Jung, S. J., Go, Y. S., Kim, H. U., Kim, J. K., Cho, H. J., ... & Suh, M. C. (2009). Two Arabidopsis 3-ketoacyl CoA synthase genes, KCS20 and KCS2/DAISY, are functionally redundant in cuticular wax and root suberin biosynthesis, but differentially controlled by osmotic stress. *The Plant Journal*, 60(3), 462-475.
- Leesutthiphonchai, W., Vu, A. L., Ah-Fong, A. M., & Judelson, H. S. (2018). How does *Phytophthora infestans* evade control efforts? Modern insight into the late blight disease. *Phytopathology*, 108(8), 916-924.
- Legay, S., Guerriero, G., André, C., Guignard, C., Cocco, E., Charton, S., ... & Hausman, J. F. (2016). MdMyb93 is a regulator of suberin deposition in russeted apple fruit skins. *New Phytologist*, 212(4), 977-991.
- Leide, J., Hildebrandt, U., Reussing, K., Riederer, M., & Vogg, G. (2007). The developmental pattern of tomato fruit wax accumulation and its impact on cuticular transpiration barrier properties: effects of a deficiency in a β -ketoacyl-coenzyme A synthase (LeCER6). *Plant Physiology*, 144(3), 1667-1679.
- Lemmon, Z. H., Reem, N. T., Dalrymple, J., Soyk, S., Swartwood, K. E., Rodriguez-Leal, D., ... & Lippman, Z. B. (2018). Rapid improvement of domestication traits in an orphan crop by genome editing. *Nature Plants*, 4(10), 766-770.
- Lenzian, K. J. (2006). Survival strategies of plants during secondary growth: barrier properties of phellements and lenticels towards water, oxygen, and carbon dioxide. *Journal of Experimental Botany*, 57(11), 2535-2546.
- Li, H., Pinot, F., Sauveplane, V., Werck-Reichhart, D., Diehl, P., Schreiber, L., ... & Zhang, D. (2010). Cytochrome P450 family member CYP704B2 catalyzes the ω -hydroxylation of fatty acids and is required for anther cutin biosynthesis and pollen exine formation in rice. *The Plant Cell*, 22(1), 173-190.
- Li, J. F., Norville, J. E., Aach, J., McCormack, M., Zhang, D., Bush, J., ... & Sheen, J. (2013). Multiplex and homologous recombination-mediated genome editing in Arabidopsis and *Nicotiana benthamiana* using guide RNA and Cas9. *Nature Biotechnology*, 31(8), 688-691.
- Li, Y., Beisson, F., Koo, A. J., Molina, I., Pollard, M., & Ohlrogge, J. (2007). Identification of acyltransferases required for cutin biosynthesis and production of cutin with suberin-like monomers. *Proceedings of the National Academy of Sciences*, 104(46), 18339-18344.
- Lindhout, P., Meijer, D., Schotte, T., Hutten, R. C., Visser, R. G., & van Eck, H. J. (2011). Towards F 1 hybrid seed potato breeding. *Potato Research*, 54, 301-312.
- Liu, L., Zhao, L., Chen, P., Cai, H., Hou, Z., Jin, X., ... & Qin, Y. (2020). ATP binding cassette transporters ABCG1 and ABCG16 affect reproductive development via auxin signalling in Arabidopsis. *The Plant Journal*, 102(6), 1172-1186.
- Llorente, B., Alonso, G. D., Bravo-Almonacid, F., Rodríguez, V., López, M. G., Carrari, F., ... & Flawiá, M. M. (2011). Safety assessment of nonbrowning potatoes: opening the discussion about the relevance of substantial equivalence on next generation biotech crops. *Plant Biotechnology Journal*, 9(2), 136-150.
- Loomis, W. D. (1974). [54] Overcoming problems of phenolics and quinones in the isolation of plant enzymes and organelles. In *Methods in enzymology* (Vol. 31, pp. 528-544). Academic Press.
- Lulai, E. C., & Corsini, D. L. (1998). Differential deposition of suberin phenolic and aliphatic domains and their roles in resistance to infection during potato tuber (*Solanum tuberosum* L.) wound-healing. *Physiological and Molecular Plant Pathology*, 53(4), 209-222.
- Lulai, E. C. (2007). Skin-set, wound healing, and related defects. In *Potato Biology and Biotechnology* (pp. 471-500). Elsevier Science BV.
- Lulai, E. C., & Freeman, T. P. (2001). The importance of phellogen cells and their structural characteristics in susceptibility and resistance to excoriation in immature and mature potato tuber (*Solanum tuberosum* L.) periderm. *Annals of Botany*, 88(4), 555-561.

- Lulai, E. C., & Neubauer, J. D. (2014). Wound-induced suberization genes are differentially expressed, spatially and temporally, during closing layer and wound periderm formation. *Postharvest Biology and Technology*, 90, 24-33.
- Machida-Hirano, R. (2015). Diversity of potato genetic resources. *Breeding Science*, 65(1), 26-40.
- Mahmood, K., Zeisler-Diehl, V. V., Schreiber, L., Bi, Y. M., Rothstein, S. J., & Ranathunge, K. (2019). Overexpression of ANAC046 promotes suberin biosynthesis in roots of *Arabidopsis thaliana*. *International Journal of Molecular Sciences*, 20(24), 6117.
- Makarova, S. S., Khromov, A. V., Spechenkova, N. A., Taliensky, M. E., & Kalinina, N. O. (2018). Application of the CRISPR/Cas system for generation of pathogen-resistant plants. *Biochemistry (Moscow)*, 83(12-13), 1552-1562.
- Marillonnet, S., & Grütznert, R. (2020). Synthetic DNA assembly using golden gate cloning and the hierarchical modular cloning pipeline. *Current Protocols in Molecular Biology*, 130(1), e115.
- Marois, E., Van den Ackerveken, G., & Bonas, U. (2002). The Xanthomonas type III effector protein AvrBs3 modulates plant gene expression and induces cell hypertrophy in the susceptible host. *Molecular Plant-Microbe Interactions*, 15(7), 637-646.
- Millar, A. A., Clemens, S., Zachgo, S., Giblin, E. M., Taylor, D. C., & Kunst, L. (1999). CUT1, an Arabidopsis gene required for cuticular wax biosynthesis and pollen fertility, encodes a very-long-chain fatty acid condensing enzyme. *The Plant Cell*, 11(5), 825-838.
- Miller, J. C., Holmes, M. C., Wang, J., Guschin, D. Y., Lee, Y. L., Rupniewski, I., ... & Rebar, E. J. (2007). An improved zinc-finger nuclease architecture for highly specific genome editing. *Nature Biotechnology*, 25(7), 778-785.
- Minogue, K. P., & Fry, W. E. (1981). Effect of temperature, relative humidity, and rehydration rate on germination of dried sporangia of *Phytophthora infestans*. *Phytopathology*, 71(11), 1181-1184.
- Molina, I., Li-Beisson, Y., Beisson, F., Ohlrogge, J. B., & Pollard, M. (2009). Identification of an Arabidopsis feruloyl-coenzyme A transferase required for suberin synthesis. *Plant Physiology*, 151(3), 1317-1328.
- Monaghan, J., & Zipfel, C. (2012). Plant pattern recognition receptor complexes at the plasma membrane. *Current Opinion in Plant Biology*, 15(4), 349-357.
- Morant, M., Jørgensen, K., Schaller, H., Pinot, F., Møller, B. L., Werck-Reichhart, D., & Bak, S. (2007). CYP703 is an ancient cytochrome P450 in land plants catalyzing in-chain hydroxylation of lauric acid to provide building blocks for sporopollenin synthesis in pollen. *The Plant Cell*, 19(5), 1473-1487.
- Murashige, T., & Skoog, F. (1962). A revised medium for rapid growth and bio assays with tobacco tissue cultures. *Physiologia Plantarum*, 15(3), 473-497.
- Muthoni, J., Kabira, J., Shimelis, H., & Melis, R. (2015). Tetrasomic inheritance in cultivated potato and implications in conventional breeding. *Australian Journal of Crop Science*, 9(3), 185-190.
- Nadakuduti, S. S., Starker, C. G., Voytas, D. F., Buell, C. R., & Douches, D. S. (2019). Genome editing in potato with CRISPR/Cas9. *Plant genome editing with CRISPR systems: Methods and protocols*, 183-201.
- Naseer, S., Lee, Y., Lapierre, C., Franke, R., Nawrath, C., & Geldner, N. (2012). Casparian strip diffusion barrier in Arabidopsis is made of a lignin polymer without suberin. *Proceedings of the National Academy of Sciences*, 109(25), 10101-10106.
- Nekrasov, V., Staskawicz, B., Weigel, D., Jones, J. D., & Kamoun, S. (2013). Targeted mutagenesis in the model plant *Nicotiana benthamiana* using Cas9 RNA-guided endonuclease. *Nature Biotechnology*, 31(8), 691-693.
- Nicolia, A., Proux-Wéra, E., Åhman, I., Onkokesung, N., Andersson, M., Andreasson, E., & Zhu, L. H. (2015). Targeted gene mutation in tetraploid potato through transient TALEN expression in protoplasts. *Journal of Biotechnology*, 204, 17-24.
- Nomberg, G., Marinov, O., Arya, G. C., Manasherova, E., & Cohen, H. (2022). The key enzymes in the suberin biosynthetic pathway in plants: An update. *Plants*, 11(3), 392.

- Nowicki, M., Foolad, M. R., Nowakowska, M., & Kozik, E. U. (2012). Potato and tomato late blight caused by *Phytophthora infestans*: an overview of pathology and resistance breeding. *Plant Disease*, 96(1), 4-17.
- Nürnberg, T., Nennstiel, D., Jabs, T., Sacks, W. R., Hahlbrock, K., & Scheel, D. (1994). High affinity binding of a fungal oligopeptide elicitor to parsley plasma membranes triggers multiple defense responses. *Cell*, 78(3), 449-460.
- Oh, S. K., Young, C., Lee, M., Oliva, R., Bozkurt, T. O., Cano, L. M., ... & Kamoun, S. (2009). In planta expression screens of *Phytophthora infestans* RXLR effectors reveal diverse phenotypes, including activation of the *Solanum bulbocastanum* disease resistance protein Rpi-blb2. *The Plant Cell*, 21(9), 2928-2947.
- Parker, J. E., Schulte, W., Hahlbrock, K., & Scheel, D. (1991). An extracellular glycoprotein from *Phytophthora megasperma* f. sp. *glycinea* elicits phytoalexin synthesis in cultured parsley cells and protoplasts. *Mol. Plant-Microbe Interact*, 4, 19-27.
- Paro, R., Tiboni, G. M., Buccione, R., Rossi, G., Cellini, V., Canipari, R., & Cecconi, S. (2012). The fungicide mancozeb induces toxic effects on mammalian granulosa cells. *Toxicology and applied Pharmacology*, 260(2), 155-161.
- Pinot, F., & Beisson, F. (2011). Cytochrome P450 metabolizing fatty acids in plants: characterization and physiological roles. *The FEBS Journal*, 278(2), 195-205.
- Pollard, M., Beisson, F., Li, Y., & Ohlrogge, J. B. (2008). Building lipid barriers: biosynthesis of cutin and suberin. *Trends in Plant Science*, 13(5), 236-246.
- Pruitt, R. N., Gust, A. A., & Nürnberg, T. (2021). Plant immunity unified. *Nature Plants*, 7(4), 382-383.
- Qin, Y. M., Pujol, F. M., Hu, C. Y., Feng, J. X., Kastaniotis, A. J., Hiltunen, J. K., & Zhu, Y. X. (2007). Genetic and biochemical studies in yeast reveal that the cotton fibre-specific GhCER6 gene functions in fatty acid elongation. *Journal of Experimental Botany*, 58(3), 473-481.
- Ranathunge, K., Lin, J., Steudle, E., & Schreiber, L. (2011). Stagnant deoxygenated growth enhances root suberization and lignifications, but differentially affects water and NaCl permeabilities in rice (*Oryza sativa* L.) roots. *Plant, Cell & Environment*, 34(8), 1223-1240.
- Ranathunge, K., Thomas, R. H., Fang, X., Peterson, C. A., Gijzen, M., & Bernards, M. A. (2008). Soybean root suberin and partial resistance to root rot caused by *Phytophthora sojae*. *Phytopathology*, 98(11), 1179-1189.
- Rakosy-Tican, E., Thieme, R., König, J., Nachtigall, M., Hammann, T., Denes, T. E., ... & Molnár-Láng, M. (2020). Introgression of two broad-spectrum late blight resistance genes, Rpi-Blb1 and Rpi-Blb3, from *Solanum bulbocastanum* Dun plus race-specific R genes into potato pre-breeding lines. *Frontiers in Plant Science*, 11, 699.
- Reeve, R. M., Hautala, E., & Weaver, M. L. (1969). Anatomy and compositional variation within potatoes. *American Potato Journal*, 46, 361-373.
- Reddick, D. (1930). Frost-tolerant and blight-resistant Potatoes. *Phytopathology*, 20(12).
- Robatzek, S., & Saijo, Y. (2008). Plant immunity from A to Z.
- Rommens, C. M., Ye, J., Richael, C., & Swords, K. (2006). Improving potato storage and processing characteristics through all-native DNA transformation. *Journal of Agricultural and Food Chemistry*, 54(26), 9882-9887.
- Rowland, O., Zheng, H., Hepworth, S. R., Lam, P., Jetter, R., & Kunst, L. (2006). CER4 encodes an alcohol-forming fatty acyl-coenzyme A reductase involved in cuticular wax production in *Arabidopsis*. *Plant Physiology*, 142(3), 866-877.
- Ruffell, D. (2018). The EU Court of Justice extends the GMO Directive to gene-edited organisms. *FEBS Letters*, 592(22), 3653-3657.

- Runge, P. (2013). Dissertation: Charakterisierung und funktionelle Analyse eines ABC-Promotors aus *Solanum tuberosum*. Available in <<https://opendata.uni-halle.de/handle/1981185920/12438>>. Accessed 01 February 2022.
- Sánchez-Fernández, R., Davies, T. E., Coleman, J. O., & Rea, P. A. (2001). The *Arabidopsis thaliana* ABC protein superfamily, a complete inventory. *Journal of Biological Chemistry*, 276(32), 30231-30244.
- Sauveplane, V., Kandel, S., Kastner, P. E., Ehling, J., Compagnon, V., Werck-Reichhart, D., & Pinot, F. (2009). *Arabidopsis thaliana* CYP77A4 is the first cytochrome P450 able to catalyze the epoxidation of free fatty acids in plants. *The FEBS journal*, 276(3), 719-735.
- Sawai, S., Ohyama, K., Yasumoto, S., Seki, H., Sakuma, T., Yamamoto, T., ... & Umemoto, N. (2014). Sterol side chain reductase 2 is a key enzyme in the biosynthesis of cholesterol, the common precursor of toxic steroidal glycoalkaloids in potato. *The Plant Cell*, 26(9), 3763-3774.
- Scholze, H., & Boch, J. (2010). TAL effector-DNA specificity. *Virulence*, 1(5), 428-432.
- Schorneck, S., Peter, K., Bonas, U., & Lahaye, T. (2005). Expression levels of avrBs3-like genes affect recognition specificity in tomato Bs4-but not in pepper Bs3-mediated perception. *Molecular Plant-Microbe Interactions*, 18(11), 1215-1225.
- Schreiber, L., Franke, R., & Hartmann, K. (2005). Wax and suberin development of native and wound periderm of potato (*Solanum tuberosum* L.) and its relation to peridermal transpiration. *Planta*, 220, 520-530.
- Serra, O., Hohn, C., Franke, R., Prat, S., Molinas, M., & Figueras, M. (2010). A feruloyl transferase involved in the biosynthesis of suberin and suberin-associated wax is required for maturation and sealing properties of potato periderm. *The Plant Journal*, 62(2), 277-290.
- Serra, O., Soler, M., Hohn, C., Franke, R., Schreiber, L., Prat, S., ... & Figueras, M. (2009a). Silencing of StKCS6 in potato periderm leads to reduced chain lengths of suberin and wax compounds and increased peridermal transpiration. *Journal of Experimental Botany*, 60(2), 697-707.
- Serra, O., Soler, M., Hohn, C., Sauveplane, V., Pinot, F., Franke, R., ... & Figueras, M. (2009b). CYP86A33-targeted gene silencing in potato tuber alters suberin composition, distorts suberin lamellae, and impairs the periderm's water barrier function. *Plant Physiology*, 149(2), 1050-1060.
- Shan, Q., Wang, Y., Li, J., Zhang, Y., Chen, K., Liang, Z., ... & Gao, C. (2013). Targeted genome modification of crop plants using a CRISPR-Cas system. *Nature Biotechnology*, 31(8), 686-688.
- Shanmugarajah, K., Linka, N., Gräfe, K., Smits, S. H., Weber, A. P., Zeier, J., & Schmitt, L. (2019). ABCG1 contributes to suberin formation in *Arabidopsis thaliana* roots. *Scientific Reports*, 9(1), 11381.
- Shibata, Y., Ojika, M., Sugiyama, A., Yazaki, K., Jones, D. A., Kawakita, K., & Takemoto, D. (2016). The full-size ABCG transporters Nb-ABCG1 and Nb-ABCG2 function in pre-and postinvasion defense against *Phytophthora infestans* in *Nicotiana benthamiana*. *The Plant Cell*, 28(5), 1163-1181.
- Shoji, T. (2014). ATP-binding cassette and multidrug and toxic compound extrusion transporters in plants: a common theme among diverse detoxification mechanisms. *International Review of Cell and Molecular Biology*, 309, 303-346.
- Shukla, V., Han, J. P., Cléard, F., Lefebvre-Legendre, L., Gully, K., Flis, P., ... & Barberon, M. (2021). Suberin plasticity to developmental and exogenous cues is regulated by a set of MYB transcription factors. *Proceedings of the National Academy of Sciences*, 118(39), e2101730118.
- Si-Ammour, A., Mauch-Mani, B., & Mauch, F. (2003). Quantification of induced resistance against *Phytophthora* species expressing GFP as a vital marker: β -aminobutyric acid but not BTH protects potato and *Arabidopsis* from infection. *Molecular Plant Pathology*, 4(4), 237-248.
- Smit, A. L., Bengough, A. G., Engels, C., van Noordwijk, M., Pellerin, S., & van de Geijn, S. C. (Eds.). (2013). *Root methods: a handbook*. Springer Science & Business Media.
- Spooner, D. M., Núñez, J., Trujillo, G., del Rosario Herrera, M., Guzmán, F., & Ghislain, M. (2007). Extensive simple sequence repeat genotyping of potato landraces supports a major reevaluation of their gene

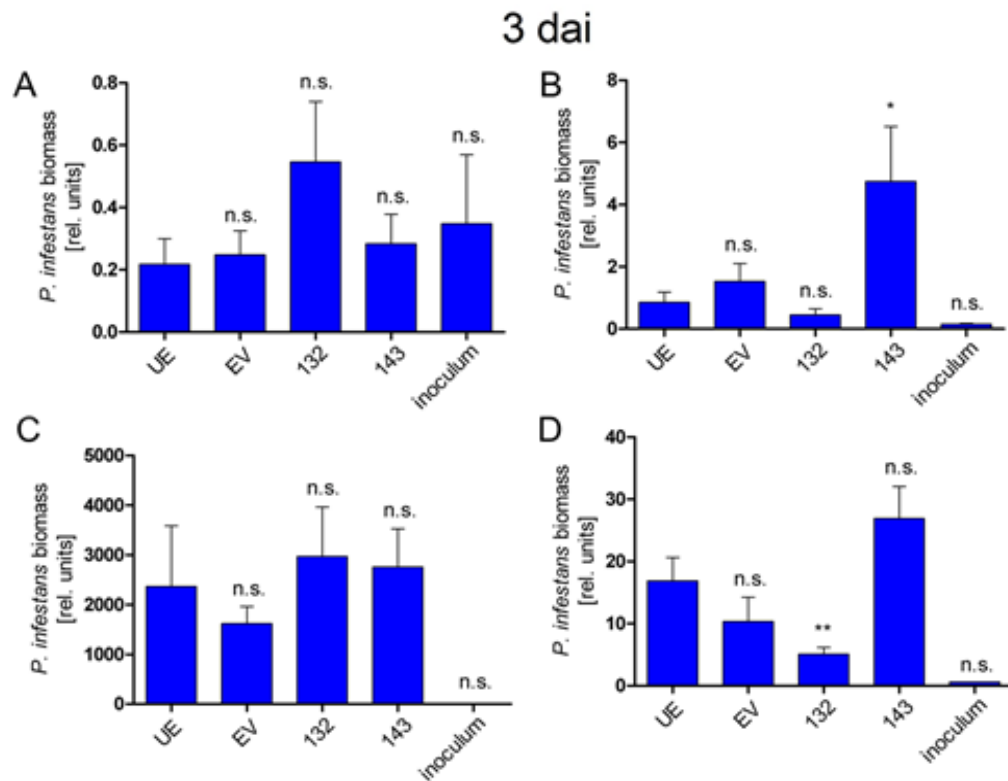
- pool structure and classification. *Proceedings of the National Academy of Sciences*, 104(49), 19398-19403.
- Soler, M., Serra, O., Molinas, M., Huguet, G., Fluch, S., & Figueras, M. (2007). A genomic approach to suberin biosynthesis and cork differentiation. *Plant Physiology*, 144(1), 419-431.
- Stumpe, M., & Feussner, I. (2006). Formation of oxylipins by CYP74 enzymes. *Phytochemistry Reviews*, 5, 347-357.
- Swanson, J. K., Yao, J., Tans-Kersten, J., & Allen, C. (2005). Behavior of *Ralstonia solanacearum* race 3 biovar 2 during latent and active infection of geranium. *Phytopathology*, 95(2), 136-143.
- Szcepek, M., Brondani, V., Büchel, J., Serrano, L., Segal, D. J., & Cathomen, T. (2007). Structure-based redesign of the dimerization interface reduces the toxicity of zinc-finger nucleases. *Nature Biotechnology*, 25(7), 786-793.
- Thomas, R., Fang, X., Ranathunge, K., Anderson, T. R., Peterson, C. A., & Bernards, M. A. (2007). Soybean root suberin: anatomical distribution, chemical composition, and relationship to partial resistance to *Phytophthora sojae*. *Plant Physiology*, 144(1), 299-311.
- Thordal-Christensen, H. (2020). A holistic view on plant effector-triggered immunity presented as an iceberg model. *Cellular and Molecular Life Sciences*, 77(20), 3963-3976.
- Todd, J., Post-Beittenmiller, D., & Jaworski, J. G. (1999). KCS1 encodes a fatty acid elongase 3-ketoacyl-CoA synthase affecting wax biosynthesis in *Arabidopsis thaliana*. *The Plant Journal*, 17(2), 119-130.
- Trenkamp, S., Martin, W., & Tietjen, K. (2004). Specific and differential inhibition of very-long-chain fatty acid elongases from *Arabidopsis thaliana* by different herbicides. *Proceedings of the National Academy of Sciences*, 101(32), 11903-11908.
- Tuncel, A., Corbin, K. R., Ahn-Jarvis, J., Harris, S., Hawkins, E., Smedley, M. A., ... & Smith, A. M. (2019). Cas9-mediated mutagenesis of potato starch-branching enzymes generates a range of tuber starch phenotypes. *Plant Biotechnology Journal*, 17(12), 2259-2271.
- Urnov, F. D., Rebar, E. J., Holmes, M. C., Zhang, H. S., & Gregory, P. D. (2010). Genome editing with engineered zinc finger nucleases. *Nature Reviews Genetics*, 11(9), 636-646.
- Ursache, R., De Jesus Vieira Teixeira, C., Déneraud Tendon, V., Gully, K., De Bellis, D., Schmid-Siegert, E., ... & Vermeer, J. E. (2021). GDSL-domain proteins have key roles in suberin polymerization and degradation. *Nature Plants*, 7(3), 353-364.
- Van den Ackerveken, G., Marois, E., & Bonas, U. (1996). Recognition of the bacterial avirulence protein AvrBs3 occurs inside the host plant cell. *Cell*, 87(7), 1307-1316.
- Verrier, P. J., Bird, D., Burla, B., Dassa, E., Forestier, C., Geisler, M., ... & Theodoulou, F. L. (2008). Plant ABC proteins—a unified nomenclature and updated inventory. *Trends in Plant Science*, 13(4), 151-159.
- Vishwanath, S. J., Delude, C., Domergue, F., & Rowland, O. (2015). Suberin: biosynthesis, regulation, and polymer assembly of a protective extracellular barrier. *Plant Cell Reports*, 34, 573-586.
- Vishwanath, S. J., Kosma, D. K., Pulsifer, I. P., Scandola, S., Pascal, S., Joubès, J., ... & Domergue, F. (2013a). Suberin-associated fatty alcohols in *Arabidopsis*: distributions in roots and contributions to seed coat barrier properties. *Plant Physiology*, 163(3), 1118-1132.
- Vishwanath, S. J. (2013b). Dissertation: Suberin-associated fatty acyl-CoA Reductases from *Arabidopsis thaliana*. Available in <<https://curve.carleton.ca/83518e7a-b25d-4581-b5d3-88f331040d9d>>. Accessed 17.01.2021.
- Vogg, G., Fischer, S., Leide, J., Emmanuel, E., Jetter, R., Levy, A. A., & Riederer, M. (2004). Tomato fruit cuticular waxes and their effects on transpiration barrier properties: functional characterization of a mutant deficient in a very-long-chain fatty acid β -ketoacyl-CoA synthase. *Journal of Experimental Botany*, 55(401), 1401-1410.

- Vulavala, V. K., Fogelman, E., Faigenboim, A., Shoseyov, O., & Ginzberg, I. (2019). The transcriptome of potato tuber phellogen reveals cellular functions of cork cambium and genes involved in periderm formation and maturation. *Scientific Reports*, 9(1), 10216.
- Vulavala, V. K., Fogelman, E., Rozental, L., Faigenboim, A., Tanami, Z., Shoseyov, O., & Ginzberg, I. (2017). Identification of genes related to skin development in potato. *Plant Molecular Biology*, 94, 481-494.
- Wahrenburg, Z., Benesch, E., Lowe, C., Jimenez, J., Vulavala, V. K., Lü, S., ... & Kosma, D. K. (2021). Transcriptional regulation of wound suberin deposition in potato cultivars with differential wound healing capacity. *The Plant Journal*, 107(1), 77-99.
- Wang, P. P., Liu, H., Gao, S., & Cheng, A. X. (2017). Functional characterization of a hydroxyacid/alcohol hydroxycinnamoyl transferase produced by the liverwort *Marchantia emarginata*. *Molecules*, 22(11), 1854.
- Wang, Y., Cheng, X., Shan, Q., Zhang, Y., Liu, J., Gao, C., & Qiu, J. L. (2014). Simultaneous editing of three homoeoalleles in hexaploid bread wheat confers heritable resistance to powdery mildew. *Nature Biotechnology*, 32(9), 947-951.
- Weber, E., Engler, C., Gruetzner, R., Werner, S., & Marillonnet, S. (2011). A modular cloning system for standardized assembly of multigene constructs. *PloS one*, 6(2), e16765.
- Wei, X., Lu, W., Mao, L., Han, X., Wei, X., Zhao, X., ... & Xu, C. (2020). ABF2 and MYB transcription factors regulate feruloyl transferase FHT involved in ABA-mediated wound suberization of kiwifruit. *Journal of Experimental Botany*, 71(1), 305-317.
- Werck-Reichhart, D., & Feyereisen, R. (2000). Cytochromes P450: a success story. *Genome Biology*, 1(6), 1-9.
- Werner, S., Engler, C., Weber, E., Gruetzner, R., & Marillonnet, S. (2012). Fast track assembly of multigene constructs using Golden Gate cloning and the MoClo system. *Bioengineered*, 3(1), 38-43.
- Woolfson, K. N., Haggitt, M. L., Zhang, Y., Kachura, A., Bjelica, A., Rey Rincon, M. A., ... & Bernards, M. A. (2018). Differential induction of polar and non-polar metabolism during wound-induced suberization in potato (*Solanum tuberosum* L.) tubers. *The Plant Journal*, 93(5), 931-942.
- Wu, E. J., Wang, Y. P., Yahuza, L., He, M. H., Sun, D. L., Huang, Y. M., ... & Zhan, J. (2020). Rapid adaptation of the Irish potato famine pathogen *Phytophthora infestans* to changing temperature. *Evolutionary Applications*, 13(4), 768-780.
- Xin, A., & Herburger, K. (2021). Mini review: transport of hydrophobic polymers into the plant apoplast. *Frontiers in Plant Science*, 11, 590990.
- Yadav, V., Molina, I., Ranathunge, K., Castillo, I. Q., Rothstein, S. J., & Reed, J. W. (2014). ABCG transporters are required for suberin and pollen wall extracellular barriers in Arabidopsis. *The Plant Cell*, 26(9), 3569-3588.
- Yamamizo, C., Kuchimura, K., Kobayashi, A., Katou, S., Kawakita, K., Jones, J. D., ... & Yoshioka, H. (2006). Rewiring mitogen-activated protein kinase cascade by positive feedback confers potato blight resistance. *Plant Physiology*, 140(2), 681-692.
- Yang, W., Pollard, M., Li-Beisson, Y., Beisson, F., Feig, M., & Ohlrogge, J. (2010). A distinct type of glycerol-3-phosphate acyltransferase with sn-2 preference and phosphatase activity producing 2-monoacylglycerol. *Proceedings of the National Academy of Sciences*, 107(26), 12040-12045.
- Yildiz, M., & Ozgen, Y. (Eds.). (2021). *Solanum tuberosum: A Promising Crop for Starvation Problem*. BoD-Books on Demand.
- Yim, S., Khare, D., Kang, J., Hwang, J. U., Liang, W., Martinoia, E., ... & Lee, Y. (2016). Postmeiotic development of pollen surface layers requires two Arabidopsis ABCG-type transporters. *Plant Cell Reports*, 35, 1863-1873.

- Yogendra, K. N., Kumar, A., Sarkar, K., Li, Y., Pushpa, D., Mosa, K. A., ... & Kushalappa, A. C. (2015). Transcription factor StWRKY1 regulates phenylpropanoid metabolites conferring late blight resistance in potato. *Journal of Experimental Botany*, 66(22), 7377-7389.
- Yogendra, K. N., Kushalappa, A. C., Sarmiento, F., Rodriguez, E., & Mosquera, T. (2014). Metabolomics deciphers quantitative resistance mechanisms in diploid potato clones against late blight. *Functional Plant Biology*, 42(3), 284-298.
- Zhang, H. X., Zhang, Y., & Yin, H. (2019a). Genome editing with mRNA encoding ZFN, TALEN, and Cas9. *Molecular Therapy*, 27(4), 735-746.
- Zhang, L., Zhang, X., Wang, X., Xu, J., Wang, M., Li, L., ... & Yang, X. (2019b). Seed Carotenoid Deficient functions in isoprenoid biosynthesis via the plastid MEP pathway. *Plant Physiology*, 179(4), 1723-1738.
- Zhang, Y., Huber, D. J., Hu, M., Jiang, G., Gao, Z., Xu, X., ... & Zhang, Z. (2018). Delay of postharvest browning in litchi fruit by melatonin via the enhancing of antioxidative processes and oxidation repair. *Journal of Agricultural and Food Chemistry*, 66(28), 7475-7484.
- Zhou, X., Zha, M., Huang, J., Li, L., Imran, M., & Zhang, C. (2017). StMYB44 negatively regulates phosphate transport by suppressing expression of PHOSPHATE1 in potato. *Journal of Experimental Botany*, 68(5), 1265-1281.
- Zhu, H., Chen, C., Zeng, J., Yun, Z., Liu, Y., Qu, H., ... & Xia, R. (2020). Micro RNA 528, a hub regulator modulating ROS homeostasis via targeting of a diverse set of genes encoding copper-containing proteins in monocots. *New Phytologist*, 225(1), 385-399.

8. APPENDICES

8.1. Supplementary figures



Supplementary figure 1: *P. infestans* biomass 3 days after inoculation (dai) performed by Ulrike Smolka (IPB/Halle). *P. infestans* DNA was determined by qPCR in leaf disks 3 days after inoculation of wild-type (WT), empty vector (EV) and two different *StABCG1*-CrisprCas (#132 and #143) plants. DNA was isolated from inoculated leaves (1×10^5 zoospores/mL) of 3-week-old plants grown in a phytochamber. Error bars represent SEM. For each graph, data are derived from one independent experiment ($n = 8$ for UE, EV, #132 and #143 and $n = 2$ for inoculum). Statistical differences between growth on WT and other plants were determined by t-test – Mann-Whitney (*, $0.01 < p < 0.05$; **, $0.001 < p < 0.1$; n.s., not significant).

8.2. Primers Table

Supplementary table 1: List of primers and sequence use in this work.

Number	Name	Sequence	Use for	Section
27	pvs3p1	tt ggtctc a acat GGAGTATAGCACTCTATTCATGTTGTAATTTGGC	Golden Gate cloning	2.8.1
28	pvs3p2	tt ggtctc a acaa CATCAACTTGAAAAAATATAGCATTACATAAAATCTTAGTATG	Golden Gate cloning	2.8.1
29	pvs3p3	tt ggtctc a acat GATGACGGAAACAATAGCATTGGATCAAG	Golden Gate cloning	2.8.1
30	pvs3p4	tt ggtctc a acaa CATTCTTCGGAAACGGGTCTAATTAGC	Golden Gate cloning	2.8.1
31	CYP1_GG	tt ggtctc a acat aATGGATCCTATACTAGTTTATTCTGG	Golden Gate cloning	2.8.2
32	CYP2_GG	tt ggtctc a acaa CgCCACCGGTTCGAGAGCCATC	Golden Gate cloning	2.8.2
33	CYP3_GG	tt ggtctc a acat GGcGACCGGTTCGAACCGCCAAAAG	Golden Gate cloning	2.8.2
34	CYP4_GG	tt ggtctc a acaa AAGCTCATGCAGACATAGCAATCTTTGGAG	Golden Gate cloning	2.8.2
35	KCS1_GG	tt ggtctc a acat aATGCCAGAACCAGTCCCAAATTC	Golden Gate cloning	2.8.2
36	KCS2_GG	tt ggtctc a acaa AtGACGATGATGTGTTACCTGTTC	Golden Gate cloning	2.8.2
37	KCS3_GG	tt ggtctc a acat TCaTCACTATGGTATGAGATGAGTTAC	Golden Gate cloning	2.8.2
38	KCS4_GG	tt ggtctc a acaa AAGCTTACAGCTTCACAATCTC	Golden Gate cloning	2.8.2
39	ABC_F	GTACAACAAGCCATGGAGATGTCAC	Genotype confirmation	2.12.1
40	ABC_R	GTTTCATAGGTGACCCACTATAAAC	Genotype confirmation	2.12.1
44	FHT1_GG	tt gaagac a aa ATGGAGAGTGGTAAACACAATGTTG	Golden Gate cloning	2.8.2

45	FHT2_GG	tt gaagac a a aagc TTAGATCTCCATAAGTTCTTCAAATGTTTTTC	Golden Gate cloning	2.8.2
46	ABC1_GG	tt gaagac a aa ATGTCAAGGATAGTGGCGGAAAATATGTTACAAG	Golden Gate cloning	2.8.2
47	ABC2_GG	tt gaagac a a aagc TCACCTTCTCTTGTTCTTACTTCCAAGCAAC	Golden Gate cloning	2.8.2
55	KCSqF	AAGCGTTCGAACATTTTTGC	qPCR	2.12.7
56	KCSqR	CTTCTGAAGCTCATCAATAACAGC	qPCR	2.12.7
57	CYPqF	TTGGCTTACCTCCAAATGAAA	qPCR	2.12.7
58	CYPqR	CGGTAATAGCCGGTAACGAA	qPCR	2.12.7
59	FHTqF	TTGACAATTAGCCAGGAAATGA	qPCR	2.12.7
60	FHTqR	TGCTTCTGCCTCAACAAAA	qPCR	2.12.7
61	ABCqF	GGTCGCGATCCTAGCCTATT	qPCR	2.12.7
62	ABCqR	ATCCTATCGCGATTGATGAAG	qPCR	2.12.7
67	ABCG1_sg RNA	cctctaatacgactcactata GGCGAGATAGTCGCCGTCCT gtttaagagctatgc	gRNA - Genotype confirmation	2.12.1
126	AtMYB39- qPCR-F	GGCAAATTTTCCGATGGAG	qPCR	2.12.7
127	AtMYB39- qPCR-R	ATGACCCGCAATTTTCGAC	qPCR	2.12.7
132	ABCG1-P5- F	tcgtcggcagcgtcagatgtgtataagagacag TCATCTCACTCTTCTTTTGT	Illumina sequencing	2.12.4
133	ABCG1-P7- R	gtctcgtgggctcggagatgtgtataagagacag TAAACTCTCCTTCGCGATCC	Illumina sequencing	2.12.4
134	FAR3_F	TCCTAAACTTTGCCAAGAAGTG	qPCR	2.12.7
135	FAR3_R	TTTTCCAACATCAACCCTTCC	qPCR	2.12.7
136	FAR1_F	ATGTCCTCAACTTTGCTAAGAG	qPCR	2.12.7
137	FAR1_R	ACTCCTTCACCTTCTCCAC	qPCR	2.12.7
138	KCS11_F	GGCGATGCTCTAAAGACAAAC	qPCR	2.12.7
139	KCS11_R	AAGAAAAGGAACTGCTCAGAC	qPCR	2.12.7
140	GPAT4_F	AAGTTCCGCCAAGAGAACG	qPCR	2.12.7
141	GPAT4_R	CCACACATACATCCAATCTACC	qPCR	2.12.7

142	PPO_F	AAGCGTTCGAACATTTTTGC	qPCR	2.12.7
143	PPO_R	AGCACCATCACAATAAGCAC	qPCR	2.12.7
144	LAC14_F	TGCACTTATTATACGTCCTGC	qPCR	2.12.7
145	LAC14_R	TCACTTTTCCACCACTCCC	qPCR	2.12.7
-	EF1alphaF	ACTGCCCAAGGTCATCATCATC	qPCR	2.12.7
-	EF1alphaR	GCACTGGAGCATATCCGTTT	qPCR	2.12.7
	PIO8-3-3F	CGTACGGCCAATGTAGTTCC	Biomass	2.3
	PIO8-3-3R	TTTGACACAGTATCACGCAAGT	Biomass	2.3
	NOXF	TCAATGCATAGGTATGAAGGAATC	Biomass	2.3
	NOXR	TCTCTTCCTAGCTAGAGCATCAAAT	Biomass	2.3

Capital letters denote sequence homologous to the respective gene;

Lowercase letters denote tails or sequences non-homologous to the respective gene (see the respective section).

8.3. Plasmids and constructs table

Supplementary table 2: List of plasmids and constructs used in this work.

Plasmid	Construct description	Verification
<i>20ABQQQP</i>	AtMYB39	ThermoFisher Scientific – GeneArt
<i>pAGR21</i>	<i>pAGM1311</i> :frag. 1 from <i>StPVS3</i> promoter	sequenced
<i>pAGR22</i>	<i>pAGM1311</i> :frag. 2 from <i>StPVS3</i> promoter	sequenced
<i>pAGR23</i>	<i>pICH41295</i> : <i>StPVS3</i> promoter	sequenced
<i>pAGR24</i>	<i>pAGR1311</i> :frag. 1 from <i>StCYP86A33</i>	sequenced
<i>pAGR25</i>	<i>pAGM1311</i> :frag. 2 from <i>StCYP86A33</i>	sequenced
<i>pAGR26</i>	<i>pICH41308</i> : <i>StCYP86A33</i>	<i>Bsa</i> I; <i>Eco</i> 47I; <i>Ssp</i> I
<i>pAGR27</i>	<i>pAGM1311</i> :frag. 1 from <i>StKCS6</i>	sequenced
<i>pAGR28</i>	<i>pAGM1311</i> :frag. 2 from <i>StKCS6</i>	sequenced
<i>pAGR29</i>	<i>pICH41308</i> : <i>StKCS6</i>	<i>Bsa</i> I; <i>Pag</i> I; <i>Ssp</i> I
<i>pAGR30A2</i>	<i>pICH41308</i> : <i>StFHTA2</i>	sequenced
<i>pAGR30A3</i>	<i>pICH41308</i> : <i>StFHTA3</i>	sequenced
<i>pAGR33</i>	<i>pAGM38499</i>:<i>StPVS3</i>promoter (GFP)	<i>Eco</i> RI; <i>Hind</i> III; <i>Ksp</i> I
<i>pAGR34</i>	<i>pAGM38501</i>:<i>StPVS3</i>promoter (GUS)	<i>Eco</i> RI; <i>Ksp</i> I; <i>Ssp</i> I
<i>pAGR35</i>	<i>pICH41308</i> : <i>StABCG1</i>	sequenced
<i>pAGR38</i>	<i>pICH47742</i> : <i>pICH71037</i> : <i>StKCS6</i> : <i>pICH41414</i>	<i>Alw</i> 44I; <i>Bbs</i> I; <i>Bgl</i> II
<i>pAGR39</i>	<i>pICH47751</i> : <i>pICH71037</i> : <i>StCYP86A33</i> : <i>pICH41421</i>	<i>Bbs</i> I; <i>Eco</i> 47I; <i>Ssp</i> I
<i>pAGR40A2</i>	<i>pICH47761</i> : <i>pICH71037</i> : <i>StFHTA2</i> : <i>pICH41432</i>	<i>Bbs</i> I; <i>Eco</i> 47I; <i>Eco</i> RI
<i>pAGR40A3</i>	<i>pICH47761</i> : <i>pICH71037</i> : <i>StFHTA3</i> : <i>pICH41432</i>	<i>Eco</i> RI; <i>Bsm</i> I; <i>Bpi</i> I; <i>Hind</i> III
<i>pAGR41</i>	<i>pICH47772</i> : <i>pICH71037</i> : <i>StABCG1</i> : <i>pICH77901</i>	<i>Alw</i> 44I; <i>Bpi</i> I; <i>Eco</i> 47I
<i>pAGR42</i>	<i>pICH47781</i> : <i>StPVS3</i> promoter: <i>pICH73103</i> : <i>pICH72400</i>	<i>Alw</i> 44I; <i>Hind</i> III; <i>Ssp</i> I
<i>pAGR43</i>	<i>pICH47742</i> : <i>StPVS3</i> promoter: <i>pICH73103</i> : <i>pICH72400</i>	<i>Alw</i> 44I; <i>Hind</i> III; <i>Ssp</i> I
<i>pAGR44A2</i>	<i>pAGM37443</i>:<i>pICH67131</i>:<i>StKCS6</i>:<i>StCYP86A33</i>:<i>StFHTA2</i>:<i>StABCG1</i>:<i>pICH41800</i>	<i>Alw</i> 44I; <i>Bgl</i> II; <i>Bsp</i> 147I

pAGR44A3	pAGM37443:piCH67131:StKCS6:StCYP86A33:StFHTA3:StABCG1:piCH41800	<i>Alw44I; BglII; Bsp147I</i>
pAGR45A2	pAGM37443:K:StKCS6:StCYP86A33:StFHTA2:StABCG1:StPVS3promoter:piCH41822	<i>Alw44I; BglII; Bsp147I</i>
pAGR45A3	pAGM37443:piCH67131:StKCS6:StCYP86A33:StFHTA3:StABCG1:StPVS3promoter:piCH41822	<i>Alw44I; BglII; Bsp147I</i>
pAGR46	pAGM37443:piCH67131:StPVS3promoter:piCH41744	<i>Alw44I; BglII; Bsp147I</i>
<i>pAGR47</i>	<i>StPVS3promoter:StKCS6:piCH41414</i>	<i>Alw44I; BpiI; EcoRI; HindIII</i>
<i>pAGR48</i>	<i>StPVS3promoter:StCYP86A33:piCH41414</i>	<i>Alw44I; BbsI; BglI</i>
<i>pAGR49A2</i>	<i>StPVS3promoter:StFHTA2:piCH41414</i>	<i>Alw44I; Mva1269I; SspI</i>
<i>pAGR49A3</i>	<i>StPVS3promoter:StFHTA3:piCH41414</i>	<i>Alw44I; Mva1269I; BbsI</i>
<i>pAGR50</i>	<i>StPVS3promoter:StABCG1:piCH41414</i>	<i>Alw44I; BbsI; SspI</i>
pAGR51A2	pAGM37443:piCH67131:pPVS3:StKCS6:pPVS3:StCYP86A33:pPVS3:StFHTA2:pPVS3:StABCG1:piCH41800	<i>Alw44I; EcoRI; HindIII</i>
pAGR51A3	pAGM37443:piCH67131:pPVS3:StKCS6:pPVS3:StCYP86A33:pPVS3:StFHTA3:pPVS3:StABCG1:piCH41800	<i>Alw44I; EcoRI; HindIII</i>
<i>pAGR90</i>	<i>piCH47742:piCH51266:35S:AtMYB39:35S:piCH41414</i>	<i>BpiI; Eco88I; XhoI</i>
pAGR91	pAGM37443:piCH67131:35S:AtMYB39:35S:piCH41744	<i>EcoRI; SspI; XhoI</i>

St. *Solanum tuberosum* genes; *At.* *Arabidopsis thaliana* genes; Bold letters denote binary plasmids used for stable transformation in *S. tuberosum*.

9. NOTE OF THANKS

I thank God. Who is always present in my life, guiding and comforting me in difficult times and blessing with every achievement. To Leibniz-Institute of Plant Biochemistry (IPB), to Martin-Luther-Universität Halle-Wittenberg (MLU), to International Graduate Schools in Agricultural and Polymer Science (AGRIPOLY), to the Hochschule Anhalt and all people from the Department BPI, mainly Prof. Dr. Scheel and Prof. Dr. Romeis for the opportunities and contributions to my academic experience.

My sincere thanks to my supervisor, Prof. Dr. Rosahl for the opportunity she gave me to grow as a professional and as a person, for her teachings and friendship. I couldn't be luckier than have her as advisor. To the co-supervisors Prof. Dr. Deising and Dr. Marillonnet and to Sindy and Sarah, who contributed to my work. A big "thank you so much" to my lab colleagues, Xiyuan, Jule, Nuno. And in particular, for their professional and personal relationship, to Ulrike Smolka, Dr. Gorzolka and Dr. Eschen-Lippold who were willing to help me with such limited deadlines and who managed to contribute immensely to this work, in such a short time, that they took me in their arms and taught me everything during my PhD: Thank you for your support.

It would be not possible to me to have this academic carrier without my friends Alan, Renata, Maria Paula, Kaissar, Lukas and Chris, who helped me with psychologic and scientific discussions, even at bar tables.

Thanks to my parents, Tânia and Elvio, my siblings, Daniella and Fernando for all the support, love and trust I received and still receive. You are the best family anyone could have. To my husband Raphael, who was always on my side for every decision. No one besides him can understands the moments of joy and despair that are interspersed with impressive speed. To my large and close family.

To my friends, who didn't allow insanity to take over me in the most accurate moments, and who celebrated with me when the light at the end of the tunnel was seen and that some of them were abandoned in Brazil but who have always remained present in my life: Miriam, Desirrê, Sandrielle, Bia, Diego, Marcos, Gabi, Coala, Kelly and Mara,

who in the meantime made me laugh with funny audios, photos and memes and for very special moments.

To the friends who are as family to me, and I miss them so much: Tai, Michel, Ale, Kamide, André and Paulo Vitor.

To everyone who somehow gave a portion of affection, effort, incentive to carry out this work.

10.EIDESSTÄTTLICHE ERKLÄRUNG / DECLARATION UNDER OATH

Ich erkläre an Eides statt, dass ich die Arbeit selbstständig und ohne fremde Hilfe verfasst, keine anderen als die von mir angegebenen Quellen und Hilfsmittel benutzt und die den benutzten Werken wörtlich oder inhaltlich entnommenen Stellen als solche kenntlich gemacht habe.

I declare under penalty of perjury that this thesis is my own work entirely and has been written without any help from other people. I used only the sources mentioned and included all the citations correctly both in word or content.

Halle (Saale), _____

Elvio Henrique Benatto Perino

11. CURRICULUM VITAE

PERSONAL INFORMATION

Name: Elvio Henrique Benatto Perino
Date of birth: 07/18/1988
Place of birth: Ourinhos/SP – Brazil
Nationality: Brazilian
Address: Rannische Str. 17, 06108, Halle (Saale), Germany
e-mail: ehperino@hotmail.com

WORKING EXPERIENCE

04/2015 – 12/2015 **VipAula** – Curitiba/PR, Brazil

Teacher

Teaching Math, Chemistry, Biology and Physics for elementary, middle, and high school students.

09/2014 – 01/2015 **Raízen**, Tarumã/SP, Brazil

Internship

Processing and product engineering, evaluation of process and methods to attend the security, quality and productivity.

09/2013 – 09/2014 **LabGeM (UFPR)**, Curitiba/PR, Brazil

Internship

Responsible for the collection of microorganisms and two projects: “New methods of fungi storage” and “Biological control of Citrus Black Spot”.

08/2012 – 08/2013 **Institute of Neuro Information Processing (Ulm University)**, Ulm, Germany

Internship

Developing a program to facilitate the design and preview of genetics networks (JAVA and R programming).

10/2011 – 07/2012 **SENAI**, Curitiba/PR, Brazil

Trainee

Trainee from the technical courses: Food Technology and Practical Technology in Food Industry.

Responsible for three laboratories: Food, Bread, and Microbiology.

04/2010 – 10/2011 **LabPPAm (UFPR)**, Curitiba/PR, Brazil

Internship

Use of industrial waste to produce fertilizer.

02/2009 – 11/2017 **Goethe Institut**, Curitiba/PR, Brazil

Internship (3h/week)

Client support and organization of the library. Support to the Librarian.

02/2007 – 12/2007 **Biotechnology Laboratory (UENP)**, Bandeirantes/PR, Brazil

Internship

Study of fermenting microorganisms' (yeasts) biodiversity isolated from the Alcohol industry.

EDUCATION

11/2017 – present **Leibniz Institute of Plant Biochemistry**, Halle (Saale), Germany

PhD, Focus: Biochemistry of Plant Interactions, (MLU)

Thesis: “The role of suberin biopolymers for pathogen resistance”.

03/2015 – 05/2017 **Federal University of Paraná (UFPR)**, Curitiba/PR, Brazil

Master in Genetics, Focus: Plant-pathogen Interactions

Thesis: “Analysis of expression and subcellular localization of urease and allantoicase proteins in *Colletotrichum graminicola* using mutants URE1:eGFP and ALA1:eGFP”.

02/2009 – 03/2015 **Federal University of Paraná (UFPR)**, Curitiba/PR, Brazil

Graduation in Bioprocess Engineering and Biotechnology

08/2012 – 08/2013 **Ulm University**, Ulm, Germany

Graduation in Bioinformatics – academic exchange

02/2007 – 06/2008 **State University of North Paraná (UENP)**, Bandeirantes/PR, Brazil

Graduation in Biology (3rd period completed)

PUBLICATIONS

Gorzolka, K., Perino, E. H. B., Lederer, S., Smolka, U., & Rosahl, S. (2021). Lysophosphatidylcholine 17: 1 from the Leaf Surface of the Wild Potato Species *Solanum bulbocastanum* Inhibits *Phytophthora infestans*. *Journal of Agricultural and Food Chemistry*, 69(20), 5607-5617.

Benatto Perino, E. H., Glienke, C., de Oliveira Silva, A., & Deising, H. B. (2020). Molecular Characterization of the Purine Degradation Pathway Genes ALA1 and URE1 of the Maize Anthracnose Fungus *Colletotrichum graminicola* Identified Urease as a Novel Target for Plant Disease Control. *Phytopathology*, 110(9), 1530-1540.